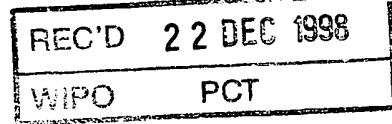




PCT/AU98/00998

S



**PRIORITY
DOCUMENT**

SUBMITTED OR TRANSMITTED IN
COMPLIANCE WITH RULE 17.1(a) OR (b)

Patent Office
Canberra

I, KIM MARSHALL, MANAGER EXAMINATION SUPPORT AND SALES, hereby certify that the annexed is a true copy of the Provisional specification in connection with Application No. PP 0585 for a patent by COMMONWEALTH SCIENTIFIC AND INDUSTRIAL RESEARCH ORGANISATION filed on 27 November 1997.

WITNESS my hand this Ninth
day of December 1998

KIM MARSHALL
MANAGER EXAMINATION SUPPORT AND
SALES



AUSTRALIA

Patents Act 1990

**COMMONWEALTH SCIENTIFIC AND INDUSTRIAL
RESEARCH ORGANISATION**

PROVISIONAL SPECIFICATION

Invention Title:

Receptor agonists and antagonists

The invention is described in the following statement:

RECEPTOR AGONISTS AND ANTAGONISTS

Field of the Invention

This invention relates to the field of receptor structure and receptor/ligand interactions. In particular it relates to the field of using receptor structure to predict the structure of related receptors and to use the determined structures and predicted structures to select and screen for agonists and antagonists of the polypeptide ligands.

Background of the Invention

Insulin is the peptide hormone that regulates glucose uptake and metabolism. The two types of diabetes are associated with either an inability to produce insulin because of destruction of the pancreatic islet cells (Homo-Delarche, F. & Boitard, C., 1996, *Immunol. Today* 10: 456-460) or poor glucose metabolism resulting from either insulin resistance at the target tissues, inadequate insulin secretion by the islets or faulty liver function (Taylor, S. I., et al., 1994, *Diabetes*, 43: 735-740).

Insulin-like growth factors-1 and 2 (IGF-1 and 2) are structurally related to insulin but are more important in tissue growth and development than in metabolism. They are primarily produced in the liver in response to growth hormone but are also produced in most other tissues where they function as paracrine/autocrine regulators. The IGFs are strong mitogens and are involved in numerous physiological states and certain cancers (Baserga, R., 1996, *TibTech* 14: 150-152).

Epidermal growth factor (EGF) is a small polypeptide cytokine that is unrelated to the insulin/IGF family. It stimulates marked proliferation of epithelial tissues and is a member of a larger family of structurally related cytokines such as transforming growth factor α , amphiregulin, betacellulin, heparin-binding EGF and some viral gene products. Abnormal EGF family signalling is a characteristic of certain cancers (Soler, C. & Carpenter, G., 1994 In Nicola, N. (ed) *Guidebook to Cytokines and Their receptors*”, Oxford Univ. Press, Oxford, pp194-197; Walker, F. & Burgess, A. W., 1994, In Nicola, N. (ed) *Guidebook to Cytokines and Their receptors*”, Oxford Univ. Press, Oxford, pp198-201).

Each of these growth factors mediate their biological actions through binding to the corresponding receptor. The IR, IGF-1R and insulin receptor-related receptor (IRR), for which the ligand is not known, are closely related to each other and are referred to as the insulin receptor subfamily. There is a

large body of information now available concerning the primary structure of these insulin receptor subfamily members (Ebina, Y., et al., 1985 *Cell* 40: 747-758; Ullrich, A., et al., 1985, *Nature* 313: 756-761; Ullrich, A. et al., 1986, *EMBO J* 5: 2503-2512; Shier, P. & Watt, V. M., 1989, *J. Biol. Chem.* 264: 14605-14608) and the identification of some of their functional domains (for reviews see De Meyts, P. 1994, *Diabetologia* 37: 135-148; Lee, J. & Pilch, P. F. 1994 *Amer. J. Physiol.* 266: C319-C334.; Schaffer, L. 1994, *Eur. J. Biochem.* 221: 1127-1132). IGF-1R, IR and IRR are members of the tyrosine kinase receptor superfamily and are closely related to the epidermal growth factor receptor (EGFR) subfamily, with which they share significant sequence identity in the extracellular region as well as in the cytoplasmic kinase domains (Ullrich, A. et al., 1984 *Nature* 309: 418-425; Ward, C. W. et al., 1995 *Proteins: Structure Function & Genetics* 22: 141-153). Both the insulin and EGF receptor subfamilies have a similar arrangement of two homologous domains (L1 and L2) separated by a cys-rich region of approximately 160 amino acids containing 22-24 cys residues (Bajaj, M., et al., 1987 *Biochim. Biophys. Acta* 916: 220-226; Ward, C. W. et al., 1995 *Proteins: Structure Function & Genetics* 22: 141-153). The C-terminal portion of the IGF-1R ectodomain (residues 463 to 906) is comprised of four domains: a connecting domain, two fibronectin type 3 (Fn3) repeats, and an insert domain (O'Bryan, J. P., et al., 1991 *Mol Cell Biol* 11: 5016-5031); the C-terminal portion of the EGFR ectodomain (residues 477-621) consists solely of a second cys-rich region containing 20 cys residues (Ullrich, A. et al., 1984, *Nature* 309: 418-425).

Little is known about the secondary, tertiary and quaternary structure of the ectodomains of these receptor subfamilies. Unlike the members of the EGFR subfamily which are transmembrane monomers which dimerise on binding ligand, the IR subfamily members are homodimers, held together by disulphide bonds. The extracellular region of the IR/IGF-1R/IRR monomers contains an α -chain (~ 703 to 735 amino acid residues) and 192-196 residues of the β -chain. There is a ~23 residue transmembrane segment, followed by the cytoplasmic portion (354 to 408 amino acids) which contains the catalytic tyrosine kinase domain flanked by juxtamembrane and C-tail regulatory regions and is responsible for mediating all receptor-specific functions (White, M. F. & Kahn, C. R. 1994 *J. Biol. Chem.* 269: 1-4). Chemical analyses of the receptor suggest that the α -chains are linked to the β -chains

via a single disulphide bond with the IR dimer being formed by at least two α - α disulphide linkages (Finn, F. M., et al., 1990, Proc. Natl. Acad. Sci. 87: 419-423; Chiacchia, K. B., 1991, Biochem. Biophys. Res. Commun. 176, 1178-1182; Schaffer, L. & Ljungqvist, L., 1992, Biochem. Biophys. Res. Comm. 189: 5 650-653; Sparrow, L. G., et al., 1997, J. Biol. Chem. 272: 29460-29467).

Although the 3D structures of the ligands EGF, TGF-alpha (Hommel, U., et al., 1992, J. Mol. Biol. 227:271-282), insulin (Dodson, E. J., et al., 1983, Biopolymers 22:281-291), IGF-1 (Sato, A., et al., 1993, Int J Peptide Protein Res 41:433-440) and IGF-2 (Torres, A. M., et al., 1995, J. Mol. Biol. 248:385-10 401) are known and numerous analytical and functional studies of ligand binding to EGFR (Soler, C. & Carpenter, G., 1994 In Nicola (ed) Guidebook to Cytokines and Their receptors", Oxford Univ. Press, Oxford, pp194-197), IGF-1R and IR (see De Meyts, P., 1994 Diabetologia, 37:135-148) have been 15 carried out, the mechanisms of ligand binding and subsequent transmembrane signalling have not been resolved.

Ligand-induced, receptor-mediated phosphorylation is the signalling mechanism by which most cytokines, polypeptide hormones and membrane-anchored ligands exert their biological effects. The primary kinase may be part of the intracellular portion of the transmembrane receptor protein as in 20 the tyrosine kinase receptors (for review see Yarden, Y., et al., 1988, Ann. Rev. Biochem. 57:443-478) or the Ser/Thr kinase receptors (Alevizopoulos, A. & Mermod, N., 1997, BioEssays, 19:581-591) or be non-covalently associated 25 with the cytoplasmic tail of the transmembrane protein(s) making up the receptor complex as in the case of the haemopoietic growth factor receptors (Stahl, N., et al., 1995, Science 267:1349-1353). The end result is the same, ligand binding leads to receptor dimerization or oligomerization or a 30 conformational change in pre-existing receptor dimers or oligomers resulting in activation by transphosphorylation, of the covalently attached or non-covalently associated protein kinase domains (Hunter, T., 1995, Cell, 80:225-236).

Many oncogenes have been shown to be homologous to growth factors, growth factor receptors or molecules in the signal transduction pathways (Baserga, R., 1994 Cell, 79:927-930; Hunter, T., 1997 Cell, 88:333-346). One of the best examples is v-Erb (related to the EGFR). Since 35 overexpression of a number of growth factor receptors results in ligand-dependent transformation an alternate strategy for oncogenes is to regulate

the expression of growth factor receptors or their ligands or to directly bind to the receptors to stimulate the same effect (Baserga, R., 1994 Cell, 79:927-930). Examples are v-Src, which activates IGF-1R intracellularly; c-Myb, which transforms cells by enhancing the expression of IGF1R and SV40 T antigen which interacts with the IGF-1R and enhances the secretion of IGF-1 (see Baserga, R., 1994 Cell, 79:927-930 for review). Cells in which the IGF-1 receptor has been knocked out cannot be transformed by SV40 T antigen. If oncogenes activate growth factors and their receptors then tumour suppressor genes should have the opposite effect. One good example of this is WT1, the Wilm's tumour suppressor gene which suppresses the expression of IGF-1R (Drummond, J. A., et al., 1992, Science, 257:275-277). Cells that are driven to proliferate by oncogenes undergo massive apoptosis when growth factor receptors are ablated since unlike normal cells, they appear unable to withdraw from the cell-cycle and enter into the G0 phase (Baserga, R., 1994 Cell, 79:927-930).

The insulin-like growth factor-1 receptor (IGF-1R) is one of several growth-factor receptors that regulate the proliferation of mammalian cells. However, its ubiquitousness and certain unique aspects of its function make IGF-1R an ideal target for therapeutic interventions against abnormal growth, with very little effect on normal cells (see Baserga, R., 1996 TIBTECH, 14:150-152). The receptor is activated by IGF1, IGF2 and insulin and plays a major role in cellular proliferation in at least three ways: it is essential for optimal growth of cells in vitro and in vivo; several cell types require IGF-1R to maintain the transformed state and activated IGF-1R has a protective effect against apoptotic cell death (Baserga, R., 1996 TIBTECH, 14:150-152). These properties alone make it an ideal target for therapeutic interventions. Transgenic experiments have shown that IGF-1R is not an absolute requirement for cell growth but is essential for the establishment of the transformed state (Baserga, R., 1994 Cell, 79: 927-930). In several cases (human glioblastoma, human melanoma; human breast carcinoma; human lung carcinoma; human ovarian carcinoma; human rhabdomyosarcoma; mouse melanoma, mouse leukaemia; rat glioblastoma; rat rhabdomyosarcoma; hamster mesothelioma) the transformed phenotype can be reversed by decreasing the expression of IGF-1R using antisense to IGF-1R (Baserga, R., 1996 TIBTECH 14:150-152); or interfering with its function by antibodies to IGF-1R (human breast carcinoma; human rhabdomyosarcoma)

or by dominant negatives of IGF-1R (rat glioblastoma; Baserga, R., 1996 TIBTECH 14:150-152).

Three effects are observed when the function of IGF-1R is impaired:

5 tumour cells undergo massive apoptosis which results in inhibition of tumourogenesis; surviving tumour cells are eliminated by a specific immune response; and such a host response can cause a regression of an established wild-type tumour (Resnicoff, M., et al., 1995, Cancer Res. 54:2218-2222). These effects, plus the fact that interference of IGF-1R function has a limited effect on normal cells (partial inhibition of growth without apoptosis) makes

10 IGF-1R a unique target for therapeutic interventions (Baserga, R., 1996 TIBTECH 14:150-152). In addition IGF-1R is downstream of many other growth factor receptors, which makes it an even more generalised target. The implication of these findings is that if you can decrease the number of IGF-1 receptors on cells or antagonise their function then tumours cease to grow

15 and can be removed immunologically. These studies establish that IGF-1R antagonists will be extremely important therapeutically.

Many cancer cells have constitutively active EGFR (Sandgreen, E. P., et al., 1990, Cell, 61:1121-135; Karnes, W. E. J., et al., 1992, Gastroenterology, 102:474-485) or other EGFR family members (Hines, N. E., 1993, Semin. 20 Cancer Biol. 4:19-26). Elevated levels of activated EGFR occur in bladder, breast, lung and brain tumours (Harris, A. L., et al., 1989, In Furth & Greaves (eds) The Molecular Diagnostics of human cancer. Cold Spring Harbor Lab. Press, CSH, NY, pp353-357). Antibodies to EGFR can inhibit ligand activation of EGFR (Sato, J. D., et al., 1983 Mol. Biol. Med. 1:511-529) and the growth of 25 many epithelial cell lines (Aboud-Pirak E., et al., 1988, J. Natl Cancer Inst. 85:1327-1331). Patients receiving repeated doses of a humanised chimeric anti-EGFR antibody showed signs of disease stabilization. The large doses required and the cost of production of humanised Mab is likely to limit the application of this type of therapy. These findings indicate that the 30 development of EGF antagonists will be attractive anticancer agents.

Summary of the Invention

The present inventors have now obtained 3D structural information concerning the insulin-like growth factor receptor (IGF-1R) and the insulin receptor (IR) which provides a rational basis for the development of 35 antagonists and agonists of the polypeptide ligands for specific therapeutic applications. This information can be used to predict the structure of related

members of the insulin receptor family and epidermal growth factor family and to develop agonists and antagonists of their respective polypeptide ligands.

Accordingly, in a first aspect the present invention provides a method 5 of screening for, or designing, an agonist of a ligand of an insulin receptor family member or EGF receptor family member which method includes

- (i) selecting or designing a substance which possesses stereochemical complementarity to a receptor site, wherein the receptor site is characterised by
 - (a) amino acids 1-462 of IGF-1R positioned at atomic coordinates substantially as shown in Figure 1 or a subset thereof; or
 - (b) amino acids derived from an insulin receptor family member or EGF receptor family member which form an equivalent structure to the amino acids defined in paragraph (a); and
- 10 (ii) testing the substance for the ability to act as an agonist of the ligand of an insulin receptor family member or EGF receptor family member.

In a second aspect the present invention provides a method of screening for, or designing, an antagonist of a ligand of an insulin receptor family member or EGF receptor family member which method includes

- 20 (i) selecting or designing a substance which possesses stereochemical complementarity to a receptor site, wherein the receptor site is characterised by
 - (a) amino acids 1-462 of IGF-1R positioned at atomic coordinates substantially as shown in Figure 1 or a subset thereof; or
 - (b) amino acids derived from an insulin receptor family member or an EGF receptor family member which form an equivalent structure to the amino acids defined in paragraph (a); and
- 25 (ii) testing the substance for the ability to act as an antagonist of the ligand of an insulin receptor family member or EGF receptor family member.

30 The phrase "insulin receptor family" encompasses, for example, IGF-1R, IR and IRR. The phrase "EGF receptor family" encompasses for example, EGFR, ErbB2, ErbB3 and ErbB4. In general, insulin receptor family members and EGF receptor family members show similar domain arrangements and share significant sequence identity (preferably at least 20% identity between 35 the families and at least 40% identity within each family).

The receptor site defined in the first and second aspects of the present invention comprises the L1-cysteine rich-L2 region (residues 1-462) of the ectodomain of IGF-1R. ~~At the centre of this structure is a groove, bounded by all three domains, of sufficient size to accommodate a ligand molecule.~~ By "stereochemical complementarity" we mean that the biologically active substance or a portion thereof correlates, in the manner of the classic "lock-and-key" visualisation of ligand-receptor interaction, with the groove in the receptor site. Preferably, the stereochemical complementarity is such that the compound has a K_I for the receptor site of less than $10^{-6}M$. More preferably, the K_I value is less than $10^{-8}M$ and more preferably less than $10^{-9}M$.

In preferred embodiments of the first and second aspects of the present invention, the method further involves selecting or designing a substance which has portions that match residues positioned on the surface of the receptor site which faces the groove. By "match" we mean that the identified portions interact with the surface residues, for example, via hydrogen bonding or by enthalpy-reducing Van der Waals interactions which promote desolvation of the biologically active substance within the site, in such a way that retention of the biologically active substance within the groove is favoured energetically.

In a preferred embodiment of the first aspect of the present invention, the method includes screening for, or designing, a substance which possesses a stereochemistry and/or geometry which allows it to interact with both the L1 and L2 domains of the receptor site. As described above, the insulin receptor exists as homodimers held together by disulphide bonds. Electron microscopy studies described herein indicate that the insulin receptor monomers dimerise in nature in such a manner that the grooves of each monomer may face each other. Accordingly, the method of the first aspect of the present invention may involve screening for, or designing, a biologically active substance which interacts with the L1 domain of one monomer and the L2 domain of the other monomer.

In a third aspect the present invention provides a method of selecting or designing an agonist of a ligand of an insulin receptor family member or EGF receptor family member which method includes

35 (i) selecting or designing a substance which interacts with

(a) a fragment of IGF-1R characterised by amino acids 1-462 positioned at atomic coordinates substantially as shown in Figure 1 or a subset thereof; or

(b) a fragment derived from an insulin family receptor member or EGF receptor family member which is equivalent to the fragment defined in paragraph (a);

5 wherein the interaction of the substance with the fragment alters the position of at least one of the L1, L2 or cys-rich domains of the fragment relative to the position of at least one of the other domains; and

10 (ii) testing the substance for the ability to act as an agonist of the ligand of an insulin receptor family member or EGF receptor family member.

In a preferred embodiment of the third aspect of the present invention the substance interacts with the fragment in the region of the L1 domain-cys rich domain interface, causing the L1 and cys-rich domains to

15 move away from each other. In a further preferred embodiment the substance interacts with the hinge region between the L2 domain and the cys-rich domain causing an alteration in the positions of the domains relative to each other. In a further preferred embodiment the substance interacts with the beta sheet of the L1 domain causing an alteration in the position of

20 the L1 domain relative to the position of the cys-rich domain or L2 domain.

In a fourth aspect the present invention provides an agonist of a ligand of an insulin receptor family member or EGF receptor family member obtained by a method according to the first or third aspects of the present invention.

25 In a fifth aspect the present invention provides an antagonist of a ligand of an insulin receptor family member or EGF receptor family member obtained by a method according to the second aspect of the present invention.

The agonists or antagonists of the fourth and fifth aspects of the

30 present invention may be mutant insulin family member or EGF family member ligands where at least one mutation occurs in the region of the ligand which interacts with residues on the surface of the receptor site facing toward the groove. For example, the IGF-1 ligand has a predominance of basic residues in the C region which may interact with the acidic patch of the

35 cys-rich region near L1. An acidic patch on the other side of the ligand may interact with the patch of basic residues (residues 307-310) on the N-terminal

end of L2. Accordingly, mutants of IGF-1 which exhibit altered activity may be generated by introducing modifications in the C region of IGF-1 or residues in the acidic patch on the other side of the hormone.

In a sixth aspect the present invention provides a substance which

- 5 possesses stereochemical complementarity to a receptor site, wherein the receptor site is characterised by
 - (a) amino acids 1-462 of IGF-1R positioned at atomic coordinates substantially as shown in Figure 1 or a subset thereof; or
 - (b) amino acids derived from an insulin receptor family
- 10 member or an EGF receptor family member which form an equivalent structure to the amino acids defined in paragraph (a); with the proviso that the substance is not a naturally occurring ligand of an insulin receptor family member or EGF receptor family member or a mutant thereof.
- 15 By "mutant" we mean a ligand which has been modified by one or more point mutations, insertions of amino acids or deletions of amino acids.

In a preferred embodiment of the sixth aspect of the present invention, the stereochemical complementarity is such that the compound has a K_I for the receptor site of less than $10^{-6}M$. More preferably, the K_I value is less than $10^{-8}M$ and more preferably less than $10^{-9}M$.

In a seventh aspect the present invention provides a pharmaceutical composition for treatment of a disease associated with reduced activity of a ligand of an insulin receptor family member or EGF receptor family member which includes an agonist obtained by a method according to the first or third aspects of the present invention and a pharmaceutically acceptable carrier or diluent.

In an eighth aspect the present invention provides a pharmaceutical composition for treatment of a disease associated with activity of a ligand of an insulin receptor family member or EGF receptor family member which includes an antagonist obtained by a method according to the second aspect of the present invention and a pharmaceutically acceptable carrier or diluent.

In a ninth aspect the present invention provides a method of preventing or treating a disease associated with reduced activity of a ligand of an insulin receptor family member or EGF receptor family member which includes administering to a subject in need thereof an agonist

obtained by a method according to the first or third aspects of the present invention.

Diseases associated with reduced activity of a ligand of an insulin receptor family member or EGF receptor family member include diabetes,
5 osteoporosis, nerve degeneration and a range of catabolic states.

In a tenth aspect the present invention provides a method of preventing or treating a disease associated with activity of a ligand of an insulin receptor family member or EGF receptor family member which method includes administering to a subject in need thereof an antagonist
10 obtained by a method according to the second aspect of the present invention.

Diseases associated with activity of a ligand of an insulin receptor family member or EGF receptor family member include cancer, leukaemia and many types of tumour states including but not restricted to breast cancer,
15 brain tumours, ovarian cancer, pancreatic tumours, lung cancer, melanoma, rhabdomyosarcoma, mesothelioma and glioblastoma.

Brief Description of the Drawings

20 **Figure 1.** IGF-1R residues 1-462, in terms of atomic coordinates refined to a resolution of 2.6 Å (average accuracy \approx 0.3Å). The coordinates are in relation to a Cartesian system of orthogonal axes.

25 **Figure 2.** Depiction of the residues lining the groove of the IGF-1R receptor fragment 1-462.

30 **Figure 3.** Gel filtration chromatography of affinity-purified IGF-1R/462 protein. The protein was purified on a Superdex S200 column (Pharmacia) fitted to a BioLogic L.C. system (Biorad), equilibrated and eluted at 0.8 ml/min with 40 mM Tris/150 mM NaCl/0.02% NaN3 adjusted to pH 8.0. (a) Protein eluting in peak 1 contained aggregated IGF-1R/462 protein, peak 2 contained monomeric protein and peak 3 contained the c-myc undecapeptide used for elution from the Mab 9E10 immunoaffinity column. (b) Non-reduced SDS-PAGE of fraction 2 from IGF-1R/462 obtained following 35 Superdex S200 (Fig.1a). Standard proteins are indicated.

Figure 4. Ion exchange chromatography of affinity-purified, truncated IGF-1R ectodomain. A mixture of gradient and isocratic elution chromatography was performed on a Resource Q column (Pharmacia) fitted to a BioLogic System (Biorad), using 20 mM Tris/pH 8.0 as buffer A and the same buffer

5 containing 1M NaCl as buffer B. Protein solution in TBSA was diluted at least 1:2 with water and loaded onto the column at 2 ml/min. Elution was monitored by absorbance (280 nm) and conductivity (mS/cm). Target protein (peak 2) eluted isocratically with 20 mM Tris/0.14 M NaCl pH 8.0. Inset: Isoelectric focusing gel (pH 3 - 7; Novex Australia Pty Ltd) of fraction 2. The 10 pI was estimated at 5.1 from standard proteins (not shown).

Figure 5. Gel filtration chromatography of affinity purified IR/485 protein. Affinity-purified material at 1 mg/ml produced a dominant peak at apparent mass ~ 140 kDa (interpreted as a dimer) (a); whereas affinity-purified

15 material at 0.02 mg/ml produced a dominant peak at apparent mass ~ 85kDa (interpreted as a monomer) (b).

Figure 6. (a) SDS-PAGE of IR/485 following gel filtration chromatography.

The protein migrated as a single broad band of apparent molecular mass ~ 78 20 kDa (reduced - lane A) or ~ 68kDa (non-reduced - lane B). (b) Isoelectric focussing of the IR/485 protein. The IR/485 fragment reacted positively in an ELISA with Mab 83-7, gave a single sequence corresponding to the N-terminal 10 residues of IR, showing several isoforms on isoelectric focussing from pI6.0-6.8. The fragment was further purified by ion-exchange 25 chromatography on Uno Q (BioRad, USA), using stepwise isocratic elution with incremental changes in salt concentrations (see Figure 7). Fractions A and D were each enriched in a component isoform from the ladder of isoforms present in the unfractionated mixture. Both these fractions produced crystals, whereas no crystals were obtained from fractions B and C.

30

Figure 7. Purification of the IR/485 protein by ion-exchange chromatography on Uno Q (BioRad, USA), using stepwise isocratic elution with incremental changes in salt concentrations.

35 **Figure 8.** Polypeptide fold for residues 1-462 of IGF-1R. The L1 domain is at the top, viewed from the N-terminal end and L2 is at the bottom. The space

at the centre is of sufficient size to accommodate IGF-1. Helices are indicated by curled ribbon and β -strands by arrows. Cysteine side chains are drawn as ball-and-stick with lines showing disulfide bonds. The arrow points in the direction of view for Figure 9.

5

Figure 9. Amino acid sequences of IGF-1R and related proteins. a, L1 and L2 domains of human IGF-1R and IR are shown based on a sequence alignment for the two proteins and a structural alignment for the L1 and L2 domains. Positions showing conservation physico-chemical properties of amino acids 10 are boxed, residues used in the structural alignment are shaded yellow and residues which form the Trp 176 pocket are in red. Secondary structure elements for L1 (above the sequences) and L2 (below) are indicated as cylinders for helices and arrows for β -strands. Strands are colour coded according to the β -sheet to which they belong. Disulfide bonds are also 15 indicated. b, Cys-rich domains of human IGF-1R, IR and EGFR (domains 2 and 4) are aligned based on sequence and structural considerations. Secondary structural elements and disulfide bonds are indicated above the sequences. The dashed bond is only present in IR. Different types of 20 disulfide bonded modules are labelled below the sequences as open, filled or broken lines. Boxed residues show conservation of physico-chemical properties and structurally conserved residues for modules 4-7 are shaded yellow. Residues from EGFR which do not conform to the pattern are shaded grey and the conserved Trp 176 and the semi-conserved Gln 182 are shaded red. This figure was prepared using ALSCRIPT (Barton, G. J., 1993, Prot. 25 Engineering, 6:37-40).

Figure 10. Stereo view of a superposition of the L1 (white) and L2 (black) domains. Residues numbers above are for L1 and below for L2. The side chain of Trp 176 which protrudes into the core of L1 is drawn as ball-and-stick. 30

Figure 11. Schematic diagram showing the association of three β -finger motifs. β -strands are drawn as arrows and disulfide bonds as zigzags.

35 **Figure 12.** GRASP [Nicolls, A. et al., 1993, Biophys. J. 64, 166-170] surface diagram of the L1 domain of IGF-1R shown in a similar view to Figure 8. The

N-terminal β -strand is at the top. The mutation L87A [Nakae, J. et al., 1995, J. Biol. Chem. 270, 22017-22022] and four regions (residues 12-15, 34-44, 64-67 and 89-91 of IR) shown to be important in insulin binding to IR [Williams, P. F. et al., 1995, J. Biol. Chem. 270, 3012-3016] correspond to a patch of

5 residues on the large β -sheet. Residues numbers for IR/IGF-1R are given and residues are coloured according to the magnitude of $K_d(\text{mutant})/K_d(\text{wild type})$, red, > 40 ; orange, 10-40; yellow, 2.5-10; green, < 2.5 ; non-secreting, white; untested, blue. All mutants on the opposite face of the domain do not affect insulin affinity.

10

Figure 13: Sequence Alignment of hIGF-1R, hIR and hIRR Ectodomains. Derived by use of the PileUp program in the software package of the Genetics Computer Group, 575 Science Drive, Madison, Wisconsin, USA. For assignment of homologous 3D structures see Figure 9.

15

Figure 14: Sequence Alignment of EGFR, ErbB2, ErbB3 and ErbB4 Ectodomains. Derived by use of the PileUp program in the software package of the Genetics Computer Group, 575 Science Drive, Madison, Wisconsin, USA. For alignment on the IGF-1R fragment and assignment of homologous 20 3D structures, see Figure 9.

25

Figure 15 Sequence Alignment and Classification of the Disulphide-bonded Modules in the Cys-rich domains of IGF-1R, IR, IRR, EGFR, ErbB2, ErbB3 and ErbB4.

30

Figure 16. Gel filtration chromatography of insulin receptor ectodomain and MFab complexes. hIR -11 ectodomain dimer (5 - 20 mg) was complexed with MFab derivatives (15-25 mg each) of the anti-hIR antibodies 18-44, 83-7 and 83-14 (Soos et al., 1986). Elution profiles were generated from samples loaded onto a Superdex S200 column (Pharmacia), connected to a BioLogic chromatography system (Biorad) and monitored at 280 nm. The column was eluted at 0.8 ml/min with 40 mM Tris/150 mM sodium chloride/0.02% sodium azide buffer adjusted to pH 8.0: Profile 0, hIR -11ectodomain, Profile 1, ectodomain mixed with MFab 18-44; Profile 2 , ectodomain mixed with 35 MFab18-44 and MFab 83-14; Profile 3, ectodomain mixed with MFab 18-44, MFab 83-14 and MFab 83-7. The apparent mass of each complex was

determined from a plot of the following standard proteins: thyroglobulin (660 kDa), ferritin (440 kDa), bovine gammaglobulin (158 kDa), bovine serum albumin (67 kDa), chicken ovalbumin (44 kDa) and equine myoglobin (17 kDa).

5

Figure 17. Micrographs of hIR and hIGF-1R ectodomains.(a) Undecorated hIR ectodomain dimer stained with methylamine tungstate showing parallel bars. (b) Undecorated hIR ectodomain dimer stained with uranyl formate, showing well-spaced parallel bars corresponding to the cartoon below.

10 (c) Undecorated hIGF-1R ectodomain dimer stained with uranyl formate. Magnification bars for (a), (b) and (c) 50nm.

Figure 18. Micrographs of hIR and hIGF-1R ectodomains. (a) Thinly stained region of undecorated hIR ectodomain dimers in uranyl formate, showing U-shaped particles (circled) as well as parallel bars as in the cartoon below. (b) Undecorated hIGF-1R ectodomain dimer under similar staining conditions. Magnification bars 50 nm.

Figure 19. hIR ectodomain dimer complexed with MFab 83-7 and stained with KPT. Three projections can be recognised: circled particles have the Fab arms displaced either clockwise as in the cartoon below left, or anticlockwise as in the cartoon below middle; arrowed particles have the Fab arms in a central position, cartoon below right. Magnification bar 50 nm.

25 **Figure 20.** hIR ectodomain dimer complexed with MFab 83-7 and stained with uranyl formate showing the parallel bar structure in particles having the Fab arms displaced (circled). Magnification bar 50 nm.

Figure 21. (a) hIR ectodomain dimer complexed with MFab 83-14 stained with potassium phosphotungstate, showing Fab arms attached near the bottom of U-shaped particles (circled). The corresponding cartoon is shown below left. (b) hIR ectodomain dimer complexed with MFab 83-14 stained with uranyl acetate, showing both the view described above (circled) and the parallel-bar view with diagonally projecting Fab arms (arrowed), as in the cartoon below right. Magnification bars 50 nm.

Figure 22 . Double complex of hIR ectodomain dimer with MFabs 83-7 and 18-44 showing particles of complex shape (circled) with four Fab arms attached, consistent with the cartoon below. Magnification bar 50 nm.

5 **Figure 23.** Images of hIR ectodomain dimer co-complexed with MFabs 83-7, 83-14 and 18-44 showing examples of complex particles (circled) where it is possible to identify that there are more than four MFabs bound to the dimeric central region. Magnification bar 50 nm.

10 **Figure 24.** Schematic illustrating the proposed model of the hIR ectodomain dimer. The dimensions of the molecular envelope are as shown in the diagram, as is the position of the two-fold axis.

Detailed Description of the Invention

15 We describe herein the expression, purification, and crystallization of a recombinant IGF-1R fragment (residues 1-462) containing the L1-cysteine-rich-L2 region of the ectodomain. The selected truncation position is just downstream of the exon 6/exon 7 junction (Abbott, A. M., et al., 1992, *J Biol Chem.*, 267:10759-10763) and occurs at a position where the sequences of the

20 IR and EGFR families diverge markedly (Ward, C. W., et al., 1995, *Proteins: Struct., Funct., Genet.* 22:141-153; Lax, I., et al., 1988, *Molec. Cellul. Biol.* 8:1970-1978) suggesting it represents a domain boundary. To limit the effects of glycosylation, the IGF-1R fragment was expressed in Lec8 cells, a glycosylation mutant of Chinese hamster ovary (CHO) cells, whose defined

25 glycosylation defect produces N-linked oligosaccharides truncated at N-acetyl glucosamine residues distal to mannose residues (Stanley, P. 1989, *Molec. Cellul. Biol.* 9:377-383). Such an approach has facilitated glycoprotein crystallization (Davis, S. J., et al., 1993, *Protein Eng.* 6:229-232; Liu, J., et al., 1996, *J. Biol. Chem.* 271:33639-33646).

30 The IGF-1R construct described herein included a c-myc peptide tag (Hoogenboom, H. R., et al., 1991, *Nucleic Acids Res.* 19:4133-4137) that is recognised by the Mab 9E10 (Evan, G. I., et al., 1985, *Mol. Cell. Biol.* 5:3610-3616) enabling the expressed product to be purified by peptide elution from an antibody affinity column followed by gel filtration over Superdex S200.

35 The purified proteins crystallized under a sparse matrix screen (Jancarik, J. & Kim, S.-H., 1991, *J. Appl. Cryst.* 24:409-411) but the crystals were of variable

quality, with the best diffracting to 3.0-3.5 Å. Isocratic gradient elution by anion-exchange chromatography yielded protein that was less heterogenous and gave crystals of sufficient quality to determine the structure of the first three domains of the human IGF-1R.

5 The IGF-1R fragment consisted of residues 1-462 of IGF-1R linked via an enterokinase-cleavable pentapeptide sequence to an eleven residue c-myc peptide tag at the C-terminal end. The fragment was expressed in Lec8 cells by continuous media perfusion in a bioreactor using porous carrier disks. It was secreted into the culture medium and purified by peptide elution from
10 an anti-c-myc antibody column followed by Superdex S200 gel filtration. The receptor fragment bound two anti-IGF-1R monoclonal antibodies, 24-31 and 24-60, which recognize conformational epitopes, but could not be shown to bind IGF-1 or IGF-2. Crystals of variable quality were grown as rhombic prisms in 1.7 M ammonium sulfate at pH 7.5 with the best diffracting to 3.0-
15 3.5 Å. Further purification by isocratic elution on an anion-exchange column gave protein which produced better quality crystals, diffracting to 2.6 Å, that were suitable for X-ray structure determination.

20 The structure of this fragment (IGF-1R residues 1-462; L1-cys rich-L2domains) has been determined to 2.6 Å resolution by X-ray diffraction. The L domains each adopt a compact shape consisting of a single stranded right-handed β-helix. The cys-rich region is composed of eight disulphide-bonded modules, seven of which form a rod-shaped domain with modules associated in a novel manner. At the centre of this reasonably extended structure is a space, bounded by all three domains, and of sufficient size to accommodate a
25 ligand molecule. Functional studies on IGF-1R and other members of the insulin receptor family show that the regions primarily responsible for hormone-binding map to this central site. Thus this structure gives a first view of how members of the insulin receptor family might interact with their ligands.

30 Another group has reported the crystallization of a related receptor, the EGFR in a complex with its ligand EGF (Weber, W., et al., 1994, J Chromat. 679:181-189). However difficulties were encountered with these crystals which diffracted to only 6 Å, insufficient for the determination of an atomic resolution structure of this complex (Weber, W., et al., 1994, J Chromat 679:181-189) or the generation of accurate models of structurally related receptor domains such as IGF-1R and IR by homology modelling.

The present inventors have applied the same process to the IR and generated a fragment (residues 1-485) that covers the first three domains of the IR. This fragment has been expressed in transformed Lec8 cells, purified, and crystallized by similar methodologies to yield crystals suitable for X-ray

5 diffraction.

The present inventors have therefore developed 3D structural information about cytokine receptors to enable a more accurate understanding of how the binding of ligand leads to signal transduction. Such information provides a rational basis for the development of antagonists 10 or agonists for specific therapeutic applications, something that heretofore could not have been predicted *de novo* from available sequence data.

The precise mechanisms underlying the binding of agonists and antagonists to the IGF-1 receptor site are not fully clarified. However, the binding of the agonists or antagonists to the receptor site, preferably with an 15 affinity in the order of 10^{-8} M or higher, is understood to arise from enhanced stereochemical complementarity, relative to naturally occurring IGF-1 ligands.

Such stereochemical complementarity, pursuant to the present invention, is characteristic of a molecule that matches intra-site surface 20 residues lining the groove of the receptor site as enumerated by the coordinates set out in Figure 1. The residues lining the groove are depicted in Figure 2. Substances which are complementary to the shape of the receptor site characterised by amino acids positioned at atomic coordinates set out in Figure 1 may be able to bind to the receptor site and, when the binding is 25 sufficiently strong, substantially prohibit binding of the naturally occurring ligands to the site.

It will be appreciated that it is not necessary that the complementarity between agonists or antagonists and the receptor site extend over all residues lining the groove in order to inhibit binding of the 30 natural ligand. Accordingly, agonists or antagonists which bind to a portion of the residues lining the groove are encompassed by the present invention.

In general, the design of a molecule possessing stereochemical complementarity can be accomplished by means of techniques that optimize, either chemically or geometrically, the "fit" between a molecule and a target 35 receptor. Known techniques of this sort are reviewed by Sheridan and Venkataraghavan, *Acc. Chem. Res.* 1987 20 322; Goodford, *J. Med. Chem.*

1984 27 557; Beddell, Chem. Soc. Reviews 1985, 279; Hol, Angew. Chem. 1986 25 767 and Verlinde C.L.M.J & Hol, W.G.J. Structure 1994, 2, 577, the respective contents of which are hereby incorporated by reference. See also Blundell et al., Nature 1987 326 347 (drug development based on information 5 regarding receptor structure).

Thus, there are two preferred approaches to designing a molecule, according to the present invention, that complements the shape of IGF-1R or a related receptor molecule. By the geometric approach, the number of internal degrees of freedom (and the corresponding local minima in the 10 molecular conformation space) is reduced by considering only the geometric (hard-sphere) interactions of two rigid bodies, where one body (the active site) contains "pockets" or "grooves" that form binding sites for the second body (the complementing molecule, as ligand). The second preferred approach entails an assessment of the interaction of respective chemical 15 groups ("probes") with the active site at sample positions within and around the site, resulting in an array of energy values from which three-dimensional contour surfaces at selected energy levels can be generated.

The geometric approach is illustrated by Kuntz et al., J. Mol. Biol. 1982 161 269, the contents of which are hereby incorporated by reference, 20 whose algorithm for ligand design is implemented in a commercial software package distributed by the Regents of the University of California and further described in a document, provided by the distributor, which is entitled "Overview of the DOCK Package, Version 1.0.", the contents of which are hereby incorporated by reference. Pursuant to the Kuntz algorithm, the 25 shape of the cavity represented by the IGF-R1 site is defined as a series of overlapping spheres of different radii. One or more extant data bases of crystallographic data, such as the Cambridge Structural Database System maintained by Cambridge University (University Chemical Laboratory, Lensfield Road, Cambridge CB2 1EW, U.K.) and the Protein Data Bank 30 maintained by Brookhaven National Laboratory (Chemistry Dept. Upton, NY 11973, U.S.A.), is then searched for molecules which approximate the shape thus defined.

Molecules identified in this way, on the basis of geometric 35 parameters, can then be modified to satisfy criteria associated with chemical complementarity, such as hydrogen bonding, ionic interactions and Van der Waals interactions.

The chemical-probe approach to ligand design is described, for example, by Goodford, *J. Med. Chem.* 1985 28 849, the contents of which are hereby incorporated by reference, and is implemented in several commercial software packages, such as GRID (product of Molecular Discovery Ltd., West

5 Way House, Elms Parade, Oxford OX2 9LL, U.K.). pursuant to this approach, the chemical prerequisites for a site-complementing molecule are identified at the outset, by probing the active site (as represented via the atomic coordinates shown in Fig. 1) with different chemical probes, e.g., water, a methyl group, an amine nitrogen, a carboxyl oxygen, and a hydroxyl.

10 Favored sites for interaction between the active site and each probe are thus determined, and from the resulting three-dimensional pattern of such sites a putative complementary molecule can be generated.

The chemical-probe approach is especially useful in defining variants of a molecule known to bind the target receptor. Accordingly, 15 crystallographic analysis of IGF-1 bound to the receptor site may provide useful information regarding the interaction between the archetype ligand and the active site of interest.

In summary, the general principles of receptor-based drug design can be applied by persons skilled in the art, using the crystallographic results 20 presented above, to produce agonists or antagonists of IGF-1R having sufficient stereochemical complementarity to exhibit high affinity binding to the receptor site.

The present invention is further described below with reference to the following, non-limiting examples.

25

EXAMPLE 1

Expression, Purification and Crystallization of the IGF-1R Fragment.

Several factors hamper macromolecular crystallization including sample selection, purity, stability, solubility (McPherson, A., et al., 1995, 30 Structure 3:759-768); Gilliland, G. L., & Ladner, J. E., 1996, *Curr. Opin. Struct. Biol.* 6:595-603), and the nature and extent of glycosylation (Davis, S. J., et al., 1993, *Protein Eng.* 6:229-232). Initial attempts to obtain structural data from soluble IGF-1R ectodomain (residues 1-906) protein, expressed in Lec8 cells (Stanley, P. 1989, *Molec. Cellul. Biol.* 9:377-383) and purified by 35 affinity chromatography, produced large, well-formed crystals (1.0 mm x 0.2 mm x 0.2 mm) which gave no discernable X-ray diffraction pattern

(unpublished data). Similar difficulties have been encountered with crystals of the structurally related epidermal growth factor receptor (EGFR) ectodomain which diffracted to only 6 Å, insufficient for the determination of an atomic resolution structure (Weber, W. et al., 1994, *J Chromat* 679:181-189).

5 This prompted us to search for a fragment of IGF-1R that was more amenable to X-ray crystallographic studies.

The fragment expressed (residues 1-462) comprises the L1-cysteine-rich-L2 region of the ectodomain. The selected truncation position at Val462 is four residues downstream of the exon 6/exon 7 junction (Abbott, A. M., et 10 al., 1992, *J Biol Chem* 267:10759-10763) and occurs at a position where the sequences of the IR and the structurally related EGFR families diverge markedly (Lax, I., et al., 1988, *Molec Cell Biol*. 8:1970-1978; Ward, C. W., et al., 1995, *Proteins: Struct., Funct., Genet.* 22:141-153), suggesting it represents a domain boundary. The expression strategy included use of the 15 pEE14 vector (Bebbington, C. R. & Hentschel, C. C. G., 1987, In: Glover, D. M., ed. *DNA Cloning*. Academic Press, San Diego. Vol 3, p163) in glycosidase-defective Lec8 cells (Stanley, P., 1989, *Molec. Cellul. Biol*. 9:377-383), which produce N-linked oligosaccharides lacking the terminal galactose and N-acetylneuraminic acid residues (Davis, S. J., et al., 1993, *Protein Eng.* 6:229-232; Liu, T., et al., 1996, *J Biol Chem* 271:33639-33646.). The construct 20 contained a C-terminal c-myc affinity tag (Hoogenboom, H. R., et al., 1991, *Nucl Acids Res*. 19:4133-4137), which facilitated immunoaffinity purification by specific peptide elution and avoided aggressive purification conditions. These procedures yielded protein which readily crystallized after a gel 25 filtration polish. This provided a general protocol to enhance crystallisation prospects for labile, multidomain glycoproteins.

The structure of this fragment is of considerable interest since it contains the major determinants governing insulin and IGF-1 binding specificity (Gustafson, T. A. & Rutter, W. J., 1990, *J. Biol. Chem.* 265:18663-30 18667; Andersen, A. S., et al., 1990, *Biochemistry*, 29:7363-7366; Schumacher, R., et al., 1991, *J. Biol. Chem.* 266:19288-19295; Schumacher, R., et al., 1993, *J. Biol. Chem.* 268:1087-1094; Schäffer, L., et al., 1993, *J. Biol. Chem.* 268:3044-3047; Williams, P. F., et al., 1995, *J. Biol. Chem.* 270:3012-3016) and is very similar to an IGF-1R fragment (residues 1-486) reported to 35 act as a strong dominant negative for several growth functions and which

induces apoptosis of tumour cells in vivo (D'Ambrosio, C., et al., 1996, *Cancer Res.* 56:4013-4020).

The expression plasmid pEE14/IGF-1R/462 was constructed by inserting the oligonucleotide cassette:

5

AatII

5' GACGTC GACGATGACGATAAG GAACAAAAACTCATC

D V D D D K E Q K L I
(EK cleavage) (c-myc tail)

10 S E E D L N (Stop)

TCAGAAGAGGATCTGAAT TAGAATTG GACGTC 3'

EcoRI *AatII*

encoding an enterokinase cleavage site, c-myc epitope tag (Hoogenboom, H. R., et al., 1991, *Nucleic acids Res.* 19:4133-4137) and stop codon into the AatII site (within codon 462) of IGF-1 receptor cDNA in the mammalian expression vector pECE (Ebina, Y., et al., 1985, *Cell*, 40:747-758; kindly supplied by W. J. Rutter, UCSF, USA), and introducing the DNA comprising the 5' 1521 bp of the cDNA (Ullrich, A., et al., 1986, *EMBO J.* 5:2503-2512)

20 ligated to the oligonucleotide cassette into the EcoRI site of the mammalian plasmid expression vector pEE14 (Bebbington, C. R. & Hentschel, C. C. G., 1987, In: Glover, D. M., ed. *DNA Cloning*. Academic Press, San Diego. Vol 3, p163; Celltech Ltd., UK). Plasmid pEE14/IGF-1R/462 was transfected into Lec8 mutant CHO cells (Stanley, P. 1989, *Molec. Cellul. Biol.* 9:377-383)

25 obtained from the American Tissue Culture Collection (CRL:1737) using Lipofectin (Gibco-BRL). Cell lines were maintained after transfection in glutamine-free medium (Glascow modification of Eagle's medium (GMEM; ICN Biomedicals, Australia) and 10% dialysed FCS (Sigma, Australia) containing 25 µM methionine sulphoximine (MSX; Sigma, Australia) as

30 described (Bebbington, C. R. & Hentschel, C. C. G., 1987, In: Glover, D. M., ed. *DNA Cloning*. Academic Press, San Diego. Vol 3, p163). Transfectants were screened for protein expression by Western blotting and sandwich enzyme-linked immunosorbant assay (ELISA) (Cosgrove, L., et al., 1995,) using monoclonal antibody (Mab) 9E10 (Evan et al., 1985) as the capture

35 antibody and either biotinylated anti-IGF-1R Mab 24-60 or 24-31 for detection (Soos et al., 1992; gifts from Ken Siddle, University of Cambridge,

UK). Large-scale cultivation of selected clones expressing IGF-1R/462 was carried out in a Celligen Plus bioreactor (New Brunswick Scientific, USA) containing 70 g Fibra-Cel Disks (Sterilin, UK) as carriers in a 1.25 L working volume. Continuous perfusion culture using GMEM medium supplemented with non-essential amino acids, nucleosides, 25 µM MSX and 10% FCS was maintained for 1 to 2 weeks followed by the more enriched DMEM/F12 without glutamine, with the same supplementation for the next 4-5 weeks. The fermentation production run was carried out three times under similar conditions and resulted in an estimated overall yield of 50 mg of receptor protein from 430 L of harvested medium. Cell growth was poor during the initial stages of the fermentation when GMEM medium was employed, but improved dramatically following the switch to the more enriched medium. Target protein productivity was essentially constant during the period from ~100 to 700 h of the 760 h fermentation, as measured by ELISA using Mab 9E10 as the capture antibody and biotinylated Mab 24-31 as the developing antibody.

Soluble IGF-1R/462 protein was recovered from harvested fermentation medium by affinity chromatography on columns prepared by coupling Mab 9E10 to divinyl sulphone-activated agarose beads (Mini Leak; Kem En Tec, Denmark) as recommended by the manufacturer. Mini-Leak Low and Medium affinity columns with antibody loadings of 1.5-4.5 mg/ml of hydrated matrix were obtained, with the loading range of 2.5-3 mg/ml giving optimal performance (data not shown). Mab 9E10 was produced by growing hybridoma cells (American Tissue Culture Collection) in serum-free medium in the Celligen Plus bioreactor and recovering the secreted antibody (4 g) using protein A glass beads (Prosep-A, Bioprocessing Limited, USA). Harvested culture medium containing IGF-1R/462 protein was adjusted to pH 8.0 with Tris-HCl (Sigma), made 0.02% (w/v) in sodium azide and passed at 3-5 ml/min over 50 ml Mab 9E10 antibody columns at 4° C. Bound protein was recovered by recycling a solution of 2-10 mg of the undecamer c-myc peptide EQKLISEEDLN (Hoogenboom et al., 1991) in 20 ml of Tris-buffered saline containing 0.02% sodium azide (TBSA). Between 65% and 75% of the product was recovered from the medium as estimated by ELISA, with a further 15-25% being recovered by a second pass over the columns. Peptide recirculation (~10 times) through the column eluted bound protein more efficiently than a single, slower elution. Residual bound protein was eluted

with sodium citrate buffer at pH 3.0 into 1 M Tris HCl pH 8.0 to neutralize the eluant, and columns were re-equilibrated with TBSA.

Gel filtration over Superdex S200 (Pharmacia, Sweden), of affinity-purified material showed a dominant protein peak at \sim 63 kDa, together with a smaller quantity of aggregated protein (Figure 3a). The peak protein migrated primarily as two closely spaced bands on reduced, sodium dodecyl sulfate polyacrylamide gel electrophoresis (SDS-PAGE; Figure 3b), reacted positively in the ELISA with both Mab 24-60 and Mab 24-31, and gave a single sequence corresponding to the N-terminal 14 residues of IGF-1R. No binding of IGF-1 or IGF-2 could be detected in the solid plate binding assay (Cosgrove et al., 1995, Protein Express Purif. 6:789-798). The IGF-1R/462 fragment was further purified by ion-exchange chromatography on Resource Q (Pharmacia, Sweden). Using shallow salt gradients, protein enriched in the slowest migrating SDS-PAGE band was obtained (data not shown), which formed relatively large, well-formed crystals (see below). Isoelectric focusing showed the presence of one major and two minor isoforms. Protein purified on Resource Q with an isocratic elution step of 0.14 M NaCl in 20 mM TrisCl at pH 8.0 (fraction 2, Figure 4) showed less heterogeneity on isoelectric focusing (Figure 4 inset) and SDS-PAGE (data not shown) and produced crystals of sufficient quality for structure determination (see below).

Crystals were grown by the hanging drop vapour diffusion method using purified protein concentrated in Centricon 10 concentrators (Amicon Inc, USA) to 5-10 mg/ml in 10-20 mM Tris-HCl pH 8.0 and 0.02% (w/v) azide, or 100 mM ammonium sulfate and 0.02% (w/v) azide. A search for crystallization conditions was performed initially using the factorial screen (Jancarik, J. & Kim, S.-H., 1991, J Appl Cryst 24:409-411) and subsequently optimised. Crystals were examined on an M18XHF rotating anode generator (Siemens, Germany) equipped with Franks mirrors (MSC, USA) and RAXIS IIC and IV image plate detectors (Rigaku, Japan).

From the initial crystallization screen of this protein, crystals of about 0.1 mm in size grew in one week. Upon refining conditions, crystals of up to 0.6 x 0.4 x 0.4 mm could be grown from a solution of 1.7-2.0 M ammonium sulfate, 0.1 M HEPES pH 7.5. The crystals varied considerably in shape and diffraction quality, growing predominantly as rhombic prisms with a length to width ratio of up to 5:1, but sometimes as rhombic bipyramids, the latter form being favoured when using material which had been eluted

from the Mab 9E10 column at pH 3.0. Each crystal showed a minor imperfection in the form of very faint lines from the centre to the vertices. Protein from dissolved crystals did not appear to be different from the protein stock solution when run on an isoelectric focusing gel. Upon X-ray

5 examination, the crystals diffracted to 3.0-4.0 Å and were found to belong to the space group $P2_12_12_1$ with $a = 76.8$ Å, $b = 99.0$ Å, $c = 119.6$ Å. In the diffraction pattern, the crystal variability noted above was manifest as a large (1-2°) and anisotropic mosaic spread, with concomitant variation in resolution. To improve the quality of the crystals, they were grown in the

10 presence of various additives or were recrystallized. These methods failed to substantially improve the crystal quality although bigger crystals were obtained by recrystallization. The variability in crystal quality appeared to be due to protein heterogeneity, as demonstrated by the observation that more highly purified protein, eluted isocratically from the Resource Q column and

15 showing one major band on isoelectric focusing (Figure 4 inset), produced crystals of sufficient quality for structure determination. These crystals diffracted to 2.6 Å resolution with cell dimensions, $a = 77.0$ Å, $b = 99.5$ Å, $c = 120.1$ Å and mosaic spread of 0.5°. Heavy metal derivatives of the IGF-1R/462 crystals have been obtained and are leading to the determination of

20 an atomic resolution structure of this fragment, which contains the L1, cysteine-rich and L2 domains of human IGF-1R.

EXAMPLE 2

Expression, Purification and Crystallization of the IR Fragment

A similar strategy was adopted for the human insulin receptor. The

25 fragment expressed (residues 1-485) comprises the L1-cysteine-rich-L2 region of the IR ectodomain but extends 13 residues further before the attachment of the 17 residue EK cleavage site linker and c-myc tail. The selected truncation position corresponds to a unique and convenient Bgl II restriction site. The expression strategy was also based on the pEE14 expression vector in

30 glycosidase-defective Lec8 cells and use of a C-terminal c-myc affinity tag for immunoaffinity purification by specific peptide elution. These procedures yielded IR protein which readily crystallized after a gel filtration polish.

The expression plasmid pHIR485 was constructed by ligating the double-stranded oligonucleotide cassette:

<i>Bgl II</i>	<i>Xba I</i>
5' AGATC TCCGACGATGACGATAAG GAACAAAAACTCATCTCAGAAGAGGATCTGAAT TAG TCTAGA 3'	
K I S D D D K E Q K L I S E E D L N	
EK cleavage	c-myc tail

5

encoding an enterokinase cleavage site, c-myc epitope tag (Hoogenboom, H. R., et al., 1991, Nucleic acids Res. 19:4133-4137) and stop codon , to the larger 11.1 kilobasepair Bgl II / Xba I fragment isolated from digestion of the mammalian expression plasmid pEH3 (a derivative of the mammalian 10 plasmid expression vector pEE14 [Bebbington, C. R. & Hentschel, C. C. G., 1987, In: Glover, D. M., ed. DNA Cloning. Academic Press, San Diego. Vol 3, p163; Celltech Ltd., UK] which holds the entire coding sequence of human insulin receptor within a Hind III /Xba I fragment). Lec8 mutant CHO cells (Stanley, P. 1989, Molec. Cellul. Biol. 9:377-383) obtained from the American 15 Tissue Culture Collection (CRL:1737) were transfected with pHIR485 using Lipofectamine (Gibco-BRL). Cell lines were maintained after transfection in glutamine-free medium (Glascow modification of Eagle's medium - GMEM; ICN Biomedicals, Australia) and 10% dialysed FCS (Sigma, Australia) containing 25 μ M methionine sulphoximine (MSX; Sigma, Australia) as 20 described (Bebbington, C. R. & Hentschel, C. C. G., 1987, In: Glover, D. M., ed. DNA Cloning. Academic Press, San Diego. Vol 3, p163). Transfectants were screened for protein expression by Western blotting and sandwich enzyme-linked immunosorbant assay (ELISA) (Cosgrove, L., et al., 1995,) using anti-hIR (Mab) 83.7 as the primary antibody and biotinylated 25 monoclonal antibody (Mab) 9E10 (Evan et al., 1985) for detection (Soos et al., 1986; gifts from Ken Siddle, University of Cambridge, UK). Large-scale cultivation of selected clones expressing IR/485 was carried out in a Celligen Plus bioreactor (New Brunswick Scientific, USA) containing 70 g Fibra-Cel Disks (Sterilin, UK) as carriers in a 1.25 L working volume. 30 Continuous perfusion culture was carried out using DMEM/F12 without glutamine medium (ICN), supplemented with non-essential amino acids, nucleosides, 25 μ M MSX and 5 - 10% FCS and resulted in an estimated overall yield of 115 mg of receptor protein from 165 L of harvested medium. Target protein productivity was essentially constant during the fermentation, 35 as measured by ELISA.

Soluble IR/485 protein was recovered from harvested fermentation medium by affinity chromatography on columns of Mab 9E10 essentially as described in Example 1. Between 92 -98% of the product was recovered from the medium by this affinity chromatography step, as estimated by ELISA.

5 Gel filtration over Superdex 200 (Pharmacia, Sweden), of the affinity-purified material at 1mg/ml produced a dominant protein peak at apparent mass ~140 kDa (Figure 5a - interpreted as dimer), whereas a peak at apparent mass ~85 kDa was obtained (Figure 5b - interpreted as monomer) at 0.02 mg/ml. The protein migrated as a single broad band of apparent molecular
10 mass ~78 kDa (reduced- lane A) or ~68 kDa (non-reduced - lane B) on sodium dodecyl sulfate polyacrylamide gel electrophoresis (SDS-PAGE; Figure 6a) The IR/485 fragment reacted positively in the ELISA with Mab 83-7, gave a single sequence corresponding to the N-terminal 10 residues of IR, showing several isoforms on isoelectric focussing from pI 6.0 - 6.8 (Figure
15 6b). Crystallisation screening trials of the fragment produced crystals too small for X-ray diffraction studies. The fragment was further purified by ion-exchange chromatography on Uno Q (BioRad, USA), using stepwise isocratic elution with incremental changes in salt concentrations (Figure 7). Fractions A and D were each enriched in a component isoform from the ladder of
20 isoforms present in the unfractionated mixture (Figure 6b). Both these fractions produced crystals, whereas no crystals were obtained from fractions B and C.

Crystals were grown by the hanging drop vapour diffusion method using purified protein concentrated in Centricon 10 concentrators (Amicon Inc, USA) to 5-10 mg/ml in 10mM Tris-HCl pH 8.0 and 0.02% (w/v) azide. A search for crystallization conditions was performed initially using the factorial screen (Jancarik, J. & Kim, S.-H., 1991, *J Appl Cryst* 24:409-411) and subsequently optimised. Crystals were examined on an M18XHF rotating anode generator (Siemens, Germany) equipped with Franks mirrors (MSC, USA) and an RAXIS IIC image plate detector (Rigaku, Japan).

From the initial crystallization screen of this protein fraction D fine needles grew in about one week. In further experiments, crystals of up to 0.04 x 0.04 x 0.2 mm could be grown from a solution of 1.9-2.0 M ammonium sulfate, 2% PEG 400, 0.1 M HEPES pH 7.5. Upon X-ray examination, the
35 crystals diffracted to 4 Å and were found to belong to the space group P2₁2₁2₁ with a = 103.2 Å, b = 130.0 Å, c = 161.6 Å. Despite their small size these

crystals diffracted sufficiently well to allow collection of a low resolution data set. Further purification of the protein and refinement of crystallisation conditions should yield larger crystals, providing data to determine the structure of this fragment at medium resolution or better.

5 **EXAMPLE 3**

Structure of the IGF-1R/1-462

Crystals were cryo-cooled to -170°C in a mother liquor containing 20% glycerol, 2.2 M ammonium sulfate and 100 mM Tris at pH 8.0. Native and derivative diffraction data were recorded on Rigaku RAXIS IIc or IV area 10 detectors using copper K α radiation from a Siemens rotating anode generator with Yale/MSC mirroroptics. The space group was P2₁2₁2₁ with $a = 77.39 \text{ \AA}$, $b = 99.72 \text{ \AA}$, and $c = 120.29 \text{ \AA}$. Data were reduced using DENZO and SCALEPACK (Otwinowski, Z. & Minor, W., 1996, *Mode. Meth. Enzym.* 276:307-326). Diffraction was notably anisotropic for all crystals examined.

15 Phasing by multiple isomorphous replacement(MIR) was performed with PROTEIN (Steigeman, W. Dissertation (Technical Univ. Munich, 1974) using anomalous scattering for both UO₂ and PIP derivatives. Statistics for data collection and phasing are given in Table 1. In the initial MIR map regions of protein and solvent could clearly be seen but the path of the 20 polypeptide was by no means obvious. That map was subject to solvent flattening and histogram matching in DM (Cowtan, K., 1994, Joint CCP4 and ESF-EACBM newslett. *Protein Crystallogr.* 31:34-38). The structure was traced and rebuilt using O (Jones, T. A., et al., 1991, *Acta Crystallogr.* A47:110-119) and refined with X-PLOR 3.851 (Brunger, A. T., 1996, X-PLOR 25 Reference Manual 3.851, Yale Univ., New Haven, CT). After 5 rounds of rebuilding and energy minimisation the R-factor dropped to 0.279 and Rfree = 0.359 for data 7-2.6 Å resolution. The current model contains 458 amino acids and 3 N-linked carbohydrates but no solvent molecules. For residues with B(Ca) > 70 Å² atomic positions are less reliable (37-42, 155-159, 305, 30 336-341, 404-406, 453-458). There is weak electron density for residues 459-461 but the c-myc tail appears completely disordered.

The 1-462 fragment consists of the N-terminal three domains of IGF-1R (L1, cys-rich, L2) and contains regions of the molecule which dictate ligand specificity (17-23). The molecule adopts a reasonably extended 35 structure (approximately 40 x 48 x 105 Å) with domain 2 (cys-rich region) making contact along the length of domain 1 (L1) but very little contact with

the third domain (L2) (see Figure 8). This leaves a space at the centre of the molecule of approximately 24 Å x 24 Å x 24 Å which is bounded on three sides by the three domains of the molecule. The space is of sufficient size to accommodate the ligand, IGF-1.

5 The L domains

Each of the L domains (residues 1-150 and 300-460) adopt a compact shape (24 x 32 x 37 Å) consisting of a single-stranded right handed β -helix and capped on the ends by short α -helices and disulfide bonds. The body of the domain looks like a loaf of bread with the base formed from a flat six-stranded β -sheet, 5 residues long and the sides being β -sheets three residues long (Figures 8 & 9). The top is irregular but in places is similar for the two domains. The two domains are superposable with an rms deviation in Ca positions of 1.6 Å for 109 atoms (Figure 10). Although this fold is reminiscent of other β -helix proteins it is much simpler and smaller with very few elaborations and thus it represents a new superfamily of domains. One notable difference between the two domains is that the indole ring of Trp 176 from the cys-rich region (Figure 9b) is inserted into the hydrophobic core of L1 and the C-terminal helix is only vestigial (Figure 8). For the insulin receptor family the sequence motif of residues which form the Trp pocket in L1 does not occur in L2 (Figure 9a). However in the EGF receptor, which has an additional cys-rich region after the L2 domain (14, 15), the pocket motif can be found in both L domains and the Trp is conserved in both cys-rich regions (Figure 9b).

The repetitive nature of the β -helix is reflected in the sequence and the first five turns were correctly identified by Bajaj, M., et al. (1987, *Biochim.Biophys. Acta* 916:220-226), the conserved Gly residues being found in turns making one bottom edge of the domain. However, their conclusions about the fold were incorrect. The "helix-like" repeat is actually a pair of bends at the top edge of the domain. In their Motif V, the Gly is not in a bend but is followed by the insertion of a conserved loop of 7-8 residues (see Figure 9a). Glycine is structurally important in the Gly bends as mutation of these residues compromises folding of the receptor [van der Vorm, E.R., et al., 1992, *J. Biol. Chem.* 267, 66-71; Wertheimer, E. et al., 1994, *J. Biol. Chem.* 269, 7587-7592].

Upon comparing the L domains with other right-handed β -helix structures such as pectate lyase (Yoder, M. D., et al., 1993, *Structure*, 1:241-

251-1507) and the p22 tailspike protein (Steinbacher, S., et al., 1997, J.Mol. Biol. 267:865-880) there are some striking similarities as well as differences. In all cases the ends of the domain are capped by α -helices but the L domains also have a disulphide bond at each end to hold the termini. The other β -helix domains are considerably longer and have significant twist to their sheets while the L domains have flat sheets. Although the sizes of the helix repeats are similar (here 24-25 residues vs 22-23 for pectate lyase) the cross-sections are quite different. The L domains have a rectangular cross-section while pectate lyase and p22 tailspike protein are V-shaped and have many, and sometimes quite large, insertions (Yoder, M. D., et al., 1993, Structure, 1:241-251-1507; Steinbacher, S., et al., 1997, J.Mol. Biol. 267:865-880). In the hydrophobic core a common feature is the stacking of aliphatic residues from successive turns of the β -helix and near the C-terminus of each L domain there is also a short Asn ladder, reminiscent of the long Asn ladder observed in pectate lyase (Yoder, M. D., et al., 1993, Structure 1:241-251-1507). On the opposite side of the L domains the Gly bend as well as the two bends and sheet preceding it have no counterpart in the other β -helix domains. Thus although the L domains are built on similar principles to the other β -helix domains they constitute a separate superfamily.

20 **The cys-rich domain**

The cys-rich domain is composed of eight disulfide-bonded modules (Figure 9b), the first of which sits at the end of L1 while the remainder make a curved rod running diagonally across L1 and reaching to L2 (Figure 8). The strands in modules 2-7 run roughly perpendicular to the axis of the rod in a manner more akin to laminin (Stetefeld, J., et al., 1996, J.Mol.Biol. 257:644-657) than to TNF receptor (Banner, D. W., et al., 1993, Cell, 73:431-445) but the modular arrangement of the cys-rich domain is different to other cys-rich proteins for which structures are known. The first 3 modules of IGF-1R have a common core, containing a pair of disulfide bonds, but show considerable variation in the loops (Figure 9b). The connectivity of these modules is the same as the first half of EGF (Cys 1-3 and 2-4) but their structures do not appear to be closely related to any member of the EGF family. Modules 4 to 7 have a different motif, β -finger, and best match residues 2152-2168 of fibrillin (Dowling, A. K., et al., 1996, Cell, 85:597-605). Each is composed of three polypeptide strands, the first and third being disulfide bonded and the latter two forming a β -ribbon. The β -ribbon of each β -finger module lines up

antiparallel to form a tightly twisted 8-stranded β -sheet (Figures 8 and 11). Module 6 deviates from the common pattern with the first segment being replaced by an α -helix followed by a large loop that is likely to have a role in ligand binding (see below). As module 5 is most similar to module 7 it is

5 possible that the four modules arose from serial gene duplications. The final module is a disulfide linked bend of five residues.

The fact that the two major types of cys-rich modules occur separately implies that these are the minimal building blocks of cys-rich domains found in many proteins. Although it can be as short as 16 residues, 10 the motif of modules 4-7 is clearly distinct and capable of forming a regular extended structure. Thus cys-rich domains such as these can be considered as made of repeat units each composed of a small number of modules.

Hormone binding

Attempts have been made to locate the IGF-1 (and insulin) binding site by examining natural (Taylor, S. I., 1992, *Diabetes*, 41:1473-1490) and site-directed mutants (Williams, P. F., et al., 1995, *J. Biol. Chem.* 270:3012-3016; Mynarcik, D. C et al., 1996, *J. Biol. Chem.* 271:2439-2442; Mynarcik, D. C., et al., 1997, *J. Biol. Chem.* 272:2077-2081), chimeric receptors (Andersen, A. S., et al., 1990, *Biochemistry* 29:7363-7366; Gustafson, T. A., & Rutter, W. 20 J., 1990, *J. Biol. Chem.* 265:18663-18667; Schäffer, L., et al., 1993, *J. Biol. Chem.* 268:3044-3047; Schumacher, R., 1993, *J. Biol. Chem.* 268:1087-1094; Kjeldsen, T., et al., 1991, *Proc. Natl Acad. Sci. USA*, 88:4404-4408) and by crosslinking studies (Wedekind, F., et al., 1989, *Biol. Chem Hoppe-Seyler*, 370:251-258; Fabry, M., 1992, *J. Biol. Chem.* 267:8950-8956; Waugh, S. M., et 25 al., 1989, *Biochemistry*, 28:3448-3458; Kurose, T., et al., 1994), *J. Biol. Chem.* 269:29190-29197-34). IGF-1R/IR chimeras not only show which regions of the receptors account for ligand specificity but also provide an efficient means of identifying some parts of the hormone binding site. Paradoxically regions controlling specificity are not the same for insulin and 30 IGF-1. Replacing the first 68 residues of IGF-1R with those of IR confers insulin binding ability on the chimeric IGF-1R (Kjeldsen, T., et al., 1991, *Proc. Natl Acad. Sci. USA*, 88:4404-4408) and replacing residues 198-300 in the cys-rich region of IR with the corresponding residues 191-290 of IGF-1R allows the chimeric receptor to bind IGF-1 (Schäffer, L., et al., 1993, *J. Biol. Chem.* 268:3044-3047). Thus a receptor can be constructed which binds both 35

IGF-1 and insulin with near native affinity. From the structure it is clear that if the hormone bound in the central space it could contact both these regions.

From analysis a series of chimeras examined by Gustafson, T. A., &

Rutter, W. J. (J. Biol. Chem. 265:18663-18667, 1990) the specificity

5 determinant in the cys-rich region can be limited further to residues 223-274. This region corresponds to modules 4-6 and includes a large and somewhat mobile loop (residues 255-263, mean B[Ca atoms] = 57 Å²) which extends into the central space (see Figure 8). In IR this loop is four residues bigger and is stabilised by an additional disulfide bond (Schäffer, L. & Hansen, 10 P.H., 1996, Exp. Clin. Endocrinol. Diabetes, 104: Suppl. 2, 89). The larger loop of IR may serve to exclude IGF-1 from the hormone binding site but allow the smaller insulin molecule to bind. It is interesting to note that mosquito IR homologue, which has a loop two residues larger than the mammalian IRs, also appears to bind insulin but not IGF-1 (Graf, R., et al., 15 1997, Insect Molec. Biol. 6:151-163). Analysis of the structure indicates that the insulin/IGF-1 specificity is controlled by residues in this loop (amino acids 253-272 in IGF-1R; amino acids 260-283 in IR)

As chimeras only address residues which differ between the two receptors a more precise analysis of the site can be obtained from single site 20 mutants. In particular, from an alanine-replacement study, four regions of L1 important for insulin binding were identified (Williams, P. F., et al., 1995, J. Biol. Chem. 270:3012-3016). The first three are at similar positions on successive turns of the β -helix and the fourth lies on the conserved bulge on the large β -sheet (Figure 12). Thus there is a footprint for insulin binding to 25 the L1 domain which lies on the first half of large β -sheet facing into the central space. Residues further along the sheet which are conserved in IGF-1R and could also be important. The conservative substitution of leucine for methionine at residue 119 of IR (113 of IGF-1R) causes a mild form of leprechaunism [Hone, J. et al., 1994, J. Med. Genet. 31, 715-716]. This 30 residue is buried and the mutation could perturb neighbouring residues to affect insulin binding.

The axis of the L2 domain is perpendicular to that of the L1 domain and N-terminal end of its β -helix is presented to the hormone-binding site. On this face of the L2 domain the only mutation studied so far is the 35 naturally occurring IR mutant, S323L, which gives rise to Rabson-Mendenhall syndrome and severe insulin resistance (Roach, P., 1994, Diabetes 43:1096-

1102). As this mutant only affects insulin binding and not cell-surface expression, residue 323 of IR (residue 313 of IGF-1R) is probably at or near the binding site. Structurally this residue lies in the middle of a region (residues 309-318 of IGF-1R) which is conserved in both IR and IGF-1R and

5 the surrounding region, 332-345 (of IGF-1R), is also quite well conserved in the these receptors (Figure 9a). Therefore this region is quite likely to form part of the hormone-binding site but would not have been detected by chimeras. It is interesting to note that in this region IRR is not as well conserved as the other two receptors (Shier, P. & Watt, V.M., 1989,

10 J.Biol.Chem. 264:4605-14608).

The distance from this putative hormone-binding region on L2 to that found on L1 is about 30 Å (Figure 8). Thus L1 and L2 appear too far apart to bind IGF-1 or insulin. However, in the crystal structure there is a deep cleft between part of the cys-rich domain (residue 262)and L2 (residue 305) and this cleft is occupied by a loop from a neighbouring molecule. Thus it seems probable that the position of the L2 domain in the receptor structure or the hormone-receptor complex adopts a different position with respect to the cys-rich domain than that found in the crystal. The movement required to bring L2 sufficiently close to L1 is small, namely a rotation of approximately 15 25° about residue 298.

20 A number of IR mutants have been identified which constitutively activate the receptor and the majority of these are found in the α chain. Curiously all α chain mutants involve changes to or from proline or the deletion of an amino acid, implying that they cause local structural rearrangements. The mutation R86N is similar to wild type but R86P reduces cell-surface expression and insulin binding while constitutively activating autophosphorylation [Grønskov, K. et al., 1993, Biochem. Biophys. Res. Commun. 192, 905-911]. The proline mutation probably disturbs residues preceding 87 which lie in the interface between the L1 and cys-rich domains 25 but it could also affect insulin binding. In the cys-rich domain residues 233, 281, 244 and 247 of IR are not conserved in IGF-1R (Figure 9b) yet L233P [Klinkhamer, M.P. et al., 1989, EMBO J. 8, 2503-2507], deletion of N281 [Debois-Mouthon, C. et al., 1996, J. Clin. Endocrinol. Metab. 81, 719-727] or the triple mutant P243R, P244R and H247D [Rafaeloff, R. et al., 1989, J. Biol. 30 Chem. 264, 15900-15904] cause constitutive kinase activation. Due to their 35 locations each of these three mutants appears likely to compromise the

folding of a β -finger domain and, in turn, the structural integrity of the rod-like cys-rich domain. The structural ramifications of these mutations could be significant for the whole receptor ectodomain as disturbing the L1/cys-rich interface or distorting the rod-like domain could affect the relative position of

5 L1 and the cys-rich domain in this context.

L1 has been further implicated as deletion of K121 on the opposite side of L1 from the cys-rich domain was also found to cause autophosphorylation [Jospe, N. et al., 1994, *J. Clin. Endocrinol. Metab.* 79, 1294-1302]. By contrast this mutation does not affect insulin binding. Thus a 10 possible mechanism emerges for insulin binding and signal transduction. When insulin binds between L1 and L2 it modifies the relative position of L1 and the cys-rich domain in the receptor, perhaps by hinge motion between L2 and the cys-rich domain like that suggested above, and the structural rearrangement is transmitted across the plasma membrane. In the absence of 15 insulin the same signal can be initiated by mutations in the cys-rich region or at the L1/cys-rich interface but at the expense on insulin binding. The signal can also be initiated more directly by mutations on the opposite side of L1 which affect the interaction of L1 with other parts of the ectodomain, possibly the other half of the receptor dimer.

20 **Ligand Studies**

Although there is no structural information about an IGF-1/IGF-1R complex a number of studies have probed the nature of this interaction. Results from cross-linking experiments with IGF-1 and insulin and their cognate receptors are consistent with the hormone binding site proposed 25 above. For example B29 of insulin can be cross-linked to the cys-rich region (residues 205-316) (Yip, C. C., et al., 1988, *Biochim. Biophys. Res. Commun.* 157:321-329) or the L1 domain (Wedekind, F., et al., 1989, *Biol. Chem Hoppe-Seyler*, 370:251-258). However these two regions are reasonably well separated and those studies may indicate that B29 is mobile. Other studies 30 unfortunately do not map the site any more precisely.

Analogues and site-directed mutants of IGF-1 and -2 have been more fruitful. Relative to insulin IGF-1 and -2 contain two extra regions, the C region between B and A and a D peptide at the C-terminus. For IGF-1 replacement of the C region by a four Gly linker reduced affinity for IGF-1R 35 by a factor of 40 but increased affinity for IR 5-fold (Bayne, M.L., et al., 1988, *J. Biol. Chem.* 264:11004-11008). Changes in affinity are consistent with the

deletion in IGF-1 complementing differences in the cys-rich regions of IGF-1R and IR noted above. Mutation of residues either side of the C region (residue 24 for IGF-1 [Cascieri, M.A., et al., 1988, Biochemistry 27:3229-3233], residues 27,43 for IGF-2, [Sakano, K., et al., 1991, J. Biol. Chem. 266:20626-20635]) also have deleterious effects on the affinity of the hormone for IGF-1R as has truncation of the nearby D peptide in IGF-2 (Roth, B.V., et al., 1991, Biochem. Biophys. Res. Commun. 181:907-914). Insulin has been extensively mutated. Binding studies [summarised in Kristensen, C. et al., 1997, J. Biol. Chem. 272, 12978-12983] indicate that insulin may bind its receptor via a hydrophobic patch (residues A2, A3, A19, B8, B11, B12, B15 and possibly B23 & B24). However this patch is normally buried and requires the removal of the B chain's C-terminus from the observed position. Assuming IGF-1, -2 and insulin bind their receptors in the same orientation, these data suggest an approximate orientation for the hormone when bound to the receptor.

One notable feature of IGF-1 and -2 is the large number of charged residues and their uneven distribution over the surface. Basic residues are predominantly found in the C region and, in solution, this region is not well ordered in either IGF-1 or -2 (Sato, A., et al., 1993, Int J Peptide Protein Res. 41:433-440; Torres, A. M., et al., 1995, J. Mol. Biol. 248:385-401). In contrast the binding site of the receptor has a sizable patch of acidic residues in the corner where the cys-rich domain departs from L1. Other acidic residues which are specific to this receptor are found along the inside face of the cys-rich domain and the loop (residues 255-263) extending from module 6. Thus it is possible that electrostatics play an important part in IGF-1 binding with the C region binding to the acidic patch of the cys-rich region near L1 and the acidic patch on the other side of the hormone directed towards a small patch of basic residues (residues 307-310) on the N-terminal end of L2.

Although the structure of this fragment gives significant information about the nature of the hormone binding site, residues outside this region have also been shown to affect binding of ligand. A number of studies have implicated residues 704-715 of IR (Mynarcik, D. C et al., 1996, J. Biol. Chem. 271, 2439-2442; Kurose, T., et al., 1994, J. Biol. Chem. 269:29190-29197). These residues could contact insulin on one of the sides left open in the current structure. Using insulin labelled at the B1 residue, Fabry, M., et al., (1992, J. Biol. Chem. 267:8950-8956) cross linked insulin to the fragment

390-488, part of which is not near the site as described. The explanation for this could be either 488 reaches back to the hormone binding site, or this region could contact another hormone bound to the other half of the receptor.

Further structural information is needed to establish how these other regions

5 contact the hormone and to elucidate how binding of the hormone is communicated to the kinase inside the cell.

The structure of the L1-cys-rich-L2 domains of IGF-1R presented here represents the first structural information for the extracellular portion of a member of the insulin receptor family. The L domains display a novel fold

10 which is common to the EGF receptor family and the modular architecture of the cys-rich domain implies that smaller building blocks should be used to describe the composition of cysteine-rich domains. This fragment contains the major specificity determinants of receptors of this class for their ligands. It has an elongated structure with a space in the middle which could

15 accommodate the ligand. The three sides of this site correspond to regions which have been implicated in hormone binding. Although other sites are present in the receptor ectodomain which interact with the ligand this structure gives us an initial view of how the insulin, IGF-1 and -2 might interact with their cell surface receptors to control their metabolic and

20 mitogenic effects

Such information will provide valuable insight into the structure of the corresponding domains of the IR and insulin receptor-related receptor as well as members of the related EGFR family (Bajaj, M., et al., 1987, *Biochim Biophys Acta* 916:220-226; Ward, C. W. et al., 1995, *Proteins: Struct Funct Genet* 22:141-153).

EXAMPLE 4

Prediction of 3D Structure of the Corresponding Domains of IRR and IR Based on Structure of IGF-1R Fragment.

The sequence identities between the different members of the insulin

30 receptor family are sufficient to allow accurate sequence alignments to facilitate 3D structure predictions by homology modelling. The alignments of the ectodomains of human IGF-1R, IR, and IRR are shown in Figure 13.

EXAMPLE 5**Prediction of 3D Structure of EGFR and its Family Members ERB2, ERB3 and ERB4.**

The sequence identities between the different members of the EGFR receptor family and the insulin receptor family are sufficient to allow accurate sequence alignments to facilitate 3D structure predictions by homology modelling. The alignments of the ectodomains of human EGFR, ERB2, ERB3 and ERB4 are shown in Figure 14. The ectodomains of the EGFR family members are composed of four domains : L1 domain, cys-rich domain, L2 domain and a second cys-rich domain all of which can be modelled from the structure of the IGF-1R fragment residues 1-462.

5 receptor family and the insulin receptor family are sufficient to allow accurate sequence alignments to facilitate 3D structure predictions by homology modelling. The alignments of the ectodomains of human EGFR, ERB2, ERB3 and ERB4 are shown in Figure 14. The ectodomains of the EGFR family members are composed of four domains : L1 domain, cys-rich domain, 10 L2 domain and a second cys-rich domain all of which can be modelled from the structure of the IGF-1R fragment residues 1-462.

10 receptor family and the insulin receptor family are sufficient to allow accurate sequence alignments to facilitate 3D structure predictions by homology modelling. The alignments of the ectodomains of human EGFR, ERB2, ERB3 and ERB4 are shown in Figure 14. The ectodomains of the EGFR family members are composed of four domains : L1 domain, cys-rich domain, 15 L2 domain and a second cys-rich domain all of which can be modelled from the structure of the IGF-1R fragment residues 1-462.

15 receptor family and the insulin receptor family are sufficient to allow accurate sequence alignments to facilitate 3D structure predictions by homology modelling. The alignments of the ectodomains of human EGFR, ERB2, ERB3 and ERB4 are shown in Figure 14. The ectodomains of the EGFR family members are composed of four domains : L1 domain, cys-rich domain, 20 L2 domain and a second cys-rich domain all of which can be modelled from the structure of the IGF-1R fragment residues 1-462.

The sequence alignment analysis and characterization of the repeat modules in the cys-rich region of IGF-1R and the homologous regions of the IR, IRR and the first and second cys-rich regions of EGFR, ErbB2, ErbB3 and ErbB4 are shown in Figure 15. A representative of each subtype of cys repeat is found in the IGF-1R fragment 1-462 and is used to model each of these modules in the other receptors. Note the nature and order of modules in the second cys-rich repeat of the EGFR family is different to that seen in the first cys-rich region.

EXAMPLE 6**Single-Molecule Imaging of Human Insulin Receptor Ectodomain and its Fab Complexes****Cloning and expression of hIR -11 ectodomain protein**

A full length clone of the human IR exon -11 form (hIR -11) was prepared by exchanging an Aat II fragment, nucleotides 1195 to 2987 , of the exon +11 clone (plasmid pET; Ellis et al., 1986; gift from Dr W. J. Rutter, UCSF) of hIR (Ebina et al., 1985, *Cell* **40**, 747-758) with the equivalent Aat II fragment from a plasmid (pHIR/P12-1, ATCC 57493) encoding part of the extracellular domain and the entire cytoplasmic domain of hIR -11 (Ullrich et al., 1985, *Nature* **313** , 756-761). The ectodomain fragment of hIR -11 (2901 bp, coding for the 27 residue signal sequence and residues His1-Asn914) was produced by SalI and SspI digestion and inserted into the mammalian expression vector pEE6.HCMV-GS (Celltech Limited, Slough, Berkshire, UK) into which a stop codon linker had been inserted, as described previously (Cosgrove et al., 1995, *Protein Expression and Purification* **6**, 789-798) for the hIR exon +11 ectodomain.

The resulting recombinant plasmid pHIR II (2 µg) was transfected into glycosylation deficient Chinese hamster ovary (Lec 8) cells (Stanley, 1989, *Molec. Cellul. Biol.* **9**, 377-383) with Lipofectin (Gibco-BRL). After

transfection, the cells were maintained in glutamine-free medium GMEM
 5 (ICN Biomedicals, Australia) as described previously (Bebbington & Hentschel, 1987, In *DNA Cloning* (Glover, D., ectodomain.), Vol III, Academic Press, san Diego; Cosgrove et al., 1995, *Protein Expression and Purification* **6**, 789-798). Expressing cell lines were selected for growth in GMEM with 25 µM methionine sulphoximine (MSX, Sigma). Transfectants were screened for
 10 protein expression using sandwich ELISA with anti-IR monoclonal antibodies 83-7 and 83-14. Metabolic labelling of cells, immunoprecipitations, insulin binding assays and Scatchard analyses were performed as described previously for the exon +11 form of hIR ectodomain (Cosgrove et al., 1995, , *Protein Expression and Purification* **6**, 789-798).

15 **hIR -11 ectodomain production and purification**

The selected clone (inoculum of 1.28 x 108 cells) was grown in a spinner flask packed with 10 g of Fibra-cel disc carriers (Sterilin, U.K.) in 500 ml of GMEM medium containing 10% fetal calf serum (FCS) and 25 µM MSX. Selection pressure was maintained for the duration of the culture.

20 Ectodomain was recovered from harvested media by affinity chromatography on immobilized insulin and further purified by gel filtration chromatography on Superdex S200 (Pharmacia; 1 x 40 cm) in Tris-buffered saline containing 0.02% sodium azide (TBSA) as described previously (Cosgrove et al., 1995, *Protein Expression and Purification* **6**, 789-798).

25 Solutions of purified hIR -11 ectodomain were stored at 4° C prior to use.

Production of Fab fragments and their complexes with ectodomain

Purification of Mabs 83-7, 83-14 and 18-44 from ascites fluid by affinity chromatography using Protein A-Sepharose, and the production of Fabs, were based on the methodologies described in Coligan et al., 1993, 30 Current Protocols in Immunology, Vol 1, pp 2.7.1-2.8.9, Greene Publishing Associates & Wiley - Interscience, John Wiley and Sons. Fab was produced from monoclonal antibody by mercuripapain digestion for 1-4 h, followed by gel filtration on Superdex S200. Products were monitored by reducing and non-reducing SDS-PAGE. For 83-7 Mab, an IgG Type 1 monoclonal antibody, 35 the bivalent (Fab)2' isolated by this method was reduced to monovalent Fab 83-7 by mild reduction with mM L-cysteine.HCl in 100 mM Tris pH 8.0

(Coligan et al., 1993, Current Protocols in Immunology, Vol 1, pp 2.7.1-2.8.9, Greene Publishing Associates & Wiley - Interscience, John Wiley and Sons).

Complexes of Fab with hIR -11 ectodomain were produced by mixing

~ 2.5 to 3.5 molar excess of Fab with hIR -11 ectodomain at ambient

5 temperature in TBSA at pH 8.0. After 1-3 h, the complex was separated from unbound Fab by gel filtration over a Superdex S200 column in the same buffer.

Electron microscopy

10 Uncomplexed hIR -11 ectodomain and the Fab complexes described above were diluted in phosphate-buffered saline (PBS) to concentrations of the order of 0.01-0.03 mg/ml. Prior to dilution, 10% glutaraldehyde (Fluka) was added to the PBS to achieve a final concentration of 1% glutaraldehyde. Droplets of ~ 3ml of this solution were applied to thin carbon film on 700-mesh gold grids after glow-discharging in nitrogen for 30 s. After 1 min. the 15 excess protein solution was drawn off and followed by application and withdrawal of 4-5 droplets of negative stain [2% uranyl acetate (Agar), 2% uranyl formate (K and K), 2% potassium phosphotungstate (Probing and Structure) adjusted to pH 6.0 with KOH, or 2% methylamine tungstate (Agar) adjusted to pH 6.8 with NH4OH]. In the case of both uranyl acetate and 20 uranyl formate staining, an intermediate wash with 2 or 3 droplets of PBS was included prior to application of the stain. The grids were air-dried and then examined at 60kV accelerating voltage in a JEOL 100B transmission electron microscope at a magnification of 100,000x. It was found that there was a typical thickness of negative stain in which Fabs were most easily 25 seen, hence areas for photography had to be chosen from particular zones of the grid. Electron micrographs were recorded on Kodak SO-163 film and developed in undiluted Kodak D19 developer. The electron-optical magnification was calibrated under identical imaging conditions by recording single-molecule images of the antigen-antibody complex of influenza virus 30 neuraminidase heads and NC10 MFab (Tulloch et al., 1986, *J.Mol. Biol.* 190, 215-225; Malby et al., 1994, *Structure*, 2, 733-746).

Image processing

35 Electron micrographs showing particles in a limited number of identifiable projections were chosen for digitisation. Micrographs were digitised on a Perkin-Elmer model 1010 GMS PDS flatbed scanning microdensitometer with a scanning aperture (square) size of 20 mm and

stepping increment of 20 nm corresponding to a distance of 0.2 nm on the specimen. Particles were selected from the digitised micrograph using the interactive windowing facility of the SPIDER image processing system (Frank et al., 1996, *J. Struct. Biol.* **116**, 190-199). Particles were scaled to an optical density range of 0.0 - 2.0 and aligned by the PSPC reference-free alignment algorithm (Marco et al., 1996, *Ultramicroscopy*, **66**, 5-10). Averages were then calculated over a subset of correctly aligned particles chosen interactively as being representative of a single view of the particle. The final average image presented here is derived from a library of 94 images.

5 **10 Biochemical characterization of expressed hIR -11 ectodomain**

The recombinant protein examined corresponded to the the first 914 residues of the 917 residue ectodomain of the exon -11 form of the human insulin receptor (Ullrich et al., 1986, *Nature* **313** , 756-761). Expressed protein was shown, by SDS-PAGE and autoradiography of immunoprecipitated

15 product from metabolically labelled cells, to exist as a homodimeric complex of ~270 - 320 kDa apparent mass, which dissociated under reducing conditions into monomeric α and β' subunits of respective apparent mass ~120 kDa and ~35 kDa (data not shown).

20 Purified hIR -11 ectodomain, expressed in Lec8 cells and purified by affinity chromatography on an insulin affinity column, ran as a symmetrical peak on a Superdex S200 gel filtration column (Figure 16). The protein eluted with an apparent mass of ~400 kDa, calculated from a standard curve generated by the elution positions of standard proteins (not shown). As expected for protein expressed in Lec 8 cells, whose glycosylation defect

25 produces truncated oligosaccharides (Stanley, 1989, *Molec. Cellul. Biol.* **9**, 377-383), this value is less than the apparent mass (450 - 500 kDa) reported for hIR +11 ectodomain expressed in wild-type CHO-K1 cells (Johnson et al., 1988, *Proc. Natl Acad. Sci USA* **85**, 7516-7520; Cosgrove et al., 1995, *Protein Expression and Purification* **6**, 789-798).

30 Radioassay of insulin binding to purified ectodomain gave linear Scatchard plots and Kd values of 1.5 - 1.8 \times 10⁻⁹ M, similar to the values of 2.4 - 5.0 \times 10⁻⁹ M reported for the hIR -11 ectodomain (Andersen et al., 1990, *Biochemistry* **29**, 7363-7366; Markussen et al., 1991, *J. Biol. Chem.* **266**, 18814-18818; Schaffer, 1994, *Eur. J. Biochem.* **221**, 1127-1132) and the values

35 of ~1.0 - 5.0 \times 10⁻⁹ M reported for the hIR +11 ectodomain (Schaefer et al., 1992, *J. Biol. Chem.* **267**, 23393-23402; Whittaker et al., 1994, *Molec.*

Endocrinol. **8**, 1521-1527; Cosgrove et al., 1995, *Protein Expression and Purification* **6**, 789-798).

Expression of hIGF-1R ectodomain

Cloning, expression and purification of this protein used elements

5 common to those described for hIR -11 ectodomain (Cosgrove et al., 1995, *Protein Expression and Purification* **6**, 789-798) and resulted in purified product that was recognised by receptor-specific Mabs 17-69, 24-31 and 24-60 (Soos et al., 1992, *J. Biol. Chem.* **267**, 12955-63) and was composed of α and β' subunits of mass similar to those of hIR ectodomain (unpublished data).

10 Preparation of hIR -11 ectodomain/MFab complexes

A complex of hIR -11 ectodomain and Fab from antibody 83-14 eluted as a symmetrical peak of 460 -500 kDa (Figure 16), as did complexes generated from a mixture of hIR -11 ectodomain with Fab from antibody 18-44 and a mixture of hIR -11 ectodomain with Fab 83-7 (not shown). A co-15 complex of ectodomain with Fabs from antibodies 18-44 and 83-14 eluted at \sim 620 kDa (Figure 12), as did a co-complex with MFabs 83-14/83-7 and another with MFabs 83-7/18-44 (not shown). A complex of hIR -11 ectodomain with all three MFab derivatives, 18-44, 83-7 and 83-14, eluted at an apparent mass of \sim 710 kDa (Figure 16).

20 **Electron microscopy**

Imaging of hIR -11 and hIGF-1R ectodomains

Single-molecule imaging of undecorated dimeric hIR -11 ectodomain was carried out under a variety of negative staining conditions, which emphasised different aspects of the structure of the molecular envelope. The 25 least aggressive or penetrative stain was potassium phosphotungstate (KPT), which revealed consistent globular particles with very little internal structure other than a suggestion of a division into two parallel bars. Staining with methylamine tungstate also revealed the parallel bar images, as shown in Figure 17a.

30 Further investigation using progressively more penetrative, but also potentially more disruptive, stains confirmed the observations above. Staining with uranyl acetate and uranyl formate showed the separation of the parallel bars most clearly (Figure 17b), but uranyl acetate showed evidence of disrupting the structure of the particles, i.e. a decrease in the consistency 35 of the particle shape and a tendency for particles to look unravelled or denatured despite having been subjected to chemical cross-linking prior to

staining. In areas of thicker stain, parallel bars predominated (Figure 17b), whereas in more thinly stained regions, U-shaped particles could be identified, sometimes outnumbering the parallel-bar structures (Figure 18a).

5 An averaged image of the parallel bars seen by staining hIR -11 ectodomain with uranyl formate is shown as an insert in Figure 17b.

In Figures 17c and 18b, images of hIGF-1R ectodomain are shown for comparison with Figure 17b and 18a, respectively, under similar staining conditions.

10 Imaging of hIR -11 ectodomain complexed with 83-7 MFab

This complex was particularly noteworthy for the consistency of the form of the particles, especially under the gentler staining conditions afforded by stains such as KPT and methylamine tungstate. The particles were interpreted as having been restricted in the views they presented, after air-drying on the carbon support film, by the almost diametrically opposite binding of the two Fab arms to the antigen to form a highly elongated complex structure. Under these conditions three distinct views could be recognised as shown in Figure 19. Two views (interpreted as top-down/bottom-up) show the Fab arms displaced clockwise or anti-clockwise as extensions of the parallel plates with two-fold symmetry. The third view shows an image with the two Fab arms in line roughly through the centre of the receptor on its opposite sides, interpreted as a side projection of binding half-way up the plates (Figure 19).

20 Figure 20 shows a field of particles of hIR -11 ectodomain complexed with 83-7 MFab, stained with uranyl formate. The use of the more aggressive uranyl stains operating at lower pHs revealed internal structure of the molecular envelope at the expense of consistency of the particle morphology. For example, staining with uranyl acetate or uranyl formate showed that parallel bars can be seen in particles in which the Fab arms are displaced either clockwise or anticlockwise but not where the intermediate central or 25 axial position of the two Fab arms is presented in projection. These observations show 83-7 MFab binding roughly half-way up the side-edge of each hIR -11 ectodomain plate. The epitope recognised by Mab 83-7 has been mapped to the cys-rich region, residues 191-297, by analysis of chimeric receptors (Zhang and Roth, 1991, *Proc. Natl. Acad. Sci. USA* **88**, 9858-9862).

Imaging of hIR -11 ectodomain complexed with either 83-14 MFab or 18-44 MFab

Figure 21a shows the complexes formed with Fabs from the most insulin-mimetic antibody Mab 83-14. Projections showing the Fab arms

5 bound to and extending out from near the base of the U-shaped particles can be identified. A second field of particles (Figure 21b) shows objects composed of two parallel bars as observed for the undecorated ectodomain, with Fab arms projecting obliquely from diametrically opposite extremities. Similar but less definitive images were also seen when MFab 18-44 was

10 bound to hIR -11 ectodomain (not shown). The epitope for Mab 83-14 is between residues 469-592 (Prigent et al., 1990) in the connecting domain. This domain contains one of the disulphide bonds (Cys524-Cys524) between the two monomers in the IR dimer (Schaffer and Ljungqvist, 1992, *Biochem. Biophys. Res. Commun.* **189**, 650-653). The epitope for Mab 18-44 is a linear

15 epitope, residues 765-770 (Prigent et al., 1990, *J. Biol. Chem.* **265**, 9970-9977) in the β -chain, near the end of the insert domain (O'Bryan et al., 1991, *Mol. Cell. Biol.* **11**, 5016-5031). The insert domain contains the second disulphide bond connecting the two monomers in the IR dimer (Sparrow et al., 1997, *J. Biol. Chem.*, 272, 29460-29467).

20 **Imaging of hIR -11 ectodomain co-complexed with two different MFabs per monomer**

The double complex of hIR -11 ectodomain with MFabs 83-7 and 18-44 was stained with 2% KPT at pH 6.0, and revealed the molecular envelopes shown in Figure 22. The particle appears complex in shape and

25 can assume a number of different orientations on the carbon support film, giving rise to a number of different projections in the micrograph. The predominant view is of an asymmetric X-shape (some examples circled). It shows the 83-7 MFab arms bound at opposite ends of the parallel bars with the two 18-44 MFabs appearing as shorter projections extending out from

30 either side of each ectodomain.

Images of the double complex of hIR -11 ectodomain with 83-7 and 83-14 MFabs gave X-shaped images similar to those seen with the 83-7/18-44 double complex (not shown). In contrast the double complex of hIR -11 ectodomain with 18-44 and 83-14 MFabs did not present the characteristic

35 asymmetric X-shapes described above (images not shown). Instead, the molecular envelope appeared to be elongated in many views, with only an

occasional X-shaped projection. While a detailed interpretation of these images would be premature, it is clear that MFabs 18-44 and 83-14, two of the more potent insulin mimetic antibodies (Prigent et al., 1990, *J. Biol. Chem.* 265, 9970-9977), can bind simultaneously to the receptor.

5 **Imaging of hIR -11 ectodomain co-complexed with three different MFabs per monomer**

Figure 23 shows a field of particles from a micrograph of hIR -11 ectodomain complexed simultaneously with MFabs 83-7, 83-14 and 18-44. In the thicker stain regions the molecular envelope is X-shaped, and looks very 10 similar to that of the double complexes of hIR -11 ectodomain with either 83-7 and 18-44 or 83-7 and 83-14. However, in the more thinly stained regions, particles of greater complexity are visible and it is possible occasionally to identify that there are in fact more than four MFabs bound to the ectodomain dimer.

15 The single-molecule imaging of hIR -11 ectodomain presented here suggests a molecular envelope for this dimeric species significantly different from that of any previously published study. However, an unequivocal determination of the molecular envelope even from the present study is not entirely straightforward. A major complicating factor here has been the 20 relative fragility of the expressed ectodomain when exposed to the rigors of electron microscope preparation by negative staining. For example, staining with potassium phosphotungstate (KPT, pH 6.0-7.0) frequently suggested a denaturation of the dimeric molecules, but when appropriate conditions were satisfied, good seemingly interpretable molecular envelope images were 25 achieved; staining with methylamine tungstate (pH ~7.0) supported the best KPT molecular envelope images, but had the suggestion of a swelling of the molecular structure at neutral pH; and the acid-pH stains of uranyl acetate (pH ~4.2) and uranyl formate (pH~3.0), with their ability to penetrate the ectodomain structure, appeared to illuminate not so much the molecular 30 envelope as the zones of high projected protein density within the dimer.

An amalgam of impressions from these various staining regimens has led to the following interpretation of single-molecule images of these undecorated, or naked, dimers: the predominant dimeric molecular image encountered here has been that of 'parallel bars' of projected protein density. 35 This view is so predominant, indeed, that it suggests there is either a single preferred orientation of the molecules on the glow-discharged carbon support

film, or that this impression of parallel bars of density may represent a mixture of superficially similar structure projections, with the subtleties of these different projections being masked by the relatively coarse resolution of this single-molecule direct imaging. The impression of parallel bars of

5 projected protein density is particularly predominant in regions of thicker negative stain. A second view of the molecular envelope, appreciably less well represented in regions of thicker stain but predominant in regions of thin staining, is that of 'open' U's, or V's. These two views of hIR -11 ectodomain were supported by the single-molecule imaging of hIGF-1R

10 ectodomain under comparable conditions of negative staining.

If the assumption is made that these two recognisable projected views, that of parallel bars and of open U's/V's, are different views of the same dimeric molecule, an assumption strongly supported by the MFab complex imaging, a coarse model of the molecular envelope can be

15 rationalized as in the schematic Figure 24. The model structure is roughly that of a cube, composed of two almost-parallel plates of high protein density, separated by a deep cleft of low protein main-chain and side-chain density able to be penetrated by stain, and connected by intermediate stain-excluding density near what is assumed here to be their base (that is,

20 nearest the membrane-anchoring region). The width of the low-density cleft appears to be of the order of 30-35Å, sufficient to accommodate the binding of the insulin molecule of diameter ca. 30Å, although we have no electron microscopical evidence to support insulin-binding in this cleft at this stage.

It has been established through imaging of bound 83-7 MFab that

25 there is a dimeric two-fold axis normal to the membrane surface between these plates of density. Occasionally, dimer images display a relative displacement of the bars of density, interpreted here as a limited capacity for a shearing of the interconnecting zone between the two plates along their horizontal axis parallel to the membrane; other images show bars skewed

30 from parallel, implying a limited capacity for the plates to rotate independently around the two-fold axis, again via this interconnecting zone. These two observations each suggest a relatively flexible connectivity between the dimer plates in the membrane-proximal region of intermediate protein density, which could possibly contribute to the transmembrane

35 signalling process.

The approximate overall measured dimensions of the ectodomain dimer depicted in Figure 24 are 110 x 90 x 120 Å, calibrated against the dimensions of imaged influenza neuraminidase heads, known from the solved X-ray structure (Varghese et al., 1983, *Nature* **303**, 35-40). It can be 5 noted that there is a compatibility here between the molecular weights and molecular dimensions of these two molecular species: the compact tetrameric influenza neuraminidase heads of Mr ~200 kDa occupy a volume almost 100 x 100 x 60 Å; the more open dimeric insulin receptor ectodomains of similar Mr ~240 kDa imaged here occupy a volume approximately 110 x 10 90 x 120 Å, roughly twice that of the neuraminidase heads, accommodating the slightly higher molecular weight and substantial central low-density cleft.

The low-resolution roughly cubic compact structure proposed here differs substantially from the T-shaped model proposed by Christiansen et al. (1991, *Proc. Natl. Acad. Sci. U. S. A.* **88**, 249-252) and Tranum-Jensen et al., 15 (1994, *J. Membrane Biol.* **140**, 215-223) for the whole receptor and the elongated model proposed by Schaefer et al. (1992, *J. Biol. Chem.* **267**, 23393-23402) for soluble ectodomain. Significantly, those previous studies did not provide any convincing independent electron microscopical evidence that their imaged objects were in fact insulin receptor.

20 In the present study, the identity of the imaged molecules as hIR -11 ectodomain has been confirmed by imaging complexes of the dimer with Fabs of the three well-established conformational Mabs against native hIR, 83-7, 83-14 and 18-44 (Soos et al., 1986, *Biochem. J.* **235**, 199-208; 1989, *Proc. Natl Acad. Sci. USA* **86**, 5217-5221), bound singly and in combination. In all 25 these instances, virtually every particle in the field of view exhibited MFab decoration through binding to conformational epitopes, establishing not only the identity of the imaged particles but also the conformational integrity of the expressed ectodomains. Furthermore, the cleanliness and uniformity of these hIR -11 ectodomain preparations, both naked and decorated, visualised 30 here by electron microscopy demonstrate their high suitability for X-ray crystallization trials.

The known flexibility of the Fab arms exacerbates image-to-image variability beyond the limited extent already described for the undecorated dimeric ectodomains, complicating any precise interpretation of these 35 antigen-antibody complexes. Such molecular flexibility also renders largely impractical any single-molecule computer image averaging to facilitate image

interpretation, progressively more so with the higher order antigen-antibody complexes studied here.

The most readily interpretable of these images, showing least image-to-image variability, are those of 83-7 MFab bound to dimers where,

5 fortuitously, the antigen-antibody complex is constrained in its degrees of rotational freedom on the carbon support film. Many projected images show the two Fab arms in line roughly through the centre of the antigen on its opposite sides (Figure 19, arrowed examples), interpreted as a side projection of binding half-way up the plates from their membrane-proximal 10 base. Other sub-sets of images (Figure 19, circled examples) show the two Fab arms still parallel but displaced clockwise or anticlockwise with 2-fold symmetry, each Fab approximating an extension of one of the parallel bars of antigen density, interpreted here as representing top or bottom projections along the 2-fold axis. The third projection, along the axis of the Fab arms, 15 could not be sampled here because of the constraining geometry of this molecular complex. These observations suggest binding of 83-7 MFab roughly half-way up the side-edge of the hIR -11 ectodomain plate. This then allows an initial attempt at spatially mapping the 83-7 MFab epitope, which has been sequence-mapped to residues 191-297 in the cys-rich region of the 20 insulin receptor (Zhang and Roth, 1991, *Proc. Natl. Acad. Sci. USA* **88**, 9858-9862). The spatial separation and relative orientations of the two binding epitopes of Mab 83-7 on the hIR -11 ectodomain dimer as indicated here appear inconsistent with the proposal that Mab 83-7 could bind intramolecularly to hIR (O'Brien et al., 1987, *Biochem J.* **6**, 4003-4010).

25 Decoration of the ectodomain dimer with 83-7 MFab established that the two plates of high protein-density are arranged with 2-fold symmetry. Decoration with either 83-14 or 18-44 MFab , on the other hand, allowed sampling of the third projection of the ectodomain dimer precluded by 83-7 MFab binding. Significantly, this third view established unequivocally the U- 30 shaped projection of the hIR -11 ectodomain dimer, something which was only able to be assumed with the undecorated ectodomain images. Further, this projection has allowed a rough spatial mapping close to the base of the U-shaped dimer for the epitopes recognised by 83-14 MFab (residues 469-592, connecting domain) and 18-44 MFab (residues 765-770, b-chain insert 35 domain; exon 11 plus numbering, Prigent et al., 1990, *J. Biol. Chem.* **265**, 9970-9977).

Inherent in the model structure presented in Figure 20 is the implication that, with the two-fold axis aligned normal to the membrane surface, the mouth of the low-density cleft where insulin binding may occur would lie most distant from the transmembrane anchor, whilst the zone of

5 intermediate density connecting the two high-density plates would be in close proximity to the membrane. It follows, in this model, that the L1/cys-rich/L2 domains(Bajaj et al., 1997, *Biochim. Biophys. Acta* **916**, 220-226; Ward et al.,1995, *Proteins: Struct., Funct., Genet.* **22**, 141-153), which comprise much of the insulin-binding region (see Mynarcik et al., 1997, *J. Biol. Chem.*

10 **272**, 2077-2081), most probably lie in the membrane-distal upper halves of the two plates, whilst the membrane-proximal lower halves contain the connecting domains, the fibronectin-type domains, the insert domains and the interchain disulphide bonds (Schaffer and Ljungqvist, 1992, *Biochem. Biophys. Res. Commun.* **189**, 650-653; Sparrow et al., 1997, *J. Biol. Chem.*, **272**,

15 29460-29467). Such a disposition of domains is supported by the images seen with the single MFab decoration, the 83-7 MFab epitope in the cys-rich region being spatially mapped roughly half-way up the side-edge of the ectodomain plates, and the 83-14 and 18-44 MFab epitopes (connecting domain and β -chain insert domain, respectively) being mapped near the base

20 of the plates. Our preference is for a single a-b β monomer to occupy a single plate, although the possibility of a single monomer straddling the two plates of protein density cannot be discounted.

The more complex images involving co-binding of two, and even more so of all three, MFabs to each monomer of the ectodomain dimer

25 (Figures 22 and 23) are not easily interpretable with respect to relative domain arrangements within the monomer at present, not least of all because of the difficulty of finding conditions of negative staining that will simultaneously maintain the integrity of the Fab binding while highlighting recognisable and reproducible details of the internal structure of the dimeric

30 IR ectodomain.

The data presented here demonstrate the ability of single-molecule imaging to give an initial insight into the topology of multidomain structures such as the ectodomain of hIR, and the value of combining this technique with that of either single or multiple monoclonal Fab attachment per

35 monomer as a potential means of epitope (and domain) mapping of the structure. By imaging Fab complexes of other members of the family (such as

hIGF-1R ectodomain) and combining available sequence-mapped epitope information with that presented here, a more comprehensive understanding of domain arrangements within the IR family ectodomains should be forthcoming.

5 It will be appreciated by persons skilled in the art that numerous variations and/or modifications may be made to the invention as shown in the specific embodiments without departing from the spirit or scope of the invention as broadly described. The present embodiments are, therefore, to be considered in all respects as illustrative and not restrictive

Dated this twenty-seventh day of November 1997

COMMONWEALTH SCIENTIFIC
AND INDUSTRIAL RESEARCH
ORGANISATION
Patent Attorneys for the Applicant:

F.B. RICE & CO.

Figure 1 (cont'd)

ATOM	325	CG2	ILE	34	44.578	2.278	48.673	1.00	29.54	AAAAA	ATOM	488	CA	ILE	51	43.330	13.615	64.097	1.00	18.06	AAAAA	
ATOM	326	CG1	ILE	34	45.030	4.674	48.117	1.00	32.29	AAAAA	ATOM	489	CB	ILE	51	42.410	12.877	63.181	1.00	17.87	AAAAA	
ATOM	327	CD1	ILE	34	45.622	4.831	49.505	1.00	36.92	AAAAA	ATOM	490	CG2	ILE	51	42.347	13.595	61.862	1.00	20.56	AAAAA	
ATOM	328	C	ILE	34	42.997	1.911	46.541	1.00	41.31	AAAAA	ATOM	491	CG1	ILE	51	42.914	11.441	62.995	1.00	19.01	AAAAA	
ATOM	329	O	ILE	34	41.816	1.677	46.767	1.00	45.84	AAAAA	ATOM	492	CD1	ILE	51	42.192	10.630	61.930	1.00	12.40	AAAAA	
ATOM	330	N	SER	35	43.843	0.938	46.228	1.00	46.80	AAAAA	ATOM	493	C	ILE	51	42.704	14.924	64.461	1.00	18.06	AAAAA	
ATOM	332	CA	SER	35	43.344	-0.421	46.209	1.00	49.73	AAAAA	ATOM	494	O	ILE	51	41.547	14.938	64.815	1.00	18.83	AAAAA	
ATOM	333	CB	SER	35	43.673	-1.112	44.905	1.00	50.47	AAAAA	ATOM	495	N	THR	52	43.450	16.022	64.394	1.00	18.18	AAAAA	
ATOM	334	OG	SER	35	42.462	-1.424	44.229	1.00	52.41	AAAAA	ATOM	497	CA	THR	52	42.895	17.284	64.825	1.00	19.65	AAAAA	
ATOM	336	C	SER	35	43.913	-1.202	47.367	1.00	53.88	AAAAA	ATOM	498	CB	THR	52	43.984	18.250	65.229	1.00	16.95	AAAAA	
ATOM	337	O	SER	35	44.271	-0.631	48.398	1.00	57.19	AAAAA	ATOM	499	OC1	THR	52	44.551	18.826	64.064	1.00	20.53	AAAAA	
ATOM	338	N	LYS	36	43.966	-2.514	47.210	1.00	56.59	AAAAA	ATOM	501	CC2	THR	52	45.049	17.554	65.975	1.00	17.67	AAAAA	
ATOM	340	CA	LYS	36	44.494	-3.385	48.248	1.00	60.80	AAAAA	ATOM	502	C	THR	52	41.961	18.002	63.874	1.00	25.70	AAAAA	
ATOM	341	CB	LYS	36	43.687	-3.225	49.533	1.00	59.09	AAAAA	ATOM	503	O	THR	52	41.647	19.180	64.091	1.00	32.66	AAAAA	
ATOM	342	C	LYS	36	44.411	-4.813	47.708	1.00	65.16	AAAAA	ATOM	504	N	GLU	53	41.505	17.310	62.828	1.00	28.12	AAAAA	
ATOM	343	O	LYS	36	44.344	-5.346	47.480	1.00	66.62	AAAAA	ATOM	506	CA	GLU	53	40.566	17.070	61.054	1.00	22.37	AAAAA	
ATOM	344	N	ALA	37	45.591	-5.402	47.475	1.00	68.90	AAAAA	ATOM	507	CB	GLU	53	41.318	18.409	60.658	1.00	14.18	AAAAA	
ATOM	346	CA	ALA	37	45.736	-6.754	46.919	1.00	71.53	AAAAA	ATOM	508	CG	GLU	53	41.622	19.828	60.894	1.00	18.95	AAAAA	
ATOM	347	CB	ALA	37	47.153	-6.950	46.387	1.00	71.74	AAAAA	ATOM	509	CD	GLU	53	42.106	20.429	59.755	1.00	23.84	AAAAA	
ATOM	348	C	ALA	37	45.435	-7.848	47.910	1.00	73.82	AAAAA	ATOM	510	OE1	GLU	53	42.405	19.724	58.744	1.00	38.01	AAAAA	
ATOM	349	O	ALA	37	46.052	-7.902	48.972	1.00	75.57	AAAAA	ATOM	511	OE2	GLU	53	42.755	21.581	59.848	1.00	25.54	AAAAA	
ATOM	350	N	GLU	38	44.494	-8.722	47.569	1.00	75.52	AAAAA	ATOM	512	C	GLU	53	39.521	16.852	61.415	1.00	26.52	AAAAA	
ATOM	352	CA	GLU	38	44.172	-9.815	48.464	1.00	77.32	AAAAA	ATOM	513	O	GLU	53	38.688	16.407	62.242	1.00	26.32	AAAAA	
ATOM	353	CB	GLU	38	43.312	-10.831	47.746	1.00	78.46	AAAAA	ATOM	514	N	TYR	54	39.550	16.455	60.146	1.00	23.93	AAAAA	
ATOM	354	CG	GLU	38	43.676	-12.133	48.144	1.00	82.68	AAAAA	ATOM	516	CA	TYR	54	38.570	15.473	59.725	1.00	23.46	AAAAA	
ATOM	356	C	GLU	38	45.540	-10.396	48.768	1.00	88.90	AAAAA	ATOM	517	CB	TYR	54	37.659	16.094	58.690	1.00	22.70	AAAAA	
ATOM	357	O	GLU	38	45.867	-10.748	49.904	1.00	78.29	AAAAA	ATOM	518	CG	TYR	54	38.346	16.500	57.403	1.00	22.22	AAAAA	
ATOM	358	N	ASP	39	46.348	-10.454	47.718	1.00	81.01	AAAAA	ATOM	519	CD1	TYR	54	38.551	15.588	56.389	1.00	23.21	AAAAA	
ATOM	360	CA	ASP	39	47.710	-10.934	47.820	1.00	83.83	AAAAA	ATOM	520	CE1	TYR	54	39.052	15.919	55.335	1.00	23.51	AAAAA	
ATOM	361	CB	ASP	39	48.237	-11.303	46.452	1.00	86.03	AAAAA	ATOM	521	CD2	TYR	54	38.666	17.819	57.153	1.00	22.12	AAAAA	
ATOM	362	CG	ASP	39	47.138	-11.457	45.455	1.00	88.51	AAAAA	ATOM	522	CE2	TYR	54	39.161	18.112	55.917	1.00	22.42	AAAAA	
ATOM	363	OD1	ASP	39	46.526	-10.429	45.090	1.00	88.03	AAAAA	ATOM	523	CZ	TYR	54	39.349	17.285	54.912	1.00	22.77	AAAAA	
ATOM	364	OD2	ASP	39	46.883	-12.612	45.052	1.00	91.17	AAAAA	ATOM	524	OH	TYR	54	39.845	17.686	53.690	1.00	21.77	AAAAA	
ATOM	365	C	ASP	39	48.464	-9.739	48.337	1.00	84.97	AAAAA	ATOM	526	C	TYR	54	39.233	14.225	59.169	1.00	21.86	AAAAA	
ATOM	366	O	ASP	39	48.888	-8.877	47.553	1.00	84.08	AAAAA	ATOM	527	O	TYR	54	40.421	14.245	58.960	1.00	21.84	AAAAA	
ATOM	367	N	TYR	40	48.606	-9.712	49.661	1.00	85.80	AAAAA	ATOM	528	N	LEU	55	38.416	13.144	58.958	1.00	15.41	AAAAA	
ATOM	369	CA	TYR	40	49.268	-8.649	50.412	1.00	87.22	AAAAA	ATOM	529	CA	LEU	55	39.027	11.934	58.184	1.00	14.49	AAAAA	
ATOM	370	CB	TYR	40	49.271	-7.326	49.643	1.00	89.17	AAAAA	ATOM	531	CB	LEU	55	38.977	10.801	59.382	1.00	16.63	AAAAA	
ATOM	371	CZ	TYR	40	50.111	-6.208	50.243	1.00	90.06	AAAAA	ATOM	532	CG	LEU	55	39.185	9.435	58.734	1.00	12.26	AAAAA	
ATOM	372	CD1	TYR	40	50.898	-5.405	49.416	1.00	90.79	AAAAA	ATOM	533	CD1	LEU	55	40.418	9.508	59.915	1.00	11.34	AAAAA	
ATOM	373	CE1	TYR	40	51.635	-4.344	49.919	1.00	89.79	AAAAA	ATOM	534	CD2	LEU	55	39.342	8.332	59.767	1.00	10.03	AAAAA	
ATOM	374	CD2	TYR	40	50.087	-5.919	51.163	1.00	89.86	AAAAA	ATOM	535	C	LEU	55	38.158	11.604	57.163	1.00	20.33	AAAAA	
ATOM	375	CE2	TYR	40	50.828	-4.850	52.129	1.00	90.33	AAAAA	ATOM	536	O	LEU	55	36.965	10.428	57.305	1.00	25.00	AAAAA	
ATOM	376	CZ	TYR	40	51.598	-4.069	51.263	1.00	89.97	AAAAA	ATOM	537	N	LEU	56	38.747	11.519	55.967	1.00	24.00	AAAAA	
ATOM	377	OH	TYR	40	52.338	-3.005	51.706	1.00	89.12	AAAAA	ATOM	539	CA	LEU	56	37.995	11.243	54.728	1.00	23.70	AAAAA	
ATOM	379	C	TYR	40	48.347	-8.502	51.592	1.00	87.00	AAAAA	ATOM	540	CB	LEU	56	37.999	12.495	53.855	1.00	22.94	AAAAA	
ATOM	380	O	TYR	40	47.168	-8.186	51.421	1.00	86.23	AAAAA	ATOM	541	CG	LEU	56	37.799	12.541	52.336	1.00	20.25	AAAAA	
ATOM	381	N	ARG	41	48.863	-8.735	52.790	1.00	88.41	AAAAA	ATOM	542	CD1	LEU	56	36.533	11.858	51.917	1.00	24.05	AAAAA	
ATOM	383	CA	ARG	41	48.007	-8.610	53.951	1.00	88.61	AAAAA	ATOM	543	CD2	LEU	56	37.704	13.993	51.944	1.00	18.90	AAAAA	
ATOM	384	CB	ARG	41	48.591	-9.396	55.162	1.00	80.32	AAAAA	ATOM	544	C	LEU	56	38.565	10.065	53.941	1.00	27.77	AAAAA	
ATOM	385	C	CG	ARG	41	47.741	-10.487	55.527	1.00	89.97	AAAAA	ATOM	545	O	LEU	56	36.692	10.125	53.450	1.00	31.41	AAAAA
ATOM	387	C	ARG	41	47.695	-7.143	54.331	1.00	85.71	AAAAA	ATOM	546	N	PHE	58	37.592	9.315	50.837	1.00	28.80	AAAAA	
ATOM	388	O	ARG	41	47.256	-6.354	53.475	1.00	87.54	AAAAA	ATOM	547	CA	PHE	58	38.610	9.288	49.539	1.00	31.21	AAAAA	
ATOM	389	N	SER	42	47.939	-6.759	55.577	1.00	79.21	AAAAA	ATOM	548	CB	PHE	58	38.080	6.614	54.093	1.00	26.29	AAAAA	
ATOM	391	CA	SER	42	47.575	-5.425	55.974	1.00	72.84	AAAAA	ATOM	549	CG	LEU	57	39.186	6.639	55.150	1.00	23.36	AAAAA	
ATOM	392	CB	SER	42	46.337	-5.509	56.858	1.00	73.48	AAAAA	ATOM	550	CD1	LEU	57	38.605	6.932	56.943	1.00	16.08	AAAAA	
ATOM	393	CG	SER	42	45.160	-6.473	56.452	1.00	75.54	AAAAA	ATOM	551	CD2	LEU	57	39.917	5.307	55.084	1.00	17.55	AAAAA	
ATOM	395	C	SER	42	48.621	-4.595	56.679	1.00	69.63	AAAAA	ATOM	552	C	LEU	57	37.377	4.955	51.845	1.00	29.41	AAAAA	
ATOM	396	O	SER	42	49.730																	

Figure 1 (cont'd)

ATOM	644	N	ASP	68	41.050	-2.279	61.101	1.00 40.43	AAAA	ATOM	803	CG	TYR	83	31.479	19.989	52.109	1.00 41.19	AAAA
ATOM	646	CA	ASP	68	42.148	-3.116	60.675	1.00 39.06	AAAA	ATOM	804	CD1	TYR	83	30.812	19.227	51.145	1.00 42.93	AAAA
ATOM	647	CB	ASP	68	41.803	-3.768	59.348	1.00 38.97	AAAA	ATOM	805	C2	TYR	83	32.440	20.928	51.725	1.00 39.25	AAAA
ATOM	648	CG	ASP	68	41.035	-5.095	59.528	1.00 43.61	AAAA	ATOM	806	C	TYR	83	31.532	20.690	55.954	1.00 30.98	AAAA
ATOM	649	OD1	ASP	68	40.891	-5.601	60.666	1.00 47.80	AAAA	ATOM	807	O	TYR	83	31.999	21.532	56.727	1.00 37.23	AAAA
ATOM	650	OD1	ASP	68	40.575	-5.641	58.513	1.00 47.13	AAAA	ATOM	808	N	ASN	84	30.655	19.811	56.398	1.00 26.48	AAAA
ATOM	651	C	ASP	68	43.340	-2.184	60.506	1.00 39.04	AAAA	ATOM	810	CA	ASN	84	30.278	19.928	57.801	1.00 24.16	AAAA
ATOM	652	O	ASP	68	44.474	-2.611	60.583	1.00 43.53	AAAA	ATOM	811	CB	ASN	84	28.789	20.218	57.975	1.00 27.22	AAAA
ATOM	653	N	LEU	69	43.086	-0.900	60.293	1.00 36.34	AAAA	ATOM	812	CG	ASN	84	28.218	21.108	56.880	1.00 35.15	AAAA
ATOM	655	CA	LEU	69	44.171	0.035	60.114	1.00 33.82	AAAA	ATOM	813	OD1	ASN	84	28.049	22.325	57.058	1.00 33.70	AAAA
ATOM	656	CB	LEU	69	43.931	0.907	58.887	1.00 31.58	AAAA	ATOM	814	ND2	ASN	84	27.905	20.503	55.733	1.00 41.22	AAAA
ATOM	657	CG	LEU	69	44.271	0.359	57.492	1.00 32.42	AAAA	ATOM	817	C	ASN	84	30.578	18.615	58.429	1.00 25.06	AAAA
ATOM	658	CD1	LEU	69	43.850	1.410	56.473	1.00 31.21	AAAA	ATOM	818	O	ASN	84	30.111	18.309	59.511	1.00 25.08	AAAA
ATOM	659	CD1	LEU	69	45.757	0.058	57.335	1.00 29.07	AAAA	ATOM	819	N	TYR	85	31.371	17.820	57.740	1.00 25.57	AAAA
ATOM	660	C	LEU	69	44.403	0.909	61.333	1.00 35.44	AAAA	ATOM	821	CA	TYR	85	31.667	16.499	58.234	1.00 24.08	AAAA
ATOM	661	O	LEU	69	45.501	0.905	61.865	1.00 38.91	AAAA	ATOM	822	CB	TYR	85	31.579	15.531	57.059	1.00 26.41	AAAA
ATOM	662	N	PHE	70	43.552	-2.657	61.777	1.00 34.80	AAAA	ATOM	823	CG	TYR	85	30.211	15.603	56.429	1.00 32.86	AAAA
ATOM	664	CA	PHE	70	43.525	2.532	62.957	1.00 34.07	AAAA	ATOM	824	CD1	TYR	85	30.017	16.201	55.184	1.00 35.46	AAAA
ATOM	665	CB	PHE	70	42.919	3.911	62.661	1.00 32.17	AAAA	ATOM	825	CE1	TYR	85	28.708	16.397	54.663	1.00 39.67	AAAA
ATOM	666	CG	PHE	70	43.349	4.500	61.356	1.00 34.96	AAAA	ATOM	826	C2	TYR	85	29.079	15.185	57.139	1.00 36.81	AAAA
ATOM	667	CD1	PHE	70	42.403	4.969	60.447	1.00 37.93	AAAA	ATOM	827	CE2	TYR	85	27.772	15.372	56.635	1.00 37.07	AAAA
ATOM	668	CD2	PHE	70	44.692	4.579	61.016	1.00 37.23	AAAA	ATOM	828	CZ	TYR	85	27.585	15.985	55.403	1.00 38.10	AAAA
ATOM	669	CE1	PHE	70	42.795	5.514	59.192	1.00 38.38	AAAA	ATOM	829	OH	TYR	85	26.294	16.253	54.952	1.00 38.56	AAAA
ATOM	670	CE2	PHE	70	45.097	5.118	59.774	1.00 38.80	AAAA	ATOM	831	C	TYR	85	32.994	16.408	58.961	1.00 22.97	AAAA
ATOM	671	CZ	PHE	70	44.136	5.585	58.860	1.00 36.98	AAAA	ATOM	832	O	TYR	85	33.864	17.243	58.806	1.00 23.68	AAAA
ATOM	672	C	PHE	70	42.888	1.984	64.268	1.00 34.58	AAAA	ATOM	833	N	ALA	86	33.119	15.387	59.784	1.00 19.80	AAAA
ATOM	673	O	PHE	70	42.028	2.632	64.870	1.00 35.55	AAAA	ATOM	835	CA	ALA	86	34.308	15.169	60.544	1.00 18.47	AAAA
ATOM	674	N	PRO	71	43.345	0.817	64.761	1.00 33.10	AAAA	ATOM	836	CB	ALA	86	34.003	15.329	62.038	1.00 16.82	AAAA
ATOM	675	CD	PRO	71	44.435	-0.034	64.264	1.00 32.31	AAAA	ATOM	837	C	ALA	86	34.769	13.752	60.243	1.00 19.67	AAAA
ATOM	676	CA	PRO	71	42.764	0.267	65.981	1.00 29.95	AAAA	ATOM	838	O	ALA	86	35.875	13.385	60.598	1.00 26.38	AAAA
ATOM	677	CB	PRO	71	41.671	-0.902	66.319	1.00 30.32	AAAA	ATOM	839	N	LEU	87	33.924	12.960	59.589	1.00 18.21	AAAA
ATOM	678	CG	PRO	71	44.287	-1.274	65.070	1.00 30.97	AAAA	ATOM	841	CA	LEU	87	34.234	11.569	59.252	1.00 17.46	AAAA
ATOM	679	C	PRO	71	42.630	1.192	67.164	1.00 30.13	AAAA	ATOM	842	CB	LEU	87	33.733	10.617	60.359	1.00 15.18	AAAA
ATOM	680	O	PRO	71	41.814	0.935	68.032	1.00 32.19	AAAA	ATOM	843	CG	LEU	87	34.392	9.248	60.579	1.00 17.81	AAAA
ATOM	681	N	ASN	72	43.403	2.269	67.227	1.00 32.30	AAAA	ATOM	844	CD1	LEU	87	33.454	8.293	61.318	1.00 15.41	AAAA
ATOM	683	CA	ASN	72	43.308	3.129	68.406	1.00 30.05	AAAA	ATOM	845	C2	LEU	87	34.808	8.664	59.242	1.00 15.94	AAAA
ATOM	684	CB	ASN	72	44.627	3.106	69.148	1.00 31.90	AAAA	ATOM	847	O	LEU	87	32.266	11.080	58.050	1.00 25.36	AAAA
ATOM	686	OD1	ASN	72	44.925	2.133	71.321	1.00 40.32	AAAA	ATOM	848	N	VAL	88	34.134	11.236	56.842	1.00 25.20	AAAA
ATOM	687	ND2	ASN	72	44.571	0.742	69.580	1.00 38.86	AAAA	ATOM	850	CA	VAL	88	33.450	10.935	55.579	1.00 23.38	AAAA
ATOM	690	C	ASN	72	42.848	4.568	68.270	1.00 28.80	AAAA	ATOM	851	CB	VAL	88	33.729	12.006	54.537	1.00 20.53	AAAA
ATOM	691	O	ASN	72	42.935	5.334	69.331	1.00 27.04	AAAA	ATOM	852	CG1	VAL	88	33.034	11.657	53.266	1.00 18.70	AAAA
ATOM	692	N	LEU	73	42.343	4.945	67.100	1.00 29.19	AAAA	ATOM	853	CG2	VAL	88	33.282	13.357	55.035	1.00 16.49	AAAA
ATOM	694	CA	LEU	73	41.863	3.317	66.924	1.00 29.71	AAAA	ATOM	854	C	VAL	88	33.976	9.607	55.054	1.00 26.49	AAAA
ATOM	695	CB	LEU	73	41.221	6.507	65.526	1.00 26.82	AAAA	ATOM	855	O	VAL	88	35.175	9.468	54.876	1.00 30.57	AAAA
ATOM	696	CG	LEU	73	40.851	7.925	65.067	1.00 23.15	AAAA	ATOM	856	N	ILE	89	33.086	8.618	54.829	1.00 28.28	AAAA
ATOM	697	CD1	LEU	73	42.074	8.766	65.023	1.00 23.71	AAAA	ATOM	858	CA	ILE	89	33.436	7.293	54.333	1.00 27.07	AAAA
ATOM	698	CD2	LEU	73	40.199	7.904	63.724	1.00 21.56	AAAA	ATOM	859	CB	ILE	89	33.091	6.197	55.374	1.00 24.54	AAAA
ATOM	699	C	LEU	73	40.842	6.495	68.040	1.00 29.01	AAAA	ATOM	860	CG2	ILE	89	33.293	4.816	54.777	1.00 27.52	AAAA
ATOM	700	O	LEU	73	40.010	5.634	68.263	1.00 32.12	AAAA	ATOM	861	CG1	ILE	89	33.973	6.141	56.606	1.00 20.83	AAAA
ATOM	701	N	THR	74	40.889	7.613	68.733	1.00 27.72	AAAA	ATOM	862	CD1	ILE	89	33.296	5.897	57.855	1.00 18.09	AAAA
ATOM	703	CA	THR	74	39.981	7.805	69.835	1.00 28.07	AAAA	ATOM	863	C	ILE	89	32.565	7.053	53.112	1.00 29.32	AAAA
ATOM	704	CB	THR	74	40.805	7.705	71.094	1.00 33.31	AAAA	ATOM	864	O	ILE	89	31.535	6.406	53.220	1.00 32.09	AAAA
ATOM	705	CG1	THR	74	41.556	6.556	65.076	1.00 36.36	AAAA	ATOM	865	N	PHE	90	33.008	7.533	51.953	1.00 29.27	AAAA
ATOM	707	CZ2	THR	74	39.949	7.732	72.347	1.00 32.71	AAAA	ATOM	867	CA	PHE	90	32.233	7.478	50.709	1.00 26.81	AAAA
ATOM	708	C	THR	74	39.247	9.122	69.756	1.00 26.87	AAAA	ATOM	868	CB	PHE	90	32.329	8.876	50.101	1.00 26.19	AAAA
ATOM	709	NH1	ARG	77	40.587	17.881	71.725	1.00 31.08	AAAA	ATOM	869	CG	PHE	90	31.564	9.053	48.845	1.00 28.17	AAAA
ATOM	739	NH2	ARG	77	40.436	20.178	71.681	1.00 36.79	AAAA	ATOM	870	CD1	PHE	90	30.331	9.678	48.859	1.00 29.79	AAAA
ATOM	742	C	ARG	77	37.717	17.784	66.005	1.00 23.31	AAAA	ATOM	871	C2	PHE	90	32.083	8.527	48.744	1.00 30.39	AAAA
ATOM	743	O	ARG	77	37.053	18.698	66.491	1.00 26.16	AAAA	ATOM	872	CE1	PHE	90	32.623	9.881	47.693	1.00 31.81	AAAA
ATOM	744	N	GLY	78	37.746	17.543	64.546	1.00 23.75	AAAA	ATOM	873	CE2	PHE	90	31.191	8.820	46.465	1.00 32.27	AAAA
ATOM	746	CA	GLY	78	36.959	18.358	63.788	1.00 19.61	AAAA	ATOM	874	CZ	PHE	90	30.150	9.454	46.489	1.00 34.74	AAAA
ATOM	747	C	GLY	78	37.196	19.859	63.881	1.00 24.91	AAAA	ATOM	890	CG1	THR	93	34.144	-0.837</			

Figure 1 (cont'd)

ATOM	950	O	GLY	99	37.444	-0.712	64.884	1.00	30.61	AAAAA	ATOM	1129	C	LYS	115	28.391	3.478	49.588	1.00	32.76	AAAAA
ATOM	951	N	LEU	100	36.304	1.118	64.206	1.00	23.75	AAAAA	ATOM	1130	O	LYS	115	29.478	3.462	49.059	1.00	37.00	AAAAA
ATOM	953	CA	LEU	100	37.041	2.075	65.016	1.00	20.90	AAAAA	ATOM	1131	N	ASN	116	28.025	2.576	50.500	1.00	34.74	AAAAA
ATOM	954	CB	LEU	100	36.784	3.507	64.495	1.00	17.96	AAAAA	ATOM	1133	CA	ASN	116	28.905	1.492	50.940	1.00	33.69	AAAAA
ATOM	955	CG	LEU	100	37.104	3.790	63.009	1.00	15.59	AAAAA	ATOM	1134	CB	ASN	116	29.448	1.815	52.310	1.00	33.99	AAAAA
ATOM	956	CD1	LEU	100	36.820	5.238	62.704	1.00	11.00	AAAAA	ATOM	1135	CG	ASN	116	30.324	1.002	52.272	1.00	34.39	AAAAA
ATOM	957	CD2	LEU	100	38.570	3.495	62.695	1.00	11.68	AAAAA	ATOM	1136	OD1	ASN	116	31.332	2.983	51.600	1.00	38.07	AAAAA
ATOM	958	C	LEU	100	36.580	1.936	66.440	1.00	19.15	AAAAA	ATOM	1137	ND2	ASN	116	29.944	4.061	52.963	1.00	35.45	AAAAA
ATOM	959	O	LEU	100	36.117	2.893	67.028	1.00	18.03	AAAAA	ATOM	1140	C	ASN	116	28.153	0.179	50.986	1.00	36.41	AAAAA
ATOM	970	N	TYR	101	36.730	0.741	66.994	1.00	23.04	AAAAA	ATOM	1141	O	ASN	116	27.932	-0.396	51.062	1.00	37.95	AAAAA
ATOM	972	CA	TYR	101	36.270	0.456	68.358	1.00	29.36	AAAAA	ATOM	1142	N	ALA	117	27.796	-0.303	49.801	1.00	36.22	AAAAA
ATOM	973	C	TYR	101	36.488	-1.023	68.722	1.00	29.53	AAAAA	ATOM	1144	CA	ALA	117	27.005	-1.512	49.636	1.00	36.19	AAAAA
ATOM	974	CG	TYR	101	37.890	-1.499	68.515	1.00	30.31	AAAAA	ATOM	1145	CB	ALA	117	27.260	-2.093	48.290	1.00	38.96	AAAAA
ATOM	975	CD1	TYR	101	38.844	-1.386	69.525	1.00	29.96	AAAAA	ATOM	1146	C	ALA	117	27.078	-2.595	50.686	1.00	38.96	AAAAA
ATOM	976	CE1	TYR	101	40.133	-1.828	69.342	1.00	29.17	AAAAA	ATOM	1147	O	ALA	117	26.036	-3.065	51.118	1.00	41.77	AAAAA
ATOM	977	CD2	TYR	101	38.268	-2.065	67.306	1.00	30.96	AAAAA	ATOM	1148	N	ASP	118	28.272	-3.003	51.106	1.00	39.97	AAAAA
ATOM	978	CG2	TYR	101	39.543	-3.510	67.100	1.00	33.23	AAAAA	ATOM	1150	CA	ASP	118	28.370	-4.080	52.778	1.00	38.19	AAAAA
ATOM	979	C	TYR	101	40.480	-2.197	68.131	1.00	36.10	AAAAA	ATOM	1151	CB	ASP	118	29.378	-5.158	51.719	1.00	44.53	AAAAA
ATOM	980	OH	TYR	101	41.755	-2.908	67.934	1.00	44.43	AAAAA	ATOM	1152	CG	ASP	118	29.527	-5.314	50.222	1.00	52.11	AAAAA
ATOM	982	C	TYR	101	36.834	1.319	69.470	1.00	32.61	AAAAA	ATOM	1153	OD1	ASP	118	28.722	-6.002	49.628	1.00	56.23	AAAAA
ATOM	983	O	TYR	101	36.387	1.213	70.628	1.00	35.65	AAAAA	ATOM	1154	OD2	ASP	118	30.452	-4.683	49.645	1.00	55.85	AAAAA
ATOM	984	N	ASN	102	37.804	2.173	69.146	1.00	34.59	AAAAA	ATOM	1155	C	ASP	118	28.759	-3.847	53.471	1.00	33.85	AAAAA
ATOM	986	CA	ASN	102	38.368	3.060	70.156	1.00	32.17	AAAAA	ATOM	1156	O	ASP	118	29.152	-4.487	54.258	1.00	33.86	AAAAA
ATOM	987	CB	ASN	102	39.883	2.919	70.153	1.00	34.62	AAAAA	ATOM	1157	N	LEU	119	28.682	-2.353	53.755	1.00	32.24	AAAAA
ATOM	988	CG	ASN	102	40.355	1.842	71.107	1.00	38.21	AAAAA	ATOM	1159	CA	LEU	119	29.050	-1.880	55.080	1.00	31.63	AAAAA
ATOM	989	OD1	ASN	102	40.312	2.018	72.328	1.00	39.16	AAAAA	ATOM	1160	CB	LEU	119	29.252	-0.351	55.121	1.00	27.83	AAAAA
ATOM	990	ND2	ASN	102	40.783	0.709	70.560	1.00	37.20	AAAAA	ATOM	1161	CG	LEU	119	29.561	0.331	56.478	1.00	24.81	AAAAA
ATOM	993	C	ASN	102	37.928	4.506	69.909	1.00	33.35	AAAAA	ATOM	1162	CD1	LEU	119	30.651	-0.392	57.220	1.00	22.15	AAAAA
ATOM	994	O	ASN	102	38.322	5.443	70.621	1.00	34.93	AAAAA	ATOM	1163	CD2	LEU	119	30.010	1.749	56.268	1.00	19.88	AAAAA
ATOM	995	N	LEU	103	37.089	4.681	68.889	1.00	33.71	AAAAA	ATOM	1164	C	LEU	119	27.975	-2.281	56.057	1.00	32.07	AAAAA
ATOM	997	CA	LEU	103	36.571	6.006	68.519	1.00	32.44	AAAAA	ATOM	1165	O	LEU	119	26.809	-1.990	55.858	1.00	34.96	AAAAA
ATOM	998	CB	LEU	103	35.879	5.969	67.157	1.00	27.71	AAAAA	ATOM	1166	N	CYS	120	28.376	-2.980	57.107	1.00	33.19	AAAAA
ATOM	999	CG	LEU	103	35.495	2.287	66.474	1.00	24.01	AAAAA	ATOM	1168	CA	CYS	120	27.448	-3.403	58.132	1.00	33.58	AAAAA
ATOM	1000	CD1	LEU	103	36.520	8.393	66.654	1.00	14.91	AAAAA	ATOM	1169	C	CYS	120	27.930	-2.883	59.481	1.00	32.10	AAAAA
ATOM	1001	CD2	LEU	103	35.342	6.955	65.028	1.00	26.24	AAAAA	ATOM	1170	O	CYS	120	28.803	-2.019	59.546	1.00	31.93	AAAAA
ATOM	1002	C	LEU	103	35.598	6.465	69.623	1.00	30.84	AAAAA	ATOM	1171	CB	CYS	120	27.352	-4.917	58.155	1.00	37.34	AAAAA
ATOM	1003	O	LEU	103	34.479	5.966	69.711	1.00	30.84	AAAAA	ATOM	1172	SG	CYS	120	26.669	-5.595	56.623	1.00	30.24	AAAAA
ATOM	1004	N	ARG	104	36.027	7.422	70.437	1.00	28.81	AAAAA	ATOM	1173	N	TYR	121	27.385	-3.430	60.558	1.00	28.35	AAAAA
ATOM	1006	CA	ARG	104	35.185	7.877	71.502	1.00	26.99	AAAAA	ATOM	1175	CA	TYR	121	27.776	-2.980	61.864	1.00	27.48	AAAAA
ATOM	1007	CB	ARG	104	35.954	7.732	72.815	1.00	31.56	AAAAA	ATOM	1176	CB	TYR	121	29.131	-3.567	62.266	1.00	26.64	AAAAA
ATOM	1008	CG	ARG	104	36.358	6.291	71.131	1.00	33.27	AAAAA	ATOM	1177	CG	TYR	121	28.977	-4.954	62.829	1.00	28.75	AAAAA
ATOM	1009	CD	ARG	104	35.132	5.480	73.542	1.00	35.96	AAAAA	ATOM	1178	CD1	TYR	121	29.360	-6.069	62.091	1.00	32.77	AAAAA
ATOM	1010	NE	ARG	104	35.425	4.504	74.671	1.00	40.69	AAAAA	ATOM	1179	CE1	TYR	121	29.080	-7.364	62.543	1.00	38.16	AAAAA
ATOM	1011	CZ	ARG	104	34.889	5.012	75.977	1.00	46.43	AAAAA	ATOM	1180	CD2	TYR	121	28.318	-5.160	64.047	1.00	33.31	AAAAA
ATOM	1015	C	ARG	104	34.577	9.269	71.408	1.00	26.61	AAAAA	ATOM	1181	CE2	TYR	121	28.030	-6.440	64.512	1.00	36.57	AAAAA
ATOM	1016	O	ARG	104	33.618	9.562	72.120	1.00	28.46	AAAAA	ATOM	1182	CZ	TYR	121	28.409	-7.543	63.750	1.00	39.97	AAAAA
ATOM	1017	N	ASN	105	35.067	10.131	70.531	1.00	24.00	AAAAA	ATOM	1183	CH	TYR	121	28.087	-8.825	64.171	1.00	45.83	AAAAA
ATOM	1019	CA	ASN	105	34.510	11.744	70.528	1.00	20.78	AAAAA	ATOM	1184	C	TYR	121	27.832	-1.496	61.770	1.00	27.62	AAAAA
ATOM	1020	CB	ASN	105	35.156	12.263	71.594	1.00	18.92	AAAAA	ATOM	1186	O	TYR	121	28.835	-5.886	62.121	1.00	31.85	AAAAA
ATOM	1021	CO	ASN	105	34.633	13.727	71.779	1.00	27.94	AAAAA	ATOM	1187	N	LEU	122	26.741	-0.934	61.246	1.00	31.58	AAAAA
ATOM	1022	OD1	ASN	105	35.159	14.694	71.595	1.00	28.87	AAAAA	ATOM	1189	CA	LEU	122	26.544	0.522	61.095	1.00	34.25	AAAAA
ATOM	1023	ND2	ASN	105	33.540	13.937	72.545	1.00	29.96	AAAAA	ATOM	1190	CB	LEU	122	26.220	0.889	59.629	1.00	34.23	AAAAA
ATOM	1025	O	ASN	105	34.895	12.254	68.930	1.00	24.92	AAAAA	ATOM	1191	CG	VAL	125	26.867	3.175	67.360	1.00	24.24	AAAAA
ATOM	1067	N	ALA	110	29.683	16.577	61.906	1.00	28.32	AAAAA	ATOM	1220	O	VAL	125	25.029	3.695	66.669	1.00	29.23	AAAAA
ATOM	1069	CA	ALA	110	28.914	15.322	61.835	1.00	23.60	AAAAA	ATOM	1230	N	TRP	127	26.111	6.596	67.776	1.00	27.25	AAAAA
ATOM	1070	CB	ALA	110	27.573	15.585	61.269	1.00	19.14	AAAAA	ATOM	1232	CA	TRP	127	26.845	7.832	67.526	1.00	23.75	AAAAA
ATOM	1071	C	ALA	110	29.628	14.307	60.974	1.00	22.79	AAAAA	ATOM	1233	CB	TRP	127	26.657	8.301	66.067	1.00	29.26	AAAAA
ATOM	1072	O	ALA	110	30.707	14.543	60.467	1.00	26.36	AAAAA	ATOM	1234</td									

Figure 1 (cont'd)

ATOM	1285	CG	ASP	132	27.203	17.299	71.583	1.00 40.20	AAAA	ATOM	1445	C	ASP	150	24.550	-8.922	63.833	1.00 41.30	AAAA	
ATOM	1286	OD1	ASP	132	26.867	16.379	72.461	1.00 46.09	AAAA	ATOM	1446	O	ASP	150	23.458	-8.771	64.376	1.00 44.58	AAAA	
ATOM	1287	OD2	ASP	132	27.531	18.454	72.055	1.00 44.38	AAAA	ATOM	1447	N	LEU	151	25.536	-9.597	64.398	1.00 37.30	AAAA	
ATOM	1288	C	ASP	132	25.570	15.814	68.876	1.00 29.06	AAAA	ATOM	1449	CA	LEU	151	25.359	-10.181	65.699	1.00 35.09	AAAA	
A...	1289	O	ASP	132	24.460	15.362	69.093	1.00 34.86	AAAA	ATOM	1450	CB	LEU	151	25.407	-11.702	65.571	1.00 38.32	AAAA	
ATOM	1290	N	ALA	133	25.913	16.511	67.792	1.00 26.57	AAAA	ATOM	1451	OC	LEU	151	24.168	-12.207	65.097	1.00 36.38	AAAA	
ATOM	1292	CA	ALA	133	25.060	16.891	66.665	1.00 22.34	AAAA	ATOM	1453	C	LEU	151	26.452	-9.655	66.624	1.00 34.61	AAAA	
ATOM	1293	CB	ALA	133	25.767	17.973	65.893	1.00 22.29	AAAA	ATOM	1454	O	LEU	151	27.640	-9.885	66.409	1.00 33.41	AAAA	
ATOM	1294	C	ALA	133	24.683	15.764	65.703	1.00 22.13	AAAA	ATOM	1455	N	CYS	152	26.045	-8.937	67.659	1.00 35.32	AAAA	
ATOM	1295	O	ALA	133	24.814	15.896	64.478	1.00 20.05	AAAA	ATOM	1457	CA	CYS	152	27.006	-8.365	68.593	1.00 40.29	AAAA	
ATOM	1296	N	VAL	134	24.194	14.667	66.252	1.00 22.27	AAAA	ATOM	1458	C	CYS	152	27.570	-9.463	69.480	1.00 43.08	AAAA	
ATOM	1298	CA	VAL	134	23.813	13.524	65.448	1.00 24.74	AAAA	ATOM	1459	O	CYS	152	26.977	-10.542	69.568	1.00 45.04	AAAA	
ATOM	1299	CB	VAL	134	23.360	12.171	66.353	1.00 23.00	AAAA	ATOM	1460	CB	CYS	152	26.342	-7.288	69.473	1.00 37.72	AAAA	
ATOM	1300	CG1	VAL	134	22.194	12.804	67.154	1.00 27.35	AAAA	ATOM	1461	SG	CYS	152	26.098	-5.631	68.736	1.00 37.05	AAAA	
ATOM	1301	CG2	VAL	134	22.996	11.152	65.547	1.00 29.73	AAAA	ATOM	1462	N	PRO	153	26.739	-9.216	70.121	1.00 45.27	AAAA	
ATOM	1302	C	VAL	134	22.699	13.884	64.478	1.00 29.00	AAAA	ATOM	1463	CD	PRO	153	29.565	-8.005	69.975	1.00 41.44	AAAA	
ATOM	1301	O	VAL	134	22.585	12.288	63.416	1.00 36.69	AAAA	ATOM	1464	CA	PRO	153	29.381	-10.190	71.012	1.00 47.26	AAAA	
ATOM	1304	N	SER	135	21.880	14.869	64.824	1.00 29.17	AAAA	ATOM	1465	C	PRO	153	30.591	-9.439	71.562	1.00 46.10	AAAA	
ATOM	1306	CA	SER	135	20.796	15.257	63.950	1.00 29.17	AAAA	ATOM	1466	CG	PRO	153	30.894	-8.438	70.530	1.00 44.99	AAAA	
ATOM	1307	CB	SER	135	20.111	16.477	64.504	1.00 27.10	AAAA	ATOM	1467	C	PRO	153	28.442	-10.694	72.113	1.00 50.81	AAAA	
ATOM	1308	OG	SER	135	21.062	17.327	65.070	1.00 23.39	AAAA	ATOM	1468	O	PRO	153	27.825	-9.923	72.865	1.00 47.27	AAAA	
ATOM	1310	C	SER	135	21.232	15.552	62.511	1.00 34.63	AAAA	ATOM	1469	N	GLY	154	28.339	-12.015	72.167	1.00 57.66	AAAA	
ATOM	1311	O	SER	135	20.404	15.509	61.586	1.00 36.08	AAAA	ATOM	1471	CA	GLY	154	27.477	-12.680	73.125	1.00 67.39	AAAA	
ATOM	1312	N	ASN	136	22.506	15.866	62.272	1.00 38.35	AAAA	ATOM	1472	C	GLY	154	26.279	-13.135	72.442	1.00 72.88	AAAA	
ATOM	1314	CA	ASN	136	22.847	16.132	60.882	1.00 39.46	AAAA	ATOM	1473	O	GLY	154	25.998	-14.517	72.652	1.00 75.86	AAAA	
ATOM	1315	CB	ASN	136	23.071	17.632	60.650	1.00 43.49	AAAA	ATOM	1474	N	THR	155	25.592	-12.553	71.612	1.00 75.09	AAAA	
ATOM	1316	CG	ASN	136	24.275	18.155	61.314	1.00 49.28	AAAA	ATOM	1476	CA	THR	155	24.400	-12.955	70.874	1.00 76.56	AAAA	
ATOM	1317	OD1	ASN	136	24.266	18.420	62.514	1.00 51.34	AAAA	ATOM	1477	CB	THR	155	24.209	-12.007	69.709	1.00 74.93	AAAA	
ATOM	1318	ND2	ASN	136	25.349	18.334	60.533	1.00 58.07	AAAA	ATOM	1478	O	CG1	THR	155	24.169	-10.665	70.210	1.00 73.48	AAAA
ATOM	1321	C	ASN	136	23.897	15.261	60.189	1.00 35.57	AAAA	ATOM	1480	CG2	THR	155	22.932	-12.329	69.965	1.00 74.24	AAAA	
ATOM	1322	O	ASN	136	24.619	15.688	59.273	1.00 35.22	AAAA	ATOM	1481	C	THR	155	24.253	-14.386	70.351	1.00 80.38	AAAA	
ATOM	1323	N	ASN	137	23.894	14.002	60.613	1.00 30.60	AAAA	ATOM	1482	O	THR	155	23.234	-15.039	70.602	1.00 80.09	AAAA	
ATOM	1325	CA	ASN	137	24.734	12.974	60.051	1.00 27.82	AAAA	ATOM	1483	N	MET	156	25.248	-18.868	69.609	1.00 85.70	AAAA	
ATOM	1326	CB	ASN	137	24.732	11.747	60.947	1.00 20.95	AAAA	ATOM	1485	CA	MET	156	25.191	-16.219	69.038	1.00 89.85	AAAA	
ATOM	1327	CG	ASN	137	25.518	11.972	62.173	1.00 17.44	AAAA	ATOM	1486	CB	MET	156	26.072	-16.305	67.777	1.00 93.38	AAAA	
ATOM	1328	OD1	ASN	137	26.000	13.072	62.395	1.00 18.82	AAAA	ATOM	1487	CG	MET	156	25.481	-15.618	68.526	1.00 96.33	AAAA	
ATOM	1329	ND2	ASN	137	25.654	10.958	62.993	1.00 17.51	AAAA	ATOM	1488	SD	MET	156	24.697	-15.732	65.287	1.00 100.00	AAAA	
ATOM	1332	C	ASN	137	24.005	12.675	58.769	1.00 30.30	AAAA	ATOM	1489	CE	MET	156	22.937	-16.735	65.851	1.00 99.65	AAAA	
ATOM	1333	O	ASN	137	22.792	12.889	58.720	1.00 32.71	AAAA	ATOM	1490	C	MET	156	25.611	-17.282	70.053	1.00 90.29	AAAA	
ATOM	1334	N	TYR	138	24.732	12.178	57.754	1.00 31.84	AAAA	ATOM	1491	O	MET	156	25.660	-18.479	69.752	1.00 90.33	AAAA	
ATOM	1336	CA	TYR	138	24.188	11.869	56.427	1.00 27.90	AAAA	ATOM	1492	N	GLU	157	25.918	-16.820	71.258	1.00 90.50	AAAA	
ATOM	1337	CB	TYR	138	24.795	12.793	55.375	1.00 30.75	AAAA	ATOM	1494	CA	GLU	157	26.315	-17.690	72.360	1.00 89.67	AAAA	
ATOM	1338	CG	TYR	138	24.084	12.786	54.027	1.00 39.45	AAAA	ATOM	1495	CB	GLU	157	27.735	-17.337	72.819	1.00 91.16	AAAA	
ATOM	1339	CD1	TYR	138	23.304	13.883	53.607	1.00 39.30	AAAA	ATOM	1496	C	GLU	157	25.320	-17.500	73.512	1.00 87.84	AAAA	
ATOM	1340	CE1	TYR	138	22.744	13.928	53.740	1.00 41.16	AAAA	ATOM	1497	O	GLU	157	25.653	-16.718	74.678	1.00 87.91	AAAA	
ATOM	1341	CD2	TYR	138	24.274	11.721	53.122	1.00 41.34	AAAA	ATOM	1498	N	GLU	158	24.103	-17.090	73.164	1.00 85.28	AAAA	
ATOM	1342	CE2	TYR	138	23.721	11.774	51.838	1.00 41.53	AAAA	ATOM	1500	CA	GLU	158	23.047	-16.845	74.135	1.00 83.35	AAAA	
ATOM	1343	CB2	TYR	138	22.966	12.866	51.439	1.00 43.01	AAAA	ATOM	1501	CB	GLU	158	22.200	-18.100	74.328	1.00 88.22	AAAA	
ATOM	1344	OR1	TYR	138	22.480	12.879	50.148	1.00 45.40	AAAA	ATOM	1502	CG	GLU	158	20.684	-17.845	74.202	1.00 94.30	AAAA	
ATOM	1346	C	TYR	138	24.480	10.462	56.060	1.00 24.71	AAAA	ATOM	1503	CD	GLU	158	20.072	-18.391	72.903	1.00 96.87	AAAA	
ATOM	1347	O	TYR	138	25.569	10.147	55.635	1.00 26.78	AAAA	ATOM	1504	OE1	GLU	158	20.829	-18.618	71.924	1.00 99.26	AAAA	
ATOM	1348	N	ILE	139	23.474	9.621	56.185	1.00 25.19	AAAA	ATOM	1505	OE2	GLU	158	18.831	-18.590	72.865	1.00 97.31	AAAA	
ATOM	1350	CA	ILE	139	23.646	8.221	55.906	1.00 25.42	AAAA	ATOM	1506	C	ILE	159	23.616	-16.384	75.460	1.00 79.85	AAAA	
ATOM	1351	C	ILE	139	23.385	7.409	51.151	1.00 24.65	AAAA	ATOM	1507	O	ILE	159	23.514	-16.080	79.509	1.00 64.85	AAAA	
ATOM	1352	CG2	ILE	139	22.731	-2.505	54.115	1.00 42.12	AAAA	ATOM	1508	CD1	GLU	163	26.573	-1.513	75.801	1.00 67.74	AAAA	
ATOM	1393	O	LYS	143	22.653	-1.998	55.237	1.00 44.30	AAAA	ATOM	1504	OE2	GLU	163	26.461	-1.824	80.510	1.00 69.44	AAAA	
ATOM	1394	N	PRO	144	21.695	-3.164	53.586	1.00 40.49	AAAA	ATOM	1505	C	GLU	163	24.061	-1.456	75.503	1.00 44.29	AAAA	
ATOM	1395	CD	PRO	144	21.559	-3.774	52.262	1.00 40.92	AAAA	ATOM	1506	CG	GLU	163	24.246	-2.644	74.300	1.00 46.58	AAAA	
ATOM	1396	CA	PRO	144	20.426	-3.286	54.365	1.00 39.12	AAAA	ATOM	1507	N	LYS	164	22.967	-1.879	75.982	1.00 40.91	AAAA	
ATOM	1397	CB	PRO	144	19.470	-3.861	53.368	1.00 40.42	AAAA	ATOM	1509	CA	LYS	164	21.879	-1.478	75.100	1.00 38.39	AAAA	
ATOM	1398	CG	PRO	144	20.108	-3.														

Figure 1 (cont'd)

ATOM	1603	OD1	ASN	169	10.912	5.715	70.234	1.00	34.96	AAAAA	ATOM	1775	O	LYS	183	32.015	3.424	75.624	1.00	44.70	AAAAA
ATOM	1604	ND2	ASN	169	10.740	5.266	68.070	1.00	37.96	AAAAA	ATOM	1776	N	MET	184	30.602	1.945	76.503	1.00	40.72	AAAAA
ATOM	1607	C	ASN	169	12.891	2.134	68.758	1.00	38.71	AAAAA	ATOM	1778	CA	MET	184	29.890	2.991	77.223	1.00	41.46	AAAAA
ATOM	1608	O	ASN	169	11.977	1.320	68.658	1.00	38.30	AAAAA	ATOM	1779	CB	MET	184	28.422	2.563	77.447	1.00	40.50	AAAAA
ATOM	1609	N	GLU	170	14.170	1.803	68.845	1.00	38.73	AAAAA	ATOM	1780	CG	MET	184	27.193	1.166	76.484	1.00	38.93	AAAAA
ATOM	1611	C	GLU	170	14.636	0.439	68.874	1.00	39.83	AAAAA	ATOM	1781	SD	MET	184	26.858	2.058	75.119	1.00	40.97	AAAAA
ATOM	1612	CB	GLU	170	15.283	0.061	67.536	1.00	49.61	AAAAA	ATOM	1782	CE	MET	184	26.902	0.624	75.907	1.00	38.40	AAAAA
ATOM	1613	CG	GLU	170	15.641	-1.439	67.359	1.00	61.29	AAAAA	ATOM	1783	C	MET	184	30.691	3.044	78.534	1.00	42.46	AAAAA
ATOM	1614	CD	GLU	170	14.986	-2.100	66.120	1.00	68.52	AAAAA	ATOM	1784	O	MET	184	31.461	2.136	78.790	1.00	42.71	AAAAA
ATOM	1615	OE1	GLU	170	14.678	-3.324	66.196	1.00	74.04	AAAAA	ATOM	1785	N	CYS	185	30.540	4.086	79.352	1.00	47.34	AAAAA
ATOM	1616	OE2	GLU	170	14.779	-1.406	65.083	1.00	69.19	AAAAA	ATOM	1787	CA	CYS	185	31.275	4.163	80.629	1.00	51.78	AAAAA
ATOM	1617	C	GLU	170	15.660	0.444	69.987	1.00	36.76	AAAAA	ATOM	1788	C	CYS	185	30.392	4.206	81.906	1.00	56.36	AAAAA
ATOM	1618	O	GLU	170	16.590	1.243	70.006	1.00	34.63	AAAAA	ATOM	1789	O	CYS	185	29.204	4.519	81.832	1.00	57.21	AAAAA
ATOM	1619	N	TYR	171	15.441	-0.436	70.943	1.00	35.62	AAAAA	ATOM	1790	CB	CYS	185	32.220	5.365	80.614	1.00	51.30	AAAAA
ATOM	1621	CA	TYR	171	16.312	-0.577	72.086	1.00	34.58	AAAAA	ATOM	1791	SG	CYS	185	33.964	4.677	80.835	1.00	51.40	AAAAA
ATOM	1622	CB	TYR	171	15.447	-0.785	71.325	1.00	12.84	AAAAA	ATOM	1792	N	PRO	186	30.974	3.014	82.104	1.00	50.68	AAAAA
ATOM	1623	CC	TYR	171	16.170	-1.153	74.595	1.00	32.37	AAAAA	ATOM	1793	CD	PRO	186	32.378	3.611	82.424	1.00	60.70	AAAAA
ATOM	1624	CD1	TYR	171	17.036	-0.249	75.207	1.00	28.71	AAAAA	ATOM	1794	CA	PRO	186	30.176	3.932	82.329	1.00	57.39	AAAAA
ATOM	1625	CE1	TYR	171	17.645	-0.536	76.382	1.00	25.22	AAAAA	ATOM	1795	CB	PRO	186	31.203	3.773	85.448	1.00	57.78	AAAAA
ATOM	1626	CD2	TYR	171	15.938	-2.381	75.217	1.00	30.01	AAAAA	ATOM	1796	CC	PRO	186	32.488	4.105	84.839	1.00	58.33	AAAAA
ATOM	1627	CE2	TYR	171	16.547	-2.677	76.401	1.00	32.15	AAAAA	ATOM	1797	C	PRO	186	29.387	5.199	84.460	1.00	56.02	AAAAA
ATOM	1628	C2	TYR	171	17.403	-1.744	76.978	1.00	32.11	AAAAA	ATOM	1798	O	PRO	186	29.923	6.303	84.386	1.00	57.19	AAAAA
ATOM	1629	OH	TYR	171	18.020	-2.018	78.167	1.00	35.12	AAAAA	ATOM	1799	N	SER	187	28.092	4.992	84.532	1.00	58.28	AAAAA
ATOM	1631	C	TYR	171	17.170	-1.804	71.798	1.00	35.29	AAAAA	ATOM	1800	CA	SER	187	27.102	6.045	84.783	1.00	61.94	AAAAA
ATOM	1632	O	TYR	171	16.658	-2.907	71.652	1.00	33.63	AAAAA	ATOM	1802	CB	SER	187	25.817	5.440	85.330	1.00	67.34	AAAAA
ATOM	1633	N	ASN	172	18.478	-1.618	71.679	1.00	36.66	AAAAA	ATOM	1803	CG	SER	187	25.839	3.985	85.161	1.00	70.00	AAAAA
ATOM	1635	CA	ASN	172	19.316	-2.760	71.416	1.00	34.29	AAAAA	ATOM	1805	C	SER	187	27.603	7.143	85.710	1.00	61.19	AAAAA
ATOM	1636	CB	ASN	172	19.231	-3.099	69.947	1.00	37.52	AAAAA	ATOM	1806	O	SER	187	27.481	8.334	85.436	1.00	60.53	AAAAA
ATOM	1637	CG	ASN	172	18.789	-4.515	69.721	1.00	43.69	AAAAA	ATOM	1807	N	THR	188	28.180	6.704	86.824	1.00	60.90	AAAAA
ATOM	1638	OD1	ASN	172	19.263	-5.438	70.384	1.00	48.62	AAAAA	ATOM	1809	CA	THR	188	28.737	7.572	87.832	1.00	58.92	AAAAA
ATOM	1639	ND2	ASN	172	17.872	-4.705	68.793	1.00	48.55	AAAAA	ATOM	1810	CB	THR	188	29.629	6.737	88.727	1.00	60.61	AAAAA
ATOM	1642	C	ASN	172	20.765	-2.644	71.842	1.00	33.14	AAAAA	ATOM	1811	OG1	THR	188	26.938	5.523	89.068	1.00	63.91	AAAAA
ATOM	1643	O	ASN	172	21.208	-1.619	72.381	1.00	29.53	AAAAA	ATOM	1813	CG2	THR	188	30.048	7.525	89.960	1.00	62.56	AAAAA
ATOM	1644	N	TYR	173	21.483	-1.738	71.619	1.00	33.30	AAAAA	ATOM	1814	C	THR	188	29.604	8.652	87.201	1.00	56.82	AAAAA
ATOM	1645	CA	TYR	173	22.899	-3.835	71.930	1.00	34.05	AAAAA	ATOM	1815	O	THR	188	29.470	9.837	87.501	1.00	57.66	AAAAA
ATOM	1647	CB	TYR	173	23.303	-5.249	71.721	1.00	31.77	AAAAA	ATOM	1816	N	CYS	189	30.508	8.197	86.337	1.00	53.62	AAAAA
ATOM	1648	CG	TYR	173	22.755	-6.251	72.513	1.00	31.54	AAAAA	ATOM	1818	CA	CYS	189	31.467	9.024	85.639	1.00	49.24	AAAAA
ATOM	1649	CD1	TYR	173	21.904	-7.206	72.107	1.00	31.55	AAAAA	ATOM	1819	C	CYS	189	30.896	10.316	85.098	1.00	48.89	AAAAA
ATOM	1650	CE1	TYR	173	21.370	-8.179	72.912	1.00	35.13	AAAAA	ATOM	1820	O	CYS	189	31.542	11.356	85.151	1.00	51.71	AAAAA
ATOM	1651	CD2	TYR	173	23.065	-6.283	73.954	1.00	33.49	AAAAA	ATOM	1821	CB	CYS	189	32.116	8.203	84.534	1.00	48.12	AAAAA
ATOM	1652	CG2	TYR	173	22.536	-7.252	74.781	1.00	37.76	AAAAA	ATOM	1822	SG	CYS	189	33.375	7.087	85.232	1.00	46.19	AAAAA
ATOM	1653	C2	TYR	173	21.684	-8.205	74.251	1.00	37.83	AAAAA	ATOM	1823	N	GLY	190	29.681	10.259	84.582	1.00	46.39	AAAAA
ATOM	1654	OH	TYR	173	21.140	-9.183	75.022	1.00	42.03	AAAAA	ATOM	1825	CA	GLY	190	29.068	11.464	84.070	1.00	42.95	AAAAA
ATOM	1656	C	TYR	173	23.664	-2.964	70.958	1.00	36.13	AAAAA	ATOM	1826	C	GLY	190	29.612	10.844	82.724	1.00	40.11	AAAAA
ATOM	1657	O	TYR	173	23.283	-2.895	69.781	1.00	38.28	AAAAA	ATOM	1827	O	GLY	190	29.877	11.002	81.884	1.00	41.46	AAAAA
ATOM	1658	N	ARG	174	24.751	-2.338	71.426	1.00	35.38	AAAAA	ATOM	1828	N	LYS	191	29.778	13.122	82.502	1.00	39.74	AAAAA
ATOM	1660	CA	ARG	174	25.569	-1.478	70.571	1.00	32.21	AAAAA	ATOM	1830	CA	LYS	191	30.300	13.532	81.228	1.00	42.54	AAAAA
ATOM	1661	CB	ARG	174	25.498	-0.037	71.086	1.00	32.61	AAAAA	ATOM	1831	CB	LYS	191	29.919	15.002	80.951	1.00	43.99	AAAAA
ATOM	1662	CG	ARG	174	24.061	0.507	71.300	1.00	33.85	AAAAA	ATOM	1832	CG	LYS	191	30.473	16.023	81.944	1.00	48.52	AAAAA
ATOM	1663	CD	ARG	174	23.277	0.687	69.980	1.00	36.54	AAAAA	ATOM	1833	CD	LYS	191	29.851	15.877	83.357	1.00	53.24	AAAAA
ATOM	1664	C2	TRP	176	31.537	-1.347	65.154	1.00	34.05	AAAAA	ATOM	1835	N	LYS	191	30.465	14.897	85.544	1.00	51.30	AAAAA
ATOM	1667	O	TRP	176	31.530	-2.901	63.929	1.00	35.55	AAAAA	ATOM	1860	CA	ALA	193	36.022	9.481	80.293	1.00	34.93	AAAAA
ATOM	1668	CE2	TRP	176	12.589	-2.332	67.343	1.00	15.57	AAAAA	ATOM	1861	CB	ALA	193	37.220	9.828	79.447	1.00	33.97	AAAAA
ATOM	1669	SE3	TRP	176	32.410	1.582	65.024	1.00	12.28	AAAAA	ATOM	1862	C	ALA	193	35.416	8.497	81.358	1.00	35.02	AAAAA
ATOM	1690	CD1	TRP	176	32.716	0.357	68.375	1.00	21.79	AAAAA	ATOM	1863	O	ALA	193	35.213	8.740	82.531	1.00	32.16	AAAAA
ATOM	1691	NE1	TRP	176	32.711	1.724	68.561	1.00	21.74	AAAAA	ATOM	1864	N	CYS	194	36.970	7.366	80.951	1.00	38.60	AAAAA
ATOM	1693	C22	TRP	176	32.521	1.685	67.022	1.00	17.48	AAAAA	ATOM	1866	CA	CYS	194	37.366	6.379	81.924	1.00	44.75	AAAAA
ATOM	1694	C23	TRP	176	32.353	0.321	64.704	1.00													

Figure 1 (cont'd)

ATOM	1940	CG	HIS	202	42.033	15.187	85.071	1.00 33.88	AAAA	ATOM	2097	CD	ARG	222	36.483	18.089	78.943	1.00 55.19	AAAA
ATOM	1941	CD2	HIS	202	42.478	15.717	86.230	1.00 34.57	AAAA	ATOM	2098	NE	ARG	222	36.491	16.622	79.070	1.00 59.31	AAAA
/	1942	ND1	HIS	202	41.801	16.250	84.229	1.00 39.51	AAAA	ATOM	2100	CZ	ARG	222	35.631	15.787	78.472	1.00 61.07	AAAA
.	1944	CE1	HIS	202	42.084	17.379	84.856	1.00 38.52	AAAA	ATOM	2101	NH1	ARG	222	34.665	16.251	77.682	1.00 62.50	AAAA
ATOM	1945	NE2	HIS	202	42.496	17.082	86.073	1.00 34.70	AAAA	ATOM	2104	NH2	ARG	222	35.727	14.476	78.673	1.00 60.03	AAAA
ATOM	1947	C	HIS	202	39.332	14.312	84.100	1.00 35.68	AAAA	ATOM	2107	C	ARG	222	39.591	19.394	75.795	1.00 43.68	AAAA
ATOM	1948	O	HIS	202	39.123	14.067	82.918	1.00 40.37	AAAA	ATOM	2108	O	ARG	222	38.794	19.842	74.961	1.00 41.43	AAAA
ATOM	1949	N	PRO	203	38.750	15.340	84.710	1.00 34.78	AAAA	ATOM	2109	N	HIS	223	40.679	20.036	76.226	1.00 43.22	AAAA
ATOM	1950	CD	PRO	203	38.881	15.735	86.115	1.00 36.37	AAAA	ATOM	2111	CA	HIS	223	41.062	21.377	75.802	1.00 40.49	AAAA
ATOM	1951	CB	PRO	203	37.850	16.233	83.982	1.00 33.97	AAAA	ATOM	2112	CB	HIS	223	41.167	22.304	76.996	1.00 40.04	AAAA
ATOM	1952	CG	PRO	203	37.614	17.389	84.954	1.00 32.34	AAAA	ATOM	2113	CG	HIS	223	39.884	22.489	77.715	1.00 42.81	AAAA
ATOM	1953	CC	PRO	203	38.582	17.198	86.058	1.00 35.27	AAAA	ATOM	2114	CD2	HIS	223	38.923	21.602	78.054	1.00 43.38	AAAA
ATOM	1954	C	PRO	203	38.381	16.724	82.642	1.00 34.97	AAAA	ATOM	2115	ND1	HIS	223	39.432	23.726	78.115	1.00 43.35	AAAA
ATOM	1955	O	PRO	203	37.614	17.144	81.765	1.00 36.16	AAAA	ATOM	2117	CE1	HIS	223	38.242	23.594	78.666	1.00 44.77	AAAA
ATOM	1956	N	GLU	204	39.693	16.676	82.477	1.00 33.97	AAAA	ATOM	2118	NE2	HIS	223	37.911	22.314	78.640	1.00 45.50	AAAA
ATOM	1958	CA	GLU	204	40.280	17.148	81.242	1.00 31.62	AAAA	ATOM	2120	C	HIS	223	47.198	21.419	75.113	1.00 43.04	AAAA
ATOM	1959	CB	GLU	204	41.545	17.955	81.552	1.00 29.26	AAAA	ATOM	2121	O	HIS	223	42.529	20.994	73.969	1.00 41.67	AAAA
ATOM	1960	CC	GLU	204	41.215	19.253	82.260	1.00 30.14	AAAA	ATOM	2122	N	TYR	224	43.386	21.939	75.843	1.00 40.87	AAAA
ATOM	1961	CD	GLU	204	40.739	20.364	81.331	1.00 34.01	AAAA	ATOM	2124	CA	TYR	224	44.740	22.109	75.351	1.00 39.54	AAAA
ATOM	1962	OE1	GLU	204	40.657	20.192	80.085	1.00 35.20	AAAA	ATOM	2125	CB	TYR	224	45.119	23.562	75.465	1.00 38.87	AAAA
ATOM	1963	OE2	GLU	204	40.434	21.445	81.868	1.00 33.07	AAAA	ATOM	2126	CG	TYR	224	44.499	24.297	74.345	1.00 43.98	AAAA
ATOM	1964	C	GLU	204	40.603	16.003	80.299	1.00 30.09	AAAA	ATOM	2127	CD1	TYR	224	43.411	25.121	74.561	1.00 42.61	AAAA
ATOM	1965	O	GLU	204	40.585	16.151	79.082	1.00 30.45	AAAA	ATOM	2128	CE1	TYR	224	42.771	25.714	73.517	1.00 45.59	AAAA
ATOM	1966	N	CYS	205	40.865	14.815	80.840	1.00 29.97	AAAA	ATOM	2129	CD2	TYR	224	44.938	24.086	73.035	1.00 45.01	AAAA
ATOM	1968	CA	CYS	205	41.180	13.767	79.931	1.00 32.60	AAAA	ATOM	2130	CE2	TYR	224	44.310	24.671	71.988	1.00 47.82	AAAA
ATOM	1969	C	CYS	205	40.046	13.710	78.966	1.00 31.35	AAAA	ATOM	2131	CZ	TYR	224	43.218	25.491	72.231	1.00 48.72	AAAA
ATOM	1970	O	CYS	205	38.908	13.801	79.362	1.00 35.49	AAAA	ATOM	2132	OH	TYR	224	42.570	26.111	71.174	1.00 59.60	AAAA
ATOM	1971	CB	CYS	205	41.327	12.444	80.662	1.00 33.33	AAAA	ATOM	2134	C	TYR	224	45.804	21.284	76.000	1.00 39.81	AAAA
ATOM	1972	SG	CYS	205	42.981	12.223	81.401	1.00 38.85	AAAA	ATOM	2135	O	TYR	224	46.017	21.370	77.202	1.00 45.49	AAAA
ATOM	1973	N	LEU	206	40.365	13.637	77.691	1.00 31.01	AAAA	ATOM	2136	N	TYR	225	46.486	20.492	75.186	1.00 39.39	AAAA
ATOM	1975	CA	LEU	206	39.345	13.523	76.577	1.00 30.91	AAAA	ATOM	2138	CA	TYR	225	47.561	19.649	75.653	1.00 36.83	AAAA
ATOM	1976	CB	LEU	206	39.466	14.655	75.537	1.00 28.62	AAAA	ATOM	2139	CB	TYR	225	47.875	18.578	74.667	1.00 34.69	AAAA
ATOM	1977	CG	LEU	206	38.601	14.521	74.370	1.00 24.69	AAAA	ATOM	2140	CG	TYR	225	49.135	17.882	75.031	1.00 36.21	AAAA
ATOM	1978	CD1	LEU	206	37.198	14.166	74.723	1.00 23.66	AAAA	ATOM	2141	CD1	TYR	225	49.118	16.785	75.876	1.00 35.50	AAAA
ATOM	1979	CD2	LEU	206	38.580	15.791	73.620	1.00 21.51	AAAA	ATOM	2142	CE1	TYR	225	50.249	16.097	75.166	1.00 37.02	AAAA
ATOM	1980	C	LEU	206	39.579	12.154	76.040	1.00 32.93	AAAA	ATOM	2143	CD2	TYR	225	50.335	18.282	74.487	1.00 38.38	AAAA
ATOM	1981	O	LEU	206	40.706	11.677	75.931	1.00 35.10	AAAA	ATOM	2144	CE2	TYR	225	51.480	17.606	74.762	1.00 42.33	AAAA
ATOM	1982	N	GLY	207	38.510	11.488	75.650	1.00 36.31	AAAA	ATOM	2145	CZ	TYR	225	51.437	16.505	75.600	1.00 42.96	AAAA
ATOM	1984	CA	GLY	207	38.688	10.195	75.033	1.00 38.16	AAAA	ATOM	2146	OH	TYR	225	52.600	15.796	75.833	1.00 51.09	AAAA
ATOM	1985	C	GLY	207	38.752	9.019	75.979	1.00 39.99	AAAA	ATOM	2148	C	TYR	225	48.781	20.484	75.794	1.00 37.42	AAAA
ATOM	1986	O	GLY	207	37.793	8.239	76.076	1.00 40.86	AAAA	ATOM	2149	O	TYR	225	49.024	21.345	74.979	1.00 39.51	AAAA
ATOM	1987	N	SER	208	39.870	8.880	76.684	1.00 38.15	AAAA	ATOM	2150	N	TYR	226	49.567	20.215	76.821	1.00 40.71	AAAA
ATOM	1989	CA	SER	208	40.026	7.745	77.576	1.00 36.49	AAAA	ATOM	2152	CA	TYR	226	50.757	20.995	77.055	1.00 41.82	AAAA
ATOM	1990	C	SER	208	40.194	6.471	76.745	1.00 36.46	AAAA	ATOM	2153	C	TYR	226	50.372	22.358	77.612	1.00 47.49	AAAA
ATOM	1991	OG	SER	208	40.426	5.334	77.554	1.00 42.23	AAAA	ATOM	2154	CG	TYR	226	51.564	23.143	78.074	1.00 56.26	AAAA
ATOM	1993	C	SER	208	41.245	7.990	78.419	1.00 36.06	AAAA	ATOM	2155	CD1	TYR	226	52.096	22.947	79.344	1.00 51.49	AAAA
ATOM	1994	O	SER	208	41.639	9.134	78.566	1.00 35.56	AAAA	ATOM	2156	CE1	TYR	226	53.251	21.613	79.750	1.00 65.13	AAAA
ATOM	1995	N	CYS	209	41.843	6.927	78.964	1.00 38.43	AAAA	ATOM	2157	CD2	TYR	226	52.210	24.033	77.215	1.00 61.56	AAAA
ATOM	1997	CA	CYS	209	43.029	7.065	79.809	1.00 41.02	AAAA	ATOM	2158	CE2	TYR	226	53.365	24.489	78.876	1.00 61.51	AAAA
ATOM	1998	C	CYS	209	43.688	5.783	80.251	1.00 44.54	AAAA	ATOM	2159	CZ	TYR	226	53.882	24.489	78.876	1.00 65.38	AAAA
ATOM	1999	O	CYS	209	43.216	4.682	79.939	1.00 45.60	AAAA	ATOM	2160	OH	TYR	226	55.030	25.136	79.280	1.00 68.79	AAAA
ATOM	2000	CB	CYS	209	42.699	7.837	81.063	1.00 41.03	AAAA	ATOM	2162	C	TYR	226	51.725	20.315	78.003	1.00 41.20	AAAA
ATOM	2001	SC	CYS	209	40.927	7.852	81.449	1.00 52.23	AAAA	ATOM	2163	O	TYR	226	51.392	20.007	79.143	1.00 42.16	AAAA
ATOM	2002	N	SER	210	44.760	5.961	81.020	1.00 46.33	AAAA	ATOM	2164	N	ALA	227	52.931	20.069	77.521	1.00 32.70	AAAA
ATOM	2004	CA	ASP	215	45.615	13.753	85.343	1.00 44.94	AAAA	ATOM	2192	CA	VAL	221	45.562	21.716	80.294	1.00 35.02	AAAA
ATOM	2042	CA	ASP	215	45.631	14.549	84.111	1.00 42.89	AAAA	ATOM	2193	CB	VAL	221	46.654	22.713	79.847	1.00 32.96	AAAA
ATOM	2043	CB	ASP	215	45.490	16.038	84.420	1.00 40.15	AAAA	ATOM	2194	CG1	VAL	221	46.621	23.964	80.671	1.00 32.73	AAAA
ATOM	2044	CG	ASP	215	46.648	16.571	85.228	1.00 42.93	AAAA	ATOM	2195	CG2	VAL	221	47.984	22.065	79.952	1.00 35.22	AAAA
ATOM	2045	OD1	ASP	215	46.522	17.676	85.803	1.00 41.96	AAAA	ATOM	2196	C	VAL	221	48.204	22.289	79.897	1.00 39.89	AAAA
ATOM	2046	OD2	ASP	215	47.689	15.885	85.297	1.00 46.15	AAAA	ATOM	2205	N	ALA	223	43.584	25.380	79.724	1.00 41.24	AAAA
ATOM																			

Figure 1 (cont'd)

ATOM	2256	CG	TYR	239	51.005	31.971	72.517	1.00	27.41	AAAAA	ATOM	2420	CA	ASN	254	50.669	29.024	63.833	1.00	41.51	AAAAA
ATOM	2257	CD1	TYR	239	52.375	31.957	72.580	1.00	26.72	AAAAA	ATOM	2421	CB	ASN	254	51.949	28.613	64.508	1.00	42.41	AAAAA
ATOM	2258	CE1	TYR	239	53.015	33.016	73.260	1.00	26.83	AAAAA	ATOM	2422	CG	ASN	254	52.825	29.791	64.764	1.00	45.51	AAAAA
ATOM	2259	CD2	TYR	239	50.304	33.070	72.938	1.00	26.63	AAAAA	ATOM	2423	OD1	ASN	254	53.493	30.320	63.846	1.00	48.66	AAAAA
ATOM	2260	CZ2	TYR	239	50.927	34.119	73.515	1.00	27.10	AAAAA	ATOM	2424	ND2	ASN	254	52.817	30.249	66.008	1.00	45.81	AAAAA
ATOM	2261	CZ	TYR	239	52.272	34.054	73.679	1.00	26.41	AAAAA	ATOM	2427	C	ASN	254	59.966	27.820	63.261	1.00	44.77	AAAAA
ATOM	2262	OH	TYR	239	52.654	35.161	74.301	1.00	32.09	AAAAA	ATOM	2428	O	ASN	254	50.551	26.739	63.150	1.00	45.62	AAAAA
ATOM	2264	C	TYR	239	49.166	28.660	72.416	1.00	32.09	AAAAA	ATOM	2429	N	ILE	255	58.718	28.053	62.854	1.00	47.11	AAAAA
ATOM	2265	O	TYR	239	49.793	27.662	72.091	1.00	34.50	AAAAA	ATOM	2431	CA	ILE	255	57.827	27.050	62.285	1.00	44.95	AAAAA
ATOM	2266	N	ARG	240	47.852	28.768	72.201	1.00	30.65	AAAAA	ATOM	2432	CB	ILE	255	56.375	27.514	62.515	1.00	39.68	AAAAA
ATOM	2268	CA	ARG	240	47.110	27.655	71.583	1.00	27.19	AAAAA	ATOM	2433	CG2	ILE	255	55.585	27.423	61.248	1.00	43.91	AAAAA
ATOM	2269	CB	ARG	240	45.626	27.940	71.580	1.00	25.69	AAAAA	ATOM	2434	CG1	ILE	255	55.740	26.688	63.625	1.00	36.11	AAAAA
ATOM	2270	CG	ARG	240	45.255	29.132	72.421	1.00	26.86	AAAAA	ATOM	2435	CD1	ILE	255	54.400	27.238	64.112	1.00	32.00	AAAAA
ATOM	2271	CD	ARG	240	43.771	29.143	72.648	1.00	29.42	AAAAA	ATOM	2436	C	ILE	255	58.126	26.778	60.787	1.00	46.54	AAAAA
ATOM	2272	NE	ARG	240	43.117	30.082	71.753	1.00	30.88	AAAAA	ATOM	2437	O	ILE	255	58.351	25.631	60.393	1.00	48.08	AAAAA
ATOM	2274	CZ	ARG	240	43.256	31.392	71.869	1.00	34.12	AAAAA	ATOM	2438	N	LEU	256	58.143	27.819	59.960	1.00	48.83	AAAAA
ATOM	2275	NH1	ARG	240	44.021	31.888	72.842	1.00	30.93	AAAAA	ATOM	2440	CA	ILE	256	59.461	27.640	58.333	1.00	32.02	AAAAA
ATOM	2276	NH2	ARG	240	42.945	32.197	71.011	1.00	33.99	AAAAA	ATOM	2441	CB	LEU	256	57.827	28.797	57.721	1.00	48.70	AAAAA
ATOM	2281	C	ARG	240	47.602	27.535	70.168	1.00	23.37	AAAAA	ATOM	2442	CG	LEU	256	56.322	29.035	57.777	1.00	49.20	AAAAA
ATOM	2282	O	ARG	240	48.038	28.509	69.505	1.00	26.68	AAAAA	ATOM	2443	CD1	LEU	256	56.004	30.443	57.261	1.00	46.78	AAAAA
ATOM	2283	N	PHE	241	47.538	26.357	69.583	1.00	20.36	AAAAA	ATOM	2444	CD2	LEU	256	55.612	27.990	56.935	1.00	49.57	AAAAA
ATOM	2285	CA	PHE	241	48.034	26.193	68.232	1.00	19.13	AAAAA	ATOM	2445	C	LEU	256	59.981	27.697	58.339	1.00	54.86	AAAAA
ATOM	2286	CB	PHE	241	49.574	26.040	68.294	1.00	20.49	AAAAA	ATOM	2446	O	LEU	256	60.483	27.900	57.235	1.00	55.37	AAAAA
ATOM	2287	CG	PHE	241	50.214	25.654	66.985	1.00	15.08	AAAAA	ATOM	2447	N	SER	257	60.706	27.505	59.431	1.00	57.82	AAAAA
ATOM	2288	CD1	PHE	241	50.346	26.569	65.967	1.00	17.58	AAAAA	ATOM	2449	CA	SER	257	62.155	27.536	59.421	1.00	61.01	AAAAA
ATOM	2289	CD2	PHE	241	50.620	24.367	66.759	1.00	16.72	AAAAA	ATOM	2450	CB	SER	257	62.705	27.201	60.815	1.00	61.83	AAAAA
ATOM	2290	CE1	PHE	241	50.868	26.193	64.732	1.00	20.68	AAAAA	ATOM	2451	OG	SER	257	63.501	26.024	60.793	1.00	63.20	AAAAA
ATOM	2291	CE2	PHE	241	51.144	23.984	65.529	1.00	20.21	AAAAA	ATOM	2453	C	SER	257	62.814	26.636	58.398	1.00	63.24	AAAAA
ATOM	2292	CZ	PHE	241	51.266	24.899	64.516	1.00	15.78	AAAAA	ATOM	2454	O	SER	257	63.828	27.006	57.818	1.00	66.36	AAAAA
ATOM	2293	C	PHE	241	47.369	24.962	67.601	1.00	22.49	AAAAA	ATOM	2455	N	ALA	258	62.276	25.452	58.165	1.00	65.73	AAAAA
ATOM	2294	O	PHE	241	47.498	23.845	68.137	1.00	22.07	AAAAA	ATOM	2457	CA	ALA	258	62.928	24.588	57.191	1.00	68.76	AAAAA
ATOM	2295	N	GLU	242	46.563	25.164	66.479	1.00	21.89	AAAAA	ATOM	2458	CB	ALA	258	62.517	23.131	57.414	1.00	69.08	AAAAA
ATOM	2297	CA	GLU	242	45.962	24.075	65.766	1.00	21.22	AAAAA	ATOM	2459	C	ALA	258	62.633	25.021	55.749	1.00	70.99	AAAAA
ATOM	2298	CB	GLU	242	46.918	22.911	65.439	1.00	25.33	AAAAA	ATOM	2460	O	ALA	258	62.947	24.288	54.802	1.00	74.18	AAAAA
ATOM	2299	CG	GLU	242	47.783	23.045	64.149	1.00	25.74	AAAAA	ATOM	2461	N	GLU	259	62.038	26.206	55.577	1.00	70.65	AAAAA
ATOM	2300	CD	GLU	242	47.099	23.768	63.007	1.00	28.55	AAAAA	ATOM	2463	CA	GLU	259	61.727	26.708	54.237	1.00	68.39	AAAAA
ATOM	2301	OE1	GLU	242	46.182	23.192	63.288	1.00	36.80	AAAAA	ATOM	2464	CB	GLU	259	60.268	26.445	53.876	1.00	69.57	AAAAA
ATOM	2302	OE2	GLU	242	47.471	24.916	67.601	1.00	28.23	AAAAA	ATOM	2465	CG	GLU	259	59.667	25.233	54.529	1.00	70.62	AAAAA
ATOM	2303	C	GLU	242	44.801	23.573	66.639	1.00	20.26	AAAAA	ATOM	2466	CD	GLU	259	58.270	25.512	55.022	1.00	74.23	AAAAA
ATOM	2304	O	GLU	242	44.369	22.426	66.573	1.00	14.94	AAAAA	ATOM	2467	OE1	GLU	259	57.651	26.472	54.495	1.00	73.42	AAAAA
ATOM	2305	N	GLY	243	44.303	24.488	67.455	1.00	25.09	AAAAA	ATOM	2468	OE2	GLU	259	57.797	24.779	55.930	1.00	76.56	AAAAA
ATOM	2307	CA	GLY	243	43.210	24.199	68.365	1.00	26.25	AAAAA	ATOM	2469	C	GLU	259	62.025	28.177	53.990	1.00	66.31	AAAAA
ATOM	2308	CB	GLY	243	43.405	22.887	69.056	1.00	27.15	AAAAA	ATOM	2470	O	GLU	259	61.764	29.058	54.808	1.00	63.93	AAAAA
ATOM	2309	O	GLY	243	42.576	22.005	68.900	1.00	35.16	AAAAA	ATOM	2471	N	SER	260	62.565	28.409	52.810	1.00	67.17	AAAAA
ATOM	2310	N	TRP	244	44.508	22.741	69.781	1.00	27.71	AAAAA	ATOM	2473	CA	SER	260	62.927	29.733	52.345	1.00	68.69	AAAAA
ATOM	2312	CA	TRP	244	44.782	20.512	70.491	1.00	27.68	AAAAA	ATOM	2474	CB	SER	260	63.983	29.606	51.221	1.00	71.38	AAAAA
ATOM	2313	CB	TRP	244	44.872	20.299	69.536	1.00	29.29	AAAAA	ATOM	2475	O	SER	260	64.829	28.470	51.396	1.00	70.87	AAAAA
ATOM	2314	CG	TRP	244	46.277	19.813	69.029	1.00	32.96	AAAAA	ATOM	2477	C	SER	260	61.673	30.448	51.814	1.00	66.68	AAAAA
ATOM	2315	CD2	TRP	244	47.154	18.860	69.666	1.00	30.71	AAAAA	ATOM	2478	O	SER	260	61.446	30.494	50.598	1.00	66.99	AAAAA
ATOM	2316	CE2	TRP	244	48.229	18.610	68.771	1.00	28.73	AAAAA	ATOM	2479	N	SER	261	60.872	31.013	52.719	1.00	60.49	AAAAA
ATOM	2317	CD1	TRP	244	47.155	18.197	70.897	1.00	29.85	AAAAA	ATOM	2481	CA	SER	261	59.633	31.704	52.325	1.00	60.29	AAAAA
ATOM	2318	CD1	TRP	244	46.858	20.089	67.795	1.00	32.81	AAAAA	ATOM	2482	CB	SER	261	58.468	21.692	53.210	1.00	58.85	AAAAA
ATOM	2319	NE1	TRP	244	48.019	19.367	67.546	1.00	31.29	AAAAA	ATOM	2483	O	SER	261	57.857	30.098	52.687	1.00	60.47	AAAAA
ATOM	2321	CZ2	TRP	244	49.260	21.735	69.574	1.00	27.63	AAAAA	ATOM	2485	C	SER	261	59.648	33.229	52.300	1.00	59.52	AAAAA
ATOM	2322	CZ1	TRP	244	51.776	25.593	70.306	1.00	25.06	AAAAA	ATOM	2486	O	SER	261	59.867	33.878	53.319	1.00	59.48	AAAAA
ATOM	2323	CG1	VAL	247	52.978	25.283	69.777	1.00	22.57	AAAAA	ATOM	2487	N	ASP	262	59.395	33.775	51.110	1.00	55.02	AAAAA
ATOM	2324	CG2	VAL	247	52.703	27.704	69.703	1.00	18.15	AAAAA	ATOM	2489	CA	ASP	262	59.321	35.213</td				

Figure 1 (cont'd)

ATOM	2578	CB	GLU	272	45.823	12.211	68.965	1.00 27.11	AAAA	ATOM	2739	O	MET	289	52.503	38.544	65.931	1.00 28.48	AAAA
ATOM	2579	CG	GLU	272	45.843	11.463	67.702	1.00 33.51	AAAA	ATOM	2740	N	TYR	290	53.445	45.997	65.744	1.00 28.07	AAAA
ATOM	2580	CD	GLU	272	44.495	30.900	67.390	1.00 37.10	AAAA	ATOM	2742	CA	TYR	290	52.377	41.409	66.314	1.00 28.86	AAAA
ATOM	2581	DE1	GLU	272	43.512	31.466	67.935	1.00 40.77	AAAA	ATOM	2743	CB	TYR	290	52.989	42.558	67.114	1.00 28.43	AAAA
ATOM	2582	OE2	GLU	272	44.426	29.906	66.617	1.00 34.64	AAAA	ATOM	2744	CG	TYR	290	53.700	42.094	68.359	1.00 28.56	AAAA
ATOM	2583	C	GLU	272	48.179	32.461	68.435	1.00 26.58	AAAA	ATOM	2745	CD1	TYR	290	55.046	41.761	68.336	1.00 26.85	AAAA
ATOM	2584	O	GLU	272	48.243	33.482	67.764	1.00 28.05	AAAA	ATOM	2746	C	TYR	290	55.681	41.314	69.466	1.00 23.77	AAAA
ATOM	2585	N	GLU	272	48.932	31.388	68.764	1.00 27.05	AAAA	ATOM	2747	CD2	TYR	290	53.017	41.960	69.554	1.00 30.41	AAAA
ATOM	2587	CA	CYS	273	49.923	31.301	67.165	1.00 27.37	AAAA	ATOM	2748	CE2	TYR	290	53.650	41.513	70.696	1.00 29.09	AAAA
ATOM	2588	C	CYS	273	49.202	30.847	65.897	1.00 29.56	AAAA	ATOM	2749	CZ	TYR	290	54.976	41.196	70.644	1.00 28.46	AAAA
ATOM	2589	O	CYS	273	48.665	29.717	65.816	1.00 27.40	AAAA	ATOM	2750	OH	TYR	290	55.604	40.788	71.794	1.00 34.58	AAAA
ATOM	2590	CB	CYS	273	51.022	30.284	67.516	1.00 26.63	AAAA	ATOM	2753	C	TYR	290	51.395	41.982	65.281	1.00 30.98	AAAA
ATOM	2591	SG	CYS	273	52.197	29.921	66.166	1.00 26.84	AAAA	ATOM	2753	O	TYR	290	51.783	42.644	64.298	1.00 27.04	AAAA
ATOM	2592	N	MET	274	49.167	31.744	64.914	1.00 29.52	AAAA	ATOM	2754	N	CYS	291	50.116	41.742	65.560	1.00 32.25	AAAA
ATOM	2594	CA	MET	274	48.562	31.487	63.637	1.00 28.78	AAAA	ATOM	2756	CA	CYS	291	49.019	41.158	64.708	1.00 33.11	AAAA
ATOM	2595	CB	MET	274	47.160	32.129	63.586	1.00 30.44	AAAA	ATOM	2757	C	CYS	291	48.287	43.394	65.207	1.00 34.88	AAAA
ATOM	2596	CG	MET	274	47.029	31.654	63.870	1.00 31.13	AAAA	ATOM	2758	O	CYS	291	47.763	43.390	66.314	1.00 36.19	AAAA
ATOM	2597	SD	MET	274	45.573	34.073	64.843	1.00 33.21	AAAA	ATOM	2759	CB	CYS	291	48.007	41.025	64.623	1.00 34.25	AAAA
ATOM	2598	CE	MET	274	45.773	35.798	65.222	1.00 26.66	AAAA	ATOM	2760	SC	CYS	291	48.552	39.512	63.781	1.00 34.00	AAAA
ATOM	2599	C	MET	274	49.456	32.084	62.573	1.00 29.64	AAAA	ATOM	2761	N	ILE	292	48.228	44.446	64.397	1.00 36.12	AAAA
ATOM	2600	O	MET	274	50.165	33.038	62.815	1.00 31.59	AAAA	ATOM	2763	CA	ILE	292	47.485	45.645	64.792	1.00 38.93	AAAA
ATOM	2601	N	GLN	275	49.426	31.506	61.387	1.00 32.42	AAAA	ATOM	2764	CB	ILE	292	48.337	46.955	64.760	1.00 36.37	AAAA
ATOM	2603	CA	GLN	275	50.139	31.900	60.357	1.00 30.77	AAAA	ATOM	2765	CG2	ILE	292	49.341	46.976	65.887	1.00 33.01	AAAA
ATOM	2604	CB	GLN	275	50.110	30.968	59.109	1.00 36.00	AAAA	ATOM	2766	CG1	ILE	292	49.005	47.100	63.403	1.00 35.12	AAAA
ATOM	2605	CG	GLN	275	49.036	31.270	58.072	1.00 40.05	AAAA	ATOM	2767	CD1	ILE	292	49.332	48.509	63.079	1.00 32.69	AAAA
ATOM	2606	CD	GLN	275	49.159	30.416	56.816	1.00 43.67	AAAA	ATOM	2768	C	ILE	292	46.278	45.878	63.873	1.00 41.13	AAAA
ATOM	2607	OE1	GLN	275	49.623	29.266	56.864	1.00 43.42	AAAA	ATOM	2770	N	PRO	293	45.255	46.577	64.395	1.00 43.88	AAAA
ATOM	2608	NE2	GLN	275	48.737	30.978	55.676	1.00 45.11	AAAA	ATOM	2771	CD	PRO	293	45.175	47.032	65.701	1.00 45.83	AAAA
ATOM	2611	C	GLN	275	49.796	33.333	58.720	1.00 27.95	AAAA	ATOM	2772	CA	PRO	293	44.026	46.912	63.679	1.00 44.79	AAAA
ATOM	2612	O	GLN	275	50.585	33.969	59.041	1.00 30.85	AAAA	ATOM	2773	CB	PRO	293	43.135	47.546	64.754	1.00 43.03	AAAA
ATOM	2613	N	GLU	276	48.583	33.779	60.000	1.00 29.24	AAAA	ATOM	2774	CG	PRO	293	43.686	47.101	66.025	1.00 45.02	AAAA
ATOM	2615	CA	GLU	276	48.129	35.061	59.478	1.00 31.66	AAAA	ATOM	2775	O	PRO	293	44.257	47.871	62.533	1.00 45.57	AAAA
ATOM	2616	CB	GLU	276	47.239	34.818	58.243	1.00 34.69	AAAA	ATOM	2776	CD	PRO	293	45.081	46.782	62.622	1.00 47.35	AAAA
ATOM	2617	CG	GLU	276	47.886	34.037	57.089	1.00 42.81	AAAA	ATOM	2777	N	CYS	294	43.492	47.660	62.470	1.00 46.89	AAAA
ATOM	2618	CD	GLU	276	48.801	34.898	56.183	1.00 49.14	AAAA	ATOM	2778	CA	CYS	294	43.519	48.582	60.346	1.00 53.79	AAAA
ATOM	2619	OE1	GLU	276	48.924	36.124	56.452	1.00 49.17	AAAA	ATOM	2779	O	CYS	294	42.490	49.582	60.346	1.00 53.79	AAAA
ATOM	2620	OE2	GLU	276	49.400	34.345	55.211	1.00 50.81	AAAA	ATOM	2781	CD	CYS	294	41.280	49.282	60.359	1.00 57.25	AAAA
ATOM	2621	C	GLU	276	47.352	35.897	60.499	1.00 29.62	AAAA	ATOM	2782	CB	CYS	294	43.197	47.642	65.967	1.00 43.85	AAAA
ATOM	2622	O	GLU	276	46.600	35.359	61.286	1.00 34.65	AAAA	ATOM	2783	SG	CYS	294	44.523	46.608	65.442	1.00 39.70	AAAA
ATOM	2623	N	CYS	277	47.513	37.209	60.488	1.00 28.03	AAAA	ATOM	2784	M	GLU	295	42.918	50.841	60.391	1.00 55.64	AAAA
ATOM	2625	CA	CYS	277	46.773	38.035	61.419	1.00 32.17	AAAA	ATOM	2785	N	PRO	297	40.566	48.936	57.456	1.00 52.72	AAAA
ATOM	2626	C	CYS	277	45.280	37.857	61.173	1.00 36.50	AAAA	ATOM	2786	CD	PRO	297	39.566	49.700	55.576	1.00 51.49	AAAA
ATOM	2627	O	CYS	277	44.871	37.405	60.112	1.00 40.78	AAAA	ATOM	2787	CB	PRO	297	39.828	50.681	54.766	1.00 50.86	AAAA
ATOM	2628	CB	CYS	277	47.060	39.492	61.177	1.00 34.42	AAAA	ATOM	2788	O	GLU	295	41.346	51.818	58.993	1.00 59.41	AAAA
ATOM	2629	SG	CYS	277	48.580	40.135	61.867	1.00 37.60	AAAA	ATOM	2789	N	GLY	295	40.165	51.219	58.903	1.00 58.10	AAAA
ATOM	2630	N	PRO	278	44.440	38.232	62.141	1.00 37.49	AAAA	ATOM	2790	CA	GLY	295	39.521	51.059	57.571	1.00 55.31	AAAA
ATOM	2631	CD	PRO	278	44.717	38.785	63.475	1.00 37.99	AAAA	ATOM	2791	C	GLY	295	40.521	51.059	57.609	1.00 55.31	AAAA
ATOM	2632	CA	PRO	278	43.011	38.077	61.908	1.00 37.70	AAAA	ATOM	2793	CD	GLY	295	39.932	49.815	56.870	1.00 53.05	AAAA
ATOM	2633	CB	PRO	278	42.412	38.332	62.276	1.00 38.57	AAAA	ATOM	2794	O	GLY	295	40.566	48.936	57.456	1.00 52.72	AAAA
ATOM	2634	CG	PRO	278	43.373	39.232	63.943	1.00 36.22	AAAA	ATOM	2795	N	PRO	297	39.566	49.700	55.576	1.00 51.49	AAAA
ATOM	2635	C	PRO	278	42.609	39.151	60.915	1.00 40.24	AAAA	ATOM	2796	CD	PRO	297	39.828	50.681	54.766	1.00 50.86	AAAA
ATOM	2636	O	PRO	278	43.221	40.218	60.892	1.00 43.77	AAAA	ATOM	2797	CA	PRO	297	40.105	49.397	54.025	1.00 39.91	AAAA
ATOM	2637	N	SER	279	41.592	38.885	60.100	1.00 41.09	AAAA	ATOM	2798	O	PRO	297	38.356	49.865	53.611	1.00 51.79	AAAA
ATOM	2638	CA	SER	279	41.248	39.861	59.109	1.00 35.74	AAAA	ATOM	2799	CD	PRO	297	41.416	48.431	54.849	1.00 48.25	AAAA
ATOM	2639	CB	SER	279	42.545	40.520	59.531	1.00 35.43	AAAA	ATOM	2800	O	PRO	297	42.115	49.423	54.607	1.00 47.82	AAAA
ATOM	2640	C	SER	279	48.951	43.966	59.820	1.00 42.12	AAAA	ATOM	2801	CD	VAL	301	40.504	47.750	55.204	1.00 47.11	AAAA
ATOM	2641	O	SER	279	48.811	44.584	61.667	1.00 45.18	AAAA	ATOM	2802	CA	CYS	301	41.324	47.042	55.326	1.00 42.12	AAAA
ATOM	2642	N	ARG	283	50.037	43.220	60.366	1.00 40.17	AAAA	ATOM	2803	CG	CYS	301	43.974	47.392	54.025	1.00 39.91	AAAA
ATOM	2643	CA	ARG	283	51.059	43.205	61.403	1.00 37.15	AAAA	ATOM	2804	CG2	CYS	301	40.516	47.738	54.331	1.00 32.38	AAAA
ATOM	2644	CB	ARG	283	52.069	42.059	61.300	1.00 32.63	AAAA	ATOM	2805	C	VAL	301	40.498	44.465	45.998	1.00 40.29	AAAA
ATOM	2645	N																	

Figure 1 (cont'd)

ATOM	2895	OGL1	THR	308	49.459	48.972	30.676	1.00	38.44	AAAA	ATOM	.1058	CE1	PHE	326	46.546	46.196	38.844	1.00	14.79	AAAA
ATOM	2897	CG2	THR	308	47.095	48.443	30.419	1.00	33.84	AAAA	ATOM	3059	CE2	PHE	326	47.334	47.984	37.480	1.00	22.55	AAAA
ATOM	2898	C	THR	308	47.326	46.497	32.350	1.00	43.89	AAAA	ATOM	3060	CZ	PHE	326	47.090	46.628	37.677	1.00	16.82	AAAA
ATOM	2899	O	THR	308	47.192	45.576	31.534	1.00	45.00	AAAA	ATOM	3061	C	PHE	326	48.694	49.614	41.394	1.00	24.23	AAAA
ATOM	2900	N	LYS	309	46.486	46.711	33.353	1.00	43.85	AAAA	ATOM	3062	O	PHE	326	48.977	50.772	41.108	1.00	36.39	AAAA
ATOM	2902	CA	LYS	309	45.214	45.878	33.516	1.00	43.17	AAAA	ATOM	3063	N	LYS	327	49.580	48.627	41.342	1.00	35.70	AAAA
ATOM	2903	CB	LYS	309	44.746	46.006	34.934	1.00	42.67	AAAA	ATOM	3065	CA	LYS	327	50.912	48.866	40.834	1.00	15.86	AAAA
ATOM	2904	CG	LYS	309	43.345	45.424	35.114	1.00	41.64	AAAA	ATOM	3066	CG	LYS	327	51.961	48.109	41.646	1.00	38.39	AAAA
ATOM	2905	CD	LYS	309	43.359	43.901	35.155	1.00	41.62	AAAA	ATOM	3067	CG	LYS	327	53.271	48.875	41.789	1.00	36.14	AAAA
ATOM	2906	CE	LYS	309	42.523	43.339	36.369	1.00	41.29	AAAA	ATOM	3068	CE	LYS	327	54.426	48.009	41.359	1.00	40.36	AAAA
ATOM	2907	NZ	LYS	309	43.106	41.972	36.731	1.00	40.17	AAAA	ATOM	3069	CE	LYS	327	55.468	48.754	40.515	1.00	43.06	AAAA
ATOM	2911	C	LYS	309	44.333	46.513	32.512	1.00	41.76	AAAA	ATOM	3070	NZ	LYS	327	56.405	47.780	39.847	1.00	32.45	AAAA
ATOM	2912	O	LYS	309	46.230	47.735	32.497	1.00	41.14	AAAA	ATOM	3074	C	LYS	327	50.894	48.402	39.393	1.00	34.84	AAAA
ATOM	2913	N	THR	310	43.806	45.694	31.645	1.00	41.60	AAAA	ATOM	3075	O	LYS	327	51.071	47.225	39.072	1.00	31.65	AAAA
ATOM	2915	CA	THR	310	43.210	45.636	29.267	1.00	45.37	AAAA	ATOM	3076	N	GLY	328	50.641	49.357	38.524	1.00	31.65	AAAA
ATOM	2916	CB	THR	310	43.210	45.636	29.267	1.00	45.37	AAAA	ATOM	3078	CA	GLY	328	50.577	49.070	37.120	1.00	30.16	AAAA
ATOM	2917	OGL1	THR	310	42.177	45.931	28.144	1.00	50.14	AAAA	ATOM	3079	C	GLY	328	49.819	50.207	36.831	1.00	29.94	AAAA
ATOM	2919	CG2	THR	310	43.353	44.123	29.342	1.00	51.13	AAAA	ATOM	3080	O	GLY	328	49.781	51.325	37.003	1.00	29.12	AAAA
ATOM	2920	C	THR	310	41.475	45.781	31.041	1.00	38.93	AAAA	ATOM	3081	N	ASN	329	49.201	49.914	35.374	1.00	31.22	AAAA
ATOM	2921	O	THR	310	41.013	44.701	30.717	1.00	40.54	AAAA	ATOM	3083	CA	ASN	329	48.445	50.909	34.682	1.00	32.69	AAAA
ATOM	2922	N	ILE	311	40.821	46.659	31.775	1.00	36.14	AAAA	ATOM	3084	CB	ASN	329	49.107	51.188	33.336	1.00	32.90	AAAA
ATOM	2924	CA	ILE	311	39.483	46.452	32.276	1.00	32.23	AAAA	ATOM	3085	CG	ASN	329	50.614	51.466	33.459	1.00	31.09	AAAA
ATOM	2925	CB	ILE	311	39.262	47.395	33.443	1.00	33.40	AAAA	ATOM	3086	OD1	ASN	329	51.056	52.197	34.350	1.00	28.29	AAAA
ATOM	2926	CG2	ILE	311	37.807	47.630	33.625	1.00	37.51	AAAA	ATOM	3087	ND2	ASN	329	51.396	50.891	32.547	1.00	27.03	AAAA
ATOM	2927	CG1	ILE	311	39.940	46.853	34.701	1.00	28.43	AAAA	ATOM	3090	C	ASN	329	47.036	50.356	34.500	1.00	36.25	AAAA
ATOM	2928	CD1	ILE	311	39.770	47.775	35.890	1.00	27.87	AAAA	ATOM	3091	O	ASN	329	46.805	49.134	34.580	1.00	37.16	AAAA
ATOM	2929	C	ILE	311	38.527	46.786	31.142	1.00	32.17	AAAA	ATOM	3092	N	LEU	330	46.091	51.264	34.287	1.00	37.34	AAAA
ATOM	2930	O	ILE	311	38.463	47.916	30.689	1.00	27.60	AAAA	ATOM	3094	CA	LEU	330	44.703	50.889	34.055	1.00	35.63	AAAA
ATOM	2931	N	ASP	312	37.790	45.789	30.681	1.00	36.21	AAAA	ATOM	3095	CB	LEU	330	43.786	51.493	35.124	1.00	32.90	AAAA
ATOM	2933	CA	ASP	312	36.871	45.960	29.560	1.00	41.14	AAAA	ATOM	3096	CG	LEU	330	43.766	50.838	36.504	1.00	32.84	AAAA
ATOM	2934	CB	ASP	312	37.416	45.228	28.330	1.00	43.85	AAAA	ATOM	3097	CD1	LEU	330	43.134	51.789	37.518	1.00	33.50	AAAA
ATOM	2935	CG	ASP	312	37.858	43.802	28.639	1.00	48.16	AAAA	ATOM	3098	CD2	LEU	330	43.000	49.552	36.438	1.00	28.87	AAAA
ATOM	2936	OD1	ASP	312	38.400	43.133	27.734	1.00	49.21	AAAA	ATOM	3099	C	LEU	330	44.291	51.429	32.692	1.00	35.17	AAAA
ATOM	2937	OD2	ASP	312	37.667	43.345	29.786	1.00	49.33	AAAA	ATOM	3100	O	LEU	330	44.554	52.583	32.342	1.00	37.16	AAAA
ATOM	2938	C	ASP	312	35.485	45.434	29.892	1.00	42.69	AAAA	ATOM	3101	N	LEU	331	43.673	50.583	31.898	1.00	34.64	AAAA
ATOM	2939	O	ASP	312	34.531	45.593	29.141	1.00	43.53	AAAA	ATOM	3103	CA	LEU	331	43.176	51.039	30.621	1.00	34.59	AAAA
ATOM	2940	N	SER	313	35.389	44.775	31.026	1.00	44.48	AAAA	ATOM	3104	CB	LEU	331	43.938	50.397	29.469	1.00	33.32	AAAA
ATOM	2942	CA	SER	313	34.125	44.264	31.476	1.00	44.15	AAAA	ATOM	3105	CC	LEU	331	43.049	50.089	28.277	1.00	28.49	AAAA
ATOM	2943	CB	SER	313	34.114	42.746	31.390	1.00	44.77	AAAA	ATOM	3106	CD1	LEU	331	43.233	51.111	27.218	1.00	27.07	AAAA
ATOM	2944	CG	SER	313	35.007	42.177	32.332	1.00	49.37	AAAA	ATOM	3107	CD2	LEU	331	43.364	48.720	27.787	1.00	31.73	AAAA
ATOM	2946	C	SER	313	34.046	44.735	32.913	1.00	45.82	AAAA	ATOM	3108	O	LEU	331	41.746	50.536	30.649	1.00	35.56	AAAA
ATOM	2947	O	SER	313	34.702	45.696	33.291	1.00	48.10	AAAA	ATOM	3109	N	ILE	331	41.511	49.345	30.389	1.00	38.42	AAAA
ATOM	2948	N	VAL	314	33.219	44.060	33.713	1.00	48.85	AAAA	ATOM	3110	O	ILE	332	40.805	51.407	31.027	1.00	32.64	AAAA
ATOM	2950	CA	VAL	314	33.053	44.399	35.110	1.00	48.19	AAAA	ATOM	3112	CA	ILE	332	39.406	51.017	31.077	1.00	32.18	AAAA
ATOM	2952	CG1	VAL	314	30.801	43.504	35.179	1.00	47.19	AAAA	ATOM	3114	CG2	ILE	332	38.770	51.272	33.479	1.00	29.20	AAAA
ATOM	2953	CG2	VAL	314	31.467	45.548	36.541	1.00	46.68	AAAA	ATOM	3115	CG1	ILE	332	39.078	53.294	32.100	1.00	35.82	AAAA
ATOM	2954	C	VAL	314	33.346	43.097	35.806	1.00	50.62	AAAA	ATOM	3116	CD1	ILE	332	39.305	53.907	33.505	1.00	36.84	AAAA
ATOM	2955	N	VAL	314	33.328	43.002	37.022	1.00	53.04	AAAA	ATOM	3117	C	ILE	332	38.914	51.233	29.668	1.00	31.94	AAAA
ATOM	2956	N	THR	315	33.550	42.072	34.993	1.00	54.43	AAAA	ATOM	3118	NE	ARG	335	33.509	48.753	21.522	1.00	73.38	AAAA
ATOM	2958	CA	THR	315	33.899	40.754	35.487	1.00	58.60	AAAA	ATOM	3119	CD2	ARG	335	33.869	49.780	22.494	1.00	69.33	AAAA
ATOM	2959	CB	THR	315	33.176	43.374	34.519	1.00	53.19	AAAA	ATOM	3120	CA	ASN	333	34.416	50.536	27.667	1.00	39.80	AAAA
ATOM	2960	CD	THR	315	33.770	42.350	32.990	1.00	51.31	AAAA	ATOM	3120	O	ASN	333	35.431	48.543	27.023	1.00	41.48	AAAA
ATOM	2961	OE2	THR	315	33.176	42.550	40.440	1.00	55.71	AAAA	ATOM	3121	N	ILE	334	35.641	50.151	28.383	1.00	43.54	AAAA
ATOM	2962	C	THR	315	33.008	42.741	41.714	1.00	55.17	AAAA	ATOM	3122	CA	ILE	334	34.277	49.571	28.446	1.00	45.40	AAAA
ATOM	2969	O	MET	319	41.757	42.877	42.775	1.00	54.41	AAAA	ATOM	3123	CB	ILE	334	33.639	49.626	29.854	1.00	42.84	AAAA
ATOM	3000	N	LEU	320	40.727	40.990	1.00	50.39	AAAA	ATOM	3124	CD2	ILE	334	32.521	49.678	28.872	1.00	85.90	AAAA	
ATOM	3002	CA	LEU	320	40.951	45.136	41.477	1.00	44.64	AAAA	ATOM	3125	ND2	ILE	334	32.407	48.219	26.632	1.00	71.93	AAAA
ATOM	3003	CB	LEU	320	40.433	46.121	40.396	1.00	37.02	AAAA	ATOM	312									

Figure 1 (cont'd)

ATOM	3225	O	LEU	344	34.029	48.845	40.528	1.00	40.28	AAAAA	ATOM	3381	NE	ARC	361	41.669	51.942	23.519	1.00	42.75	AAAAA
ATOM	3226	N	GLU	345	32.200	50.121	40.719	1.00	38.99	AAAAA	ATOM	3383	CZ	ARC	361	42.595	51.005	23.684	1.00	42.28	AAAAA
ATOM	3228	CA	GLU	345	32.626	50.715	41.973	1.00	41.32	AAAAA	ATOM	3384	NH1	ARC	361	43.881	51.302	23.544	1.00	46.14	AAAAA
ATOM	3229	CB	GLU	345	31.708	51.871	42.326	1.00	41.39	AAAAA	ATOM	3387	NW2	ARC	361	42.236	49.769	23.982	1.00	41.80	AAAAA
ATOM	3230	CG	GLU	345	31.979	52.524	43.650	1.00	48.84	AAAAA	ATOM	3390	C	ARC	361	38.486	51.782	25.256	1.00	30.62	AAAAA
ATOM	3231	CD	GLU	345	30.679	52.858	44.378	1.00	58.27	AAAAA	ATOM	3391	O	ARC	361	39.621	52.579	25.252	1.00	34.58	AAAAA
ATOM	3232	OE1	GLU	345	29.782	51.979	44.437	1.00	63.94	AAAAA	ATOM	3392	N	HYS	362	37.402	54.333	24.479	1.00	32.24	AAAAA
ATOM	3233	OE2	GLU	345	30.537	53.994	44.887	1.00	62.15	AAAAA	ATOM	3394	CA	HIS	362	36.402	51.518	24.479	1.00	34.64	AAAAA
ATOM	3234	C	GLU	345	32.708	49.749	43.130	1.00	43.01	AAAAA	ATOM	3395	CB	HIS	362	36.995	52.285	23.227	1.00	33.74	AAAAA
ATOM	3235	O	GLU	345	33.257	50.085	44.166	1.00	45.52	AAAAA	ATOM	3396	CG	HIS	362	37.843	52.621	21.986	1.00	35.37	AAAAA
ATOM	3236	N	ASN	346	32.160	48.552	42.968	1.00	45.75	AAAAA	ATOM	3397	CD2	HIS	362	38.038	51.793	23.338	1.00	35.37	AAAAA
ATOM	3238	CA	ASN	346	32.208	47.529	44.022	1.00	48.31	AAAAA	ATOM	3398	ND1	HIS	362	38.655	51.704	21.361	1.00	33.84	AAAAA
ATOM	3239	CB	ASN	346	30.852	46.771	44.058	1.00	51.54	AAAAA	ATOM	3400	CE1	HIS	362	39.313	52.296	20.383	1.00	32.38	AAAAA
ATOM	3240	CG	ASN	346	30.989	45.244	44.244	1.00	55.38	AAAAA	ATOM	3401	NE2	HIS	362	38.957	51.565	20.346	1.00	29.52	AAAAA
ATOM	3241	OD1	ASN	346	31.208	44.748	45.365	1.00	54.89	AAAAA	ATOM	3403	C	HIS	362	35.366	51.064	24.917	1.00	36.40	AAAAA
ATOM	3242	ND2	ASN	346	30.832	44.495	43.141	1.00	55.35	AAAAA	ATOM	3404	O	HIS	362	34.667	52.059	24.724	1.00	36.40	AAAAA
ATOM	3245	O	ASN	346	33.164	46.560	43.923	1.00	49.78	AAAAA	ATOM	3405	N	SER	363	35.285	51.817	26.013	1.00	37.14	AAAAA
ATOM	3246	O	ASN	346	33.530	45.494	44.226	1.00	52.95	AAAAA	ATOM	3407	CA	SER	363	34.360	53.527	27.103	1.00	36.68	AAAAA
ATOM	3247	N	PHE	347	34.112	47.105	42.884	1.00	49.92	AAAAA	ATOM	3408	CB	SER	363	34.997	53.891	28.442	1.00	37.92	AAAAA
ATOM	3249	CA	PHE	347	35.505	46.366	42.500	1.00	47.86	AAAAA	ATOM	3409	OG	SER	363	35.693	52.778	28.965	1.00	35.98	AAAAA
ATOM	3250	CD	PHE	347	35.314	45.747	41.131	1.00	46.22	AAAAA	ATOM	3411	C	SER	363	33.061	54.291	26.927	1.00	40.37	AAAAA
ATOM	3251	CG	PHE	347	34.523	44.492	41.122	1.00	45.82	AAAAA	ATOM	3412	O	SER	363	32.774	55.265	27.644	1.00	36.73	AAAAA
ATOM	3252	CD1	PHE	347	33.374	44.401	40.350	1.00	47.18	AAAAA	ATOM	3413	N	HIS	364	32.281	53.843	25.951	1.00	43.35	AAAAA
ATOM	3253	CD2	PHE	347	34.975	43.367	41.783	1.00	49.39	AAAAA	ATOM	3415	CA	HIS	364	30.995	54.464	25.951	1.00	45.91	AAAAA
ATOM	3254	CE1	PHE	347	32.687	43.207	40.225	1.00	48.19	AAAAA	ATOM	3416	CB	HIS	364	30.506	53.231	24.315	1.00	42.31	AAAAA
ATOM	3255	CE2	PHE	347	34.302	42.161	41.669	1.00	48.72	AAAAA	ATOM	3417	CG	HIS	364	31.547	54.027	23.255	1.00	40.39	AAAAA
ATOM	3256	CZ	PHE	347	33.153	42.080	40.885	1.00	50.09	AAAAA	ATOM	3418	CD2	HIS	364	32.104	53.087	22.454	1.00	37.68	AAAAA
ATOM	3257	C	PHE	347	36.690	47.336	42.397	1.00	49.37	AAAAA	ATOM	3419	ND1	HIS	364	32.202	55.208	22.973	1.00	36.18	AAAAA
ATOM	3258	O	PHE	347	37.847	46.913	42.438	1.00	52.13	AAAAA	ATOM	3421	CE1	HIS	364	33.117	54.592	22.050	1.00	37.88	AAAAA
ATOM	3259	N	MET	348	36.405	48.631	42.258	1.00	46.83	AAAAA	ATOM	3422	NE2	HIS	364	33.080	53.713	21.716	1.00	39.37	AAAAA
ATOM	3261	CA	MET	348	37.468	49.615	42.092	1.00	43.67	AAAAA	ATOM	3424	C	HIS	364	29.974	54.223	26.745	1.00	46.53	AAAAA
ATOM	3262	CB	MET	348	37.525	50.076	40.637	1.00	42.21	AAAAA	ATOM	3425	O	HIS	364	29.200	55.113	27.095	1.00	50.00	AAAAA
ATOM	3263	CG	MET	348	37.435	48.955	39.618	1.00	41.47	AAAAA	ATOM	3426	N	ALA	365	30.005	53.026	27.311	1.00	44.46	AAAAA
ATOM	3264	SD	MET	348	37.816	49.499	37.940	1.00	45.56	AAAAA	ATOM	3428	CA	ALA	365	29.102	52.673	28.383	1.00	45.94	AAAAA
ATOM	3265	CE	MET	348	37.633	51.237	38.105	1.00	45.81	AAAAA	ATOM	3429	C	ALA	365	29.247	51.212	28.675	1.00	42.23	AAAAA
ATOM	3266	C	MET	348	37.346	50.835	42.954	1.00	43.10	AAAAA	ATOM	3430	O	ALA	365	29.283	53.472	29.687	1.00	42.62	AAAAA
ATOM	3267	O	MET	348	38.237	51.679	42.971	1.00	45.33	AAAAA	ATOM	3431	N	ALA	365	28.682	53.300	30.700	1.00	47.27	AAAAA
ATOM	3268	N	GLY	349	36.242	50.944	43.667	1.00	45.75	AAAAA	ATOM	3432	N	LEU	366	30.074	54.547	29.694	1.00	37.83	AAAAA
ATOM	3270	CA	GLY	349	36.024	52.117	44.504	1.00	47.20	AAAAA	ATOM	3434	CA	LEU	366	30.303	55.397	30.935	1.00	34.43	AAAAA
ATOM	3271	C	GLY	349	37.063	52.367	45.571	1.00	46.70	AAAAA	ATOM	3435	CB	VAL	366	31.782	55.347	31.330	1.00	35.50	AAAAA
ATOM	3272	O	GLY	349	37.221	53.501	46.038	1.00	45.69	AAAAA	ATOM	3436	CG	VAL	366	32.748	54.182	31.586	1.00	37.85	AAAAA
ATOM	3273	N	LEU	350	37.796	51.312	45.944	1.00	47.30	AAAAA	ATOM	3437	CD1	LEU	366	34.151	54.791	31.721	1.00	39.21	AAAAA
ATOM	3275	CA	LEU	350	38.797	51.417	46.982	1.00	48.18	AAAAA	ATOM	3438	CD2	LEU	366	32.391	53.388	32.835	1.00	33.39	AAAAA
ATOM	3276	CB	LEU	350	38.826	50.150	47.817	1.00	47.68	AAAAA	ATOM	3439	C	LEU	366	29.872	56.711	30.782	1.00	34.59	AAAAA
ATOM	3277	CG	LEU	350	38.226	50.472	49.189	1.00	50.77	AAAAA	ATOM	3440	O	LEU	366	29.887	57.226	29.681	1.00	39.48	AAAAA
ATOM	3278	CD1	LEU	350	37.770	49.183	49.823	1.00	49.78	AAAAA	ATOM	3441	N	VAL	367	29.552	57.357	31.901	1.00	34.62	AAAAA
ATOM	3279	CD2	LEU	350	39.259	51.213	50.078	1.00	51.01	AAAAA	ATOM	3443	CA	VAL	367	29.131	58.754	31.905	1.00	34.89	AAAAA
ATOM	3280	C	LEU	350	40.214	51.767	46.568	1.00	40.86	AAAAA	ATOM	3444	CB	VAL	367	27.645	58.863	32.297	1.00	36.40	AAAAA
ATOM	3281	O	LEU	350	41.021	52.141	47.433	1.00	51.97	AAAAA	ATOM	3445	CG1	VAL	367	27.230	60.320	32.474	1.00	38.87	AAAAA
ATOM	3282	N	ILE	351	40.531	51.655	45.274	1.00	46.49	AAAAA	ATOM	3446	CG2	VAL	367	26.810	58.229	31.224	1.00	36.70	AAAAA
ATOM	3284	CA	ILE	351	41.874	51.996	44.800	1.00	41.30	AAAAA	ATOM	3447	C	VAL	367	29.981	59.577	32.872	1.00	34.18	AAAAA
ATOM	3285	CB	ILE	351	42.026	51.782	43.279	1.00	36.48	AAAAA	ATOM	3448	O	VAL	367	29.994	60.813	32.833	1.00	30.93	AAAAA
ATOM	3286	CG2	ILE	351	43.289	52.458	42.769	1.00	34.25	AAAAA	ATOM	3449	N	SER	368	30.687	58.873	33.747	1.00	37.44	AAAAA
ATOM	3287	CG1	ILE	351	42.116	54.373	43.338	1.00	47.45	AAAAA	ATOM	3450	CD1	PHE	371	34.703	52.59	37.639	1.00	38.48	AAAAA
ATOM	3288	CD1	ILE	351	45.139	53.868	43.147	1.00	26.57	AAAAA	ATOM	3480	CD2	PHE	371	33.503	54.512	36.909	1.00	41.45	AAAAA
ATOM	3289	CE	VAL	354	48.861	54.640	40.374	1.00	34.29	AAAAA	ATOM	3481	CE1	PHE	371	35.456	52.626	36.469	1.00	36.69	AAAAA
ATOM	3316	O	VAL	354	49.006	55.850	40.167	1.00	34.58	AAAAA	ATOM	3482	CE2	PHE	371	34.264	54.541	35.728	1.00	4	

Figure 1 (cont'd)

ATOM	3551	CD2	LEU	377	48.524	59.490	46.127	1.00	35.51	AAAAA	ATOM	3706	CD2	LEU	393	41.712	57.482	21.327	1.00	25.78	AAAAA
ATOM	3552	C	LEU	377	46.966	59.205	42.276	1.00	35.54	AAAAA	ATOM	3707	C	LEU	393	38.907	58.277	23.572	1.00	31.54	AAAAA
ATOM	3553	O	LEU	377	46.792	57.988	42.342	1.00	32.60	AAAAA	ATOM	3708	O	LEU	393	38.885	57.086	23.916	1.00	30.34	AAAAA
ATOM	3554	N	ILE	378	47.603	59.800	41.267	1.00	35.90	AAAAA	ATOM	3709	N	ASP	394	38.021	58.812	22.726	1.00	32.68	AAAAA
ATOM	3555	CA	ILE	378	48.258	59.087	40.169	1.00	37.38	AAAAA	ATOM	3711	CA	ASP	394	36.991	57.993	22.095	1.00	34.14	AAAAA
ATOM	3557	CB	ILE	378	47.621	59.424	38.797	1.00	36.92	AAAAA	ATOM	3712	CB	ASP	394	37.681	56.856	21.355	1.00	39.38	AAAAA
ATOM	3558	CG2	ILE	378	48.421	58.788	37.675	1.00	31.15	AAAAA	ATOM	3713	CG	ASP	394	36.891	56.352	20.184	1.00	40.62	AAAAA
ATOM	3559	CG1	ILE	378	46.186	58.870	38.737	1.00	36.11	AAAAA	ATOM	3714	OD1	ASP	394	37.510	55.716	19.279	1.00	43.56	AAAAA
ATOM	3560	CD1	ILE	378	45.373	59.423	37.585	1.00	33.62	AAAAA	ATOM	3715	OD2	ASP	394	35.665	56.592	20.190	1.00	39.59	AAAAA
ATOM	3561	C	ILE	378	49.727	59.543	40.194	1.00	39.52	AAAAA	ATOM	3716	C	ASP	394	36.051	57.428	23.131	1.00	34.44	AAAAA
ATOM	3562	O	ILE	378	50.032	60.736	40.099	1.00	40.21	AAAAA	ATOM	3717	O	ASP	394	35.968	56.205	23.339	1.00	28.78	AAAAA
ATOM	3563	N	LEU	379	50.628	58.577	40.345	1.00	40.05	AAAAA	ATOM	3718	N	ASN	395	35.338	58.341	23.772	1.00	34.65	AAAAA
ATOM	3565	CA	LEU	379	52.055	58.842	40.447	1.00	38.95	AAAAA	ATOM	3720	CA	ASN	395	34.407	57.984	24.819	1.00	36.47	AAAAA
ATOM	3566	CB	LEU	379	52.719	57.650	41.129	1.00	38.88	AAAAA	ATOM	3721	CB	ASN	395	34.991	58.434	26.157	1.00	36.56	AAAAA
ATOM	3567	CG	LEU	379	52.095	57.212	42.463	1.00	38.74	AAAAA	ATOM	3722	CG	ASN	395	36.086	57.502	26.646	1.00	35.14	AAAAA
ATOM	3568	CD1	LEU	379	52.815	56.032	43.029	1.00	37.60	AAAAA	ATOM	3723	OD1	ASN	395	35.202	56.277	26.740	1.00	35.26	AAAAA
ATOM	3569	OD2	LEU	379	56.047	56.255	43.452	1.00	36.65	AAAAA	ATOM	3724	ND2	ASN	395	37.239	58.080	26.956	1.00	37.41	AAAAA
ATOM	3570	C	LEU	379	52.733	59.165	39.128	1.00	40.01	AAAAA	ATOM	3727	C	ASN	395	33.032	58.599	24.567	1.00	36.53	AAAAA
ATOM	3571	O	LEU	379	53.593	60.044	39.076	1.00	43.96	AAAAA	ATOM	3728	O	ASN	395	32.695	59.670	25.091	1.00	37.94	AAAAA
ATOM	3572	N	GLY	380	52.354	58.463	38.064	1.00	36.71	AAAAA	ATOM	3729	N	GLN	396	32.245	57.880	23.770	1.00	38.09	AAAAA
ATOM	3574	CA	GLY	380	52.956	58.755	36.778	1.00	34.15	AAAAA	ATOM	3731	CA	GLN	396	30.911	58.302	23.339	1.00	38.47	AAAAA
ATOM	3575	C	GLY	380	54.329	57.991	36.485	1.00	35.78	AAAAA	ATOM	3732	CB	GLN	396	30.173	57.106	22.740	1.00	37.03	AAAAA
ATOM	3576	O	GLY	380	54.771	58.124	35.401	1.00	36.80	AAAAA	ATOM	3733	CG	GLN	396	29.991	57.148	21.246	1.00	35.68	AAAAA
ATOM	3577	N	GLU	381	54.705	57.186	35.432	1.00	36.39	AAAAA	ATOM	3734	CD	GLN	396	29.509	55.815	20.698	1.00	41.00	AAAAA
ATOM	3579	CA	GLU	381	55.936	56.393	37.259	1.00	36.23	AAAAA	ATOM	3735	OE1	GLN	396	28.688	55.145	21.310	1.00	47.25	AAAAA
ATOM	3580	CB	GLU	381	56.021	55.335	38.367	1.00	32.64	AAAAA	ATOM	3736	NE2	GLN	396	30.019	55.422	19.535	1.00	42.50	AAAAA
ATOM	3581	CG	GLU	381	55.842	55.837	39.673	1.00	31.08	AAAAA	ATOM	3739	C	GLN	396	29.959	59.029	24.292	1.00	38.09	AAAAA
ATOM	3582	CD	GLU	381	56.134	55.337	40.915	1.00	30.26	AAAAA	ATOM	3740	O	GLN	396	29.418	60.055	23.913	1.00	39.65	AAAAA
ATOM	3583	OE1	GLU	381	56.193	54.097	41.090	1.00	25.59	AAAAA	ATOM	3741	N	ASN	397	29.767	58.526	25.516	1.00	40.01	AAAAA
ATOM	3584	OE2	GLU	381	56.613	56.192	41.718	1.00	28.20	AAAAA	ATOM	3743	CA	ASN	397	28.794	59.115	26.467	1.00	38.64	AAAAA
ATOM	3585	C	GLU	381	56.095	55.739	35.867	1.00	38.63	AAAAA	ATOM	3744	CB	ASN	397	27.795	58.035	26.846	1.00	35.69	AAAAA
ATOM	3586	O	GLU	381	57.201	55.342	35.467	1.00	39.43	AAAAA	ATOM	3745	CG	ASN	397	27.182	57.370	25.624	1.00	39.95	AAAAA
ATOM	3587	N	GLU	382	54.992	55.637	35.133	1.00	36.87	AAAAA	ATOM	3746	OD1	ASN	397	26.447	58.014	24.865	1.00	42.85	AAAAA
ATOM	3589	CA	GLU	382	54.999	55.074	33.800	1.00	34.67	AAAAA	ATOM	3747	ND2	ASN	397	27.484	56.084	25.417	1.00	36.45	AAAAA
ATOM	3590	CB	GLU	382	54.645	53.613	33.835	1.00	31.71	AAAAA	ATOM	3750	C	ASN	397	29.264	59.795	27.750	1.00	38.08	AAAAA
ATOM	3591	CG	GLU	382	54.998	52.888	32.572	1.00	44.29	AAAAA	ATOM	3751	O	ASN	397	28.440	60.235	28.555	1.00	38.86	AAAAA
ATOM	3592	CD	GLU	382	55.450	51.444	32.833	1.00	52.79	AAAAA	ATOM	3752	N	LEU	398	30.580	59.873	27.923	1.00	38.81	AAAAA
ATOM	3593	OE1	GLU	382	55.976	51.157	33.946	1.00	51.32	AAAAA	ATOM	3754	CA	LEU	398	31.208	60.452	29.099	1.00	38.24	AAAAA
ATOM	3594	OE2	GLU	382	55.278	50.597	31.914	1.00	57.67	AAAAA	ATOM	3755	C	LEU	398	32.725	60.276	28.995	1.00	38.47	AAAAA
ATOM	3595	C	GLU	382	53.919	55.851	33.098	1.00	37.67	AAAAA	ATOM	3756	CG	LEU	398	33.536	59.791	30.199	1.00	33.50	AAAAA
ATOM	3596	O	GLU	382	52.850	56.075	33.667	1.00	40.34	AAAAA	ATOM	3757	CD1	LEU	398	34.095	58.412	29.882	1.00	35.71	AAAAA
ATOM	3597	N	GLN	383	54.205	56.286	31.869	1.00	39.42	AAAAA	ATOM	3758	CD2	LEU	398	34.660	60.760	30.498	1.00	32.89	AAAAA
ATOM	3599	CA	GLN	383	53.274	57.090	31.071	1.00	34.77	AAAAA	ATOM	3759	C	LEU	398	30.879	61.912	29.361	1.00	40.51	AAAAA
ATOM	3600	CB	GLN	383	53.599	58.572	31.212	1.00	29.45	AAAAA	ATOM	3760	O	LEU	398	31.307	62.806	28.620	1.00	41.09	AAAAA
ATOM	3601	CG	GLN	383	54.361	58.896	32.453	1.00	24.55	AAAAA	ATOM	3761	N	CLN	399	30.159	62.150	30.458	1.00	44.82	AAAAA
ATOM	3602	CD	GLN	383	54.918	60.263	32.392	1.00	24.86	AAAAA	ATOM	3763	CA	GLN	399	29.743	63.498	30.845	1.00	45.98	AAAAA
ATOM	3603	OE1	GLN	383	55.179	60.753	31.316	1.00	29.07	AAAAA	ATOM	3764	CB	GLN	399	28.298	63.458	31.344	1.00	51.82	AAAAA
ATOM	3604	NE2	GLN	383	55.097	60.906	33.541	1.00	28.28	AAAAA	ATOM	3765	CG	GLN	399	27.287	63.807	30.259	1.00	58.43	AAAAA
ATOM	3607	C	GLN	383	53.335	56.734	29.604	1.00	34.72	AAAAA	ATOM	3766	CD	GLN	399	26.083	62.897	30.283	1.00	33.27	AAAAA
ATOM	3608	O	GLN	383	54.337	56.210	27.070	1.00	34.72	AAAAA	ATOM	3767	OE1	GLN	399	24.992	63.325	30.658	1.00	65.70	AAAAA
ATOM	3609	N	LEU	384	52.255	57.029	28.891	1.00	34.39	AAAAA	ATOM	3768	NE2	GLN	399	26.271	61.627	29.888	1.00	63.89	AAAAA
ATOM	3611	CA	LEU	384	52.189	52.189	28.891	1.00	34.39	AAAAA	ATOM	3771	C	GLN	399	30.621	64.217	31.870	1.00	44.75	AAAAA
ATOM	3612	CB	LEU	384	50.753	54.474	27.221	1.00	29.04	AAAAA	ATOM	3772	OD1	TRP	402	37.854	60.898	38.833	1.00	44.35	AAAAA
ATOM	3614	CD1	TRP	384	48.674	51.231	27.177	1.00	29.25	AAAAA	ATOM	3780	CE3	TRP	402	38.553	61.609	37.846	1.00	39.33	AAAAA
ATOM	3615	CD2	TRP	384	49.539	63.417	27.707	1.00	28.46	AAAAA	ATOM	3782	CD1	TRP	402	36.516	60.091	40.462	1.00	44.07	AAAAA
ATOM	3616	C	TRP	384	49.645	49.265	27.637	1.00	24.65	AAAAA	ATOM	3783	CG	TRP	402	37.382	59.078	40.069	1.00	43.67	AAAAA
ATOM	3617	O	TRP	384	52.972	63.003	29.522	1.00	38.63	AAAAA	ATOM	3785	CD2								

Figure 1 (cont'd)

ATOM	1872	C	LEU	409	44.211	64.611	42.172	1.00	49.41	AAAAA	ATOM	4031	O	VAL	426	37.080	72.084	30.473	1.00	45.01	AAAAA
ATOM	1873	O	LEU	409	44.192	65.839	42.316	1.00	48.67	AAAAA	ATOM	4012	N	SER	427	34.966	72.579	30.000	1.00	46.62	AAAAA
ATOM	1874	N	THR	410	45.317	63.893	42.198	1.00	48.82	AAAAA	ATOM	4034	C	SER	427	34.695	73.194	31.293	1.00	48.46	AAAAA
ATOM	1876	CA	THR	410	46.605	64.527	41.952	1.00	46.46	AAAAA	ATOM	4035	C9	SER	427	33.184	73.447	31.456	1.00	49.20	AAAAA
A	1877	CB	THR	410	47.364	64.730	42.270	1.00	47.45	AAAAA	ATOM	4036	C9	SER	427	32.597	73.899	30.229	1.00	51.43	AAAAA
ATOM	1878	OCA1	THR	410	46.860	65.897	43.940	1.00	48.99	AAAAA	ATOM	4038	C	SER	427	35.237	72.316	32.421	1.00	48.91	AAAAA
ATOM	1880	CG2	THR	410	48.861	64.881	42.997	1.00	47.61	AAAAA	ATOM	4039	O	SER	427	35.928	72.733	33.318	1.00	49.65	AAAAA
ATOM	1881	C	THR	410	47.506	63.740	41.009	1.00	43.42	AAAAA	ATOM	4040	N	GLU	428	34.446	72.025	32.370	1.00	49.00	AAAAA
ATOM	1882	O	THR	410	47.716	62.551	41.191	1.00	42.61	AAAAA	ATOM	4042	CA	GLU	428	35.425	70.333	33.462	1.00	50.84	AAAAA
ATOM	1883	N	ILE	411	48.035	64.406	39.995	1.00	41.25	AAAAA	ATOM	4043	CB	GLU	428	34.693	68.747	31.392	1.00	50.84	AAAAA
ATOM	1885	CA	ILE	411	48.934	63.735	39.070	1.00	41.84	AAAAA	ATOM	4044	CG	GLU	428	33.197	68.875	31.541	1.00	53.24	AAAAA
ATOM	1886	CB	ILE	411	48.565	64.010	37.569	1.00	36.01	AAAAA	ATOM	4045	CD	GLU	428	32.829	69.284	34.969	1.00	60.59	AAAAA
ATOM	1887	CC2	ILE	411	49.253	63.011	36.662	1.00	31.64	AAAAA	ATOM	4046	OE1	GLU	428	32.667	68.380	35.839	1.00	65.08	AAAAA
ATOM	1888	CG1	ILE	411	47.050	63.889	37.375	1.00	36.00	AAAAA	ATOM	4047	OE2	GLU	428	32.696	70.514	35.209	1.00	68.29	AAAAA
ATOM	1889	CD1	ILE	411	46.594	62.884	36.336	1.00	31.18	AAAAA	ATOM	4048	C	GLU	428	36.921	69.886	33.234	1.00	51.94	AAAAA
ATOM	1890	C	ILE	411	50.338	64.265	39.407	1.00	45.51	AAAAA	ATOM	4049	O	GLU	428	37.706	69.999	34.168	1.00	56.08	AAAAA
ATOM	1891	O	ILE	411	50.710	65.175	38.002	1.00	40.16	AAAAA	ATOM	4050	N	ILE	429	37.315	69.592	32.022	1.00	50.82	AAAAA
ATOM	1892	N	LYS	412	51.061	63.468	40.195	1.00	43.71	AAAAA	ATOM	4052	CA	ILE	429	36.697	69.280	31.750	1.00	48.09	AAAAA
ATOM	1894	CA	LYS	412	52.419	63.769	40.634	1.00	41.26	AAAAA	ATOM	4053	C9	ILE	429	36.897	69.136	30.240	1.00	45.91	AAAAA
ATOM	1895	CB	LYS	412	52.972	62.563	41.369	1.00	42.01	AAAAA	ATOM	4054	CG2	ILE	429	40.359	69.094	29.893	1.00	43.32	AAAAA
ATOM	1896	CG	LYS	412	53.111	62.833	42.746	1.00	49.93	AAAAA	ATOM	4055	CG1	ILE	429	38.214	67.854	29.785	1.00	42.83	AAAAA
ATOM	1898	C	LYS	412	53.350	64.073	39.483	1.00	41.15	AAAAA	ATOM	4056	CD1	ILE	429	38.390	67.553	28.335	1.00	44.47	AAAAA
ATOM	1899	O	LYS	412	54.185	64.959	39.560	1.00	40.96	AAAAA	ATOM	4057	C	ILE	429	39.645	70.319	32.333	1.00	50.37	AAAAA
ATOM	1900	N	ALA	413	53.192	63.108	38.411	1.00	40.81	AAAAA	ATOM	4058	O	ILE	429	40.722	69.965	32.817	1.00	50.48	AAAAA
ATOM	1902	CA	ALA	413	54.043	63.445	37.255	1.00	40.95	AAAAA	ATOM	4059	N	TYR	430	39.268	71.596	32.312	1.00	53.59	AAAAA
ATOM	1903	CB	ALA	413	55.277	62.614	37.471	1.00	44.44	AAAAA	ATOM	4061	CA	TYR	430	40.189	72.001	32.854	1.00	56.94	AAAAA
ATOM	1904	C	ALA	413	53.366	62.028	35.959	1.00	40.18	AAAAA	ATOM	4062	CB	TYR	430	40.670	74.041	32.117	1.00	59.37	AAAAA
ATOM	1905	O	ALA	413	52.599	62.071	35.929	1.00	40.51	AAAAA	ATOM	4063	CG	TYR	430	39.955	74.055	30.692	1.00	61.64	AAAAA
ATOM	1906	N	GLY	414	53.694	63.729	34.884	1.00	39.10	AAAAA	ATOM	4064	C1	TYR	430	39.565	72.923	28.943	1.00	60.62	AAAAA
ATOM	1908	CA	GLY	414	53.086	64.434	33.603	1.00	40.43	AAAAA	ATOM	4065	CE1	TYR	430	39.447	72.997	28.583	1.00	61.98	AAAAA
ATOM	1909	C	GLY	414	51.983	64.453	33.371	1.00	43.42	AAAAA	ATOM	4066	CD2	TYR	430	40.073	75.277	30.013	1.00	62.01	AAAAA
ATOM	1910	O	GLY	414	51.870	65.415	34.121	1.00	43.72	AAAAA	ATOM	4067	CE2	TYR	430	39.853	75.356	28.641	1.00	61.34	AAAAA
ATOM	1911	N	LYS	415	51.161	64.247	32.347	1.00	40.85	AAAAA	ATOM	4068	C	ARG	431	39.539	74.205	27.925	1.00	51.30	AAAAA
ATOM	1913	CA	LYS	415	50.065	65.173	32.040	1.00	38.88	AAAAA	ATOM	4069	O	ARG	431	39.226	74.254	26.595	1.00	62.51	AAAAA
ATOM	1914	CB	LYS	415	50.556	66.241	31.084	1.00	39.32	AAAAA	ATOM	4071	C	TYR	430	40.068	72.726	34.366	1.00	55.10	AAAAA
ATOM	1915	CG	LYS	415	50.938	65.625	29.744	1.00	40.34	AAAAA	ATOM	4072	O	TYR	430	40.961	72.266	35.026	1.00	56.49	AAAAA
ATOM	1916	CD	LYS	415	51.401	66.633	28.746	1.00	38.47	AAAAA	ATOM	4073	N	ARG	431	38.964	72.229	34.908	1.00	52.81	AAAAA
ATOM	1917	CE	LYS	415	52.618	66.153	28.048	1.00	35.12	AAAAA	ATOM	4075	CA	ARG	431	38.776	72.253	36.346	1.00	52.51	AAAAA
ATOM	1918	N	LYS	415	52.669	66.925	26.813	1.00	43.52	AAAAA	ATOM	4076	C	ARG	431	37.377	71.782	36.742	1.00	54.84	AAAAA
ATOM	1922	C	LYS	415	48.885	64.446	31.383	1.00	37.63	AAAAA	ATOM	4077	O	ARG	431	37.349	71.386	38.106	1.00	57.04	AAAAA
ATOM	1923	O	LYS	415	48.834	63.201	31.334	1.00	37.93	AAAAA	ATOM	4079	C	ARG	431	39.770	71.250	36.828	1.00	51.03	AAAAA
ATOM	1924	N	MET	416	47.962	65.234	30.834	1.00	35.60	AAAAA	ATOM	4080	D	ARG	431	40.703	71.582	37.554	1.00	49.10	AAAAA
ATOM	1926	CA	MET	416	46.759	64.690	30.204	1.00	30.58	AAAAA	ATOM	4081	N	MET	432	39.516	70.009	36.427	1.00	52.81	AAAAA
ATOM	1927	CB	MET	416	45.548	65.090	31.032	1.00	31.10	AAAAA	ATOM	4083	CA	MET	432	40.376	68.866	36.766	1.00	55.38	AAAAA
ATOM	1928	CG	MET	416	45.916	65.605	32.386	1.00	32.69	AAAAA	ATOM	4084	CB	MET	432	40.049	67.712	35.823	1.00	52.88	AAAAA
ATOM	1929	SD	MET	416	46.485	65.721	32.416	1.00	30.47	AAAAA	ATOM	4085	CC	MET	432	40.286	66.348	36.402	1.00	50.22	AAAAA
ATOM	1930	CE	MET	416	44.258	67.553	33.513	1.00	30.89	AAAAA	ATOM	4086	SD	MET	432	41.440	65.457	35.165	1.00	47.27	AAAAA
ATOM	1931	C	MET	416	46.474	65.039	28.755	1.00	26.23	AAAAA	ATOM	4087	CE	MET	432	40.515	63.999	34.999	1.00	42.56	AAAAA
ATOM	1932	O	MET	416	46.851	66.096	28.258	1.00	24.44	AAAAA	ATOM	4088	C	MET	432	41.852	69.213	36.641	1.00	58.02	AAAAA
ATOM	1933	N	TYR	417	45.797	64.114	28.090	1.00	24.40	AAAAA	ATOM	4089	O	MET	432	42.710	68.694	37.346	1.00	59.47	AAAAA
ATOM	1935	CA	TYR	417	45.375	64.284	26.710	1.00	25.54	AAAAA	ATOM	4090	N	GLU	433	42.131	70.161	35.722	1.00	59.97	AAAAA
ATOM	1936	CB	TYR	417	44.931	63.954	26.401	1.00	31.64	AAAAA	ATOM	4092	CA	GLU	433	43.480	70.643	35.483	1.00	60.19	AAAAA
ATOM	1937	CG	TYR	417	44.303	64.124	26.175	1.00	35.34	AAAAA	ATOM	4093	CB	GLU	433	44.232	71.299	36.996	1.00	62.11	AAAAA
ATOM	1938	CD1	TYR	417	43.916	63.782	26.732	1.00	35.56	AAAAA	ATOM	4094	O	GLU	434	43.147	72.035	37.416	1.00	60.35	AAAAA
ATOM	1939	CE2	TYR	417	43.509	63.292	17.517	1.00	33.63	AAAAA	ATOM	4095	C	TYR	434	43.541	72.770	38.603	1.00	60.47	AAAAA
ATOM	1940	C	TYR	417	43.345	62.735	16.898	1.00	35.86	AAAAA	ATOM	4096	O	TYR	434	45.309	72.285	39.767	1.00	46.23	AAAAA
ATOM	1941	N	TYR	417	43.777	62.191	17.177	1.00	32.67	AAAAA	ATOM	4097	CG	TYR	434	46.904	71.511	37.436	1.00	45.6	

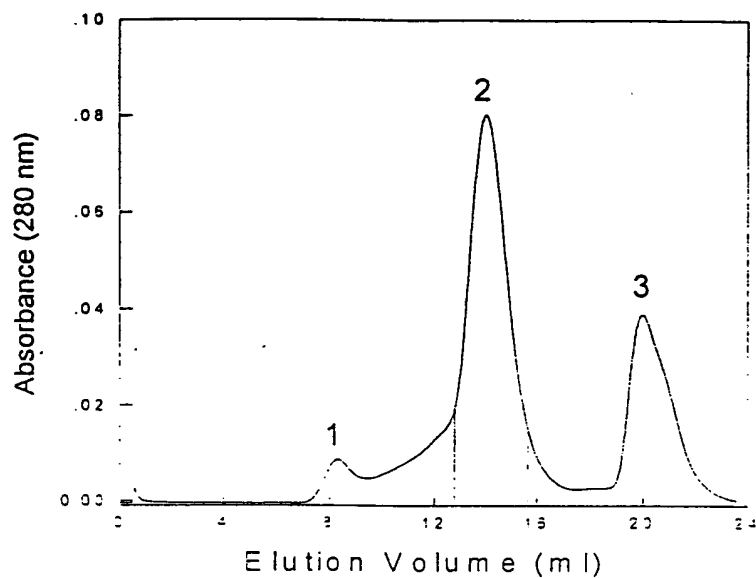
Figure 1 (cont'd)

ATOM	4194	O	LYS	444	45.682	71.789	22.581	1.00	65.94	AAAAA	ATOM	4190	C3	NAG	105B	30.646	22.028	75.808	1.00	65.10	BBBBB
ATOM	4195	N	GLY	445	47.086	70.421	21.445	1.00	63.29	AAAAA	ATOM	4192	O1	NAG	105B	29.991	23.215	75.373	1.00	72.19	BBBBB
ATOM	4197	CA	GLY	445	46.066	69.423	21.117	1.00	59.11	AAAAA	ATOM	4194	C4	NAG	105B	29.721	21.268	76.792	1.00	65.51	BBBBB
ATOM	4198	C	GLY	445	45.622	68.522	22.247	1.00	55.66	AAAAA	ATOM	4196	O4	NAG	105B	29.607	21.997	78.009	1.00	65.49	BBBBB
ATOM	4199	O	GLY	445	44.792	67.610	22.064	1.00	52.13	AAAAA	ATOM	4198	C5	NAG	105B	30.330	19.889	77.043	1.00	64.84	BBBBB
ATOM	4200	N	ASP	446	46.199	68.806	23.414	1.00	53.96	AAAAA	ATOM	4400	O5	NAG	105B	30.415	19.199	75.797	1.00	62.03	BBBBB
ATOM	4202	CA	ASP	446	45.932	68.099	24.668	1.00	49.82	AAAAA	ATOM	4401	C6	NAG	105B	29.654	18.950	78.009	1.00	67.03	BBBBB
ATOM	4203	CB	ASP	446	46.726	68.767	25.819	1.00	46.80	AAAAA	ATOM	4404	O6	NAG	105B	30.323	17.684	78.007	1.00	67.68	BBBBB
ATOM	4204	CC	ASP	446	48.109	68.141	26.059	1.00	43.77	AAAAA	ATOM	4405	C1	NAG	284A	55.225	45.501	66.582	1.00	43.05	BBBBB
ATOM	4205	OD1	ASP	446	48.659	67.456	25.174	1.00	39.45	AAAAA	ATOM	4406	C2	NAG	284A	56.197	46.668	66.564	1.00	40.21	BBBBB
ATOM	4206	OD2	ASP	446	48.655	68.350	27.162	1.00	45.58	AAAAA	ATOM	4410	N2	NAG	284A	56.745	46.859	65.232	1.00	43.34	BBBBB
ATOM	4207	C	ASP	446	44.425	68.197	24.955	1.00	46.31	AAAAA	ATOM	4412	C7	NAG	284A	56.896	48.078	64.713	1.00	39.06	BBBBB
ATOM	4208	O	ASP	446	43.707	67.202	25.011	1.00	43.03	AAAAA	ATOM	4413	O7	NAG	284A	56.610	49.107	65.308	1.00	42.15	BBBBB
ATOM	4209	N	ILE	447	43.959	69.423	25.115	1.00	43.79	AAAAA	ATOM	4414	C8	NAG	284A	57.462	48.164	63.316	1.00	39.13	BBBBB
ATOM	4211	CA	ILE	447	42.574	69.646	25.407	1.00	44.45	AAAAA	ATOM	4418	C3	NAG	284A	57.273	46.321	67.579	1.00	39.39	BBBBB
ATOM	4212	CB	ILE	447	42.435	70.389	26.758	1.00	42.60	AAAAA	ATOM	4420	O3	NAG	284A	58.265	47.338	67.593	1.00	41.03	BBBBB
ATOM	4213	CG2	ILE	447	40.978	70.386	27.225	1.00	41.47	AAAAA	ATOM	4422	C4	NAG	284A	56.610	46.174	68.961	1.00	37.74	BBBBB
ATOM	4214	CG1	ILE	447	43.208	50.600	27.014	1.00	40.40	AAAAA	ATOM	4424	O4	NAG	284A	57.613	45.720	69.912	1.00	36.85	BBBBB
ATOM	4215	CD1	ILE	447	43.069	70.172	29.231	1.00	37.75	AAAAA	ATOM	4425	C5	NAG	284A	55.474	45.177	68.945	1.00	41.49	BBBBB
ATOM	4216	C	ILE	447	41.916	70.438	24.292	1.00	46.85	AAAAA	ATOM	4427	O5	NAG	284A	54.559	45.483	67.862	1.00	45.44	BBBBB
ATOM	4217	ILE	447	41.633	71.632	24.450	1.00	49.18	AAAAA	ATOM	4428	C6	NAG	284A	54.668	45.071	70.260	1.00	42.30	BBBBB	
ATOM	4218	N	ASN	448	41.662	69.790	23.156	1.00	50.47	AAAAA	ATOM	4431	O6	NAG	284A	53.894	46.229	70.570	1.00	42.86	BBBBB
ATOM	4220	CA	ASN	448	41.019	70.514	23.056	1.00	55.78	AAAAA	ATOM	4433	C1	NAG	284A	57.951	46.656	70.868	1.00	33.26	BBBBB
ATOM	4221	CB	ASN	448	41.106	69.766	20.718	1.00	59.98	AAAAA	ATOM	4435	C2	NAG	284A	58.542	45.990	72.101	1.00	30.90	BBBBB
ATOM	4222	CG	ASN	448	40.575	68.378	20.800	1.00	65.00	AAAAA	ATOM	4437	N2	NAG	284B	57.525	45.115	72.646	1.00	27.21	BBBBB
ATOM	4223	OD1	ASN	448	41.207	67.421	20.347	1.00	71.20	AAAAA	ATOM	4439	C7	NAG	284B	57.806	43.866	72.976	1.00	27.34	BBBBB
ATOM	4224	ND2	ASN	448	39.408	68.246	21.395	1.00	72.69	AAAAA	ATOM	4440	O7	NAG	284B	58.931	43.376	72.865	1.00	30.07	BBBBB
ATOM	4227	C	ASN	448	39.572	70.820	22.370	1.00	55.89	AAAAA	ATOM	4441	C8	NAG	284B	56.655	43.038	71.531	1.00	20.62	BBBBB
ATOM	4228	O	ASN	448	38.872	70.064	23.027	1.00	56.11	AAAAA	ATOM	4445	C3	NAG	284B	58.883	47.107	73.114	1.00	33.39	BBBBB
ATOM	4229	N	THR	449	39.334	71.910	21.692	1.00	55.64	AAAAA	ATOM	4447	O3	NAG	284B	59.643	46.597	74.200	1.00	35.36	BBBBB
ATOM	4231	CA	THR	449	37.782	72.433	22.128	1.00	55.58	AAAAA	ATOM	4449	C4	NAG	284B	59.673	48.263	72.497	1.00	34.34	BBBBB
ATOM	4232	CB	THR	449	37.815	73.914	22.423	1.00	57.21	AAAAA	ATOM	4451	O4	NAG	284B	59.645	49.360	73.422	1.00	38.30	BBBBB
ATOM	4233	OG1	THR	449	38.125	74.629	21.212	1.00	59.40	AAAAA	ATOM	4452	C5	NAG	284B	59.108	48.710	71.134	1.00	32.15	BBBBB
ATOM	4235	CG2	THR	449	38.913	74.198	23.479	1.00	59.39	AAAAA	ATOM	4454	O5	NAG	284B	58.880	47.565	70.294	1.00	32.44	BBBBB
ATOM	4236	C	THR	449	36.981	72.185	20.880	1.00	53.18	AAAAA	ATOM	4455	C6	NAG	284B	60.065	49.586	70.360	1.00	30.53	BBBBB
ATOM	4237	THR	449	35.785	72.445	20.812	1.00	52.99	AAAAA	ATOM	4458	O6	NAG	284B	60.325	50.803	71.022	1.00	36.64	BBBBB	
ATOM	4238	N	ARG	450	37.658	71.655	19.885	1.00	52.04	AAAAA	ATOM	4460	C1	MAN	284C	60.861	49.875	73.828	1.00	47.37	BBBBB
ATOM	4240	CA	ARG	450	37.009	71.401	18.632	1.00	52.59	AAAAA	ATOM	4462	C2	MAN	284C	60.651	51.284	74.321	1.00	52.82	BBBBB
ATOM	4241	CB	ARG	450	37.957	71.755	17.483	1.00	51.20	AAAAA	ATOM	4463	O2	MAN	284C	59.718	51.284	75.398	1.00	56.09	BBBBB
ATOM	4242	CG	ARG	450	38.604	70.561	16.048	1.00	48.17	AAAAA	ATOM	4466	C3	MAN	284C	62.000	51.840	74.779	1.00	54.95	BBBBB
ATOM	4243	CD	ARG	450	39.869	70.955	16.073	1.00	46.87	AAAAA	ATOM	4468	O3	MAN	284C	61.827	53.180	75.284	1.00	61.94	BBBBB
ATOM	4244	NE	ARG	450	41.030	70.821	16.942	1.00	47.57	AAAAA	ATOM	4469	C4	MAN	284C	62.581	50.949	75.858	1.00	50.28	BBBBB
ATOM	4246	CZ	ARG	450	41.612	69.664	17.230	1.00	45.63	AAAAA	ATOM	4471	O4	MAN	284C	63.871	51.404	76.227	1.00	49.51	BBBBB
ATOM	4247	NH1	ARG	450	41.143	68.530	15.713	1.00	45.69	AAAAA	ATOM	4473	C5	MAN	284C	62.673	49.529	75.341	1.00	48.06	BBBBB
ATOM	4250	NH2	ARG	450	42.654	69.643	18.051	1.00	46.29	AAAAA	ATOM	4475	O5	MAN	284C	61.374	49.072	74.897	1.00	49.19	BBBBB
ATOM	4252	C	ARG	450	36.633	69.958	18.546	1.00	53.95	AAAAA	ATOM	4476	C6	MAN	284C	63.121	48.619	76.445	1.00	47.11	BBBBB
ATOM	4254	O	ARG	450	35.498	69.603	18.214	1.00	52.79	AAAAA	ATOM	4479	O6	MAN	284C	62.888	49.221	77.701	1.00	46.51	BBBBB
ATOM	4255	N	ASN	451	37.601	69.118	18.877	1.00	57.18	AAAAA	ATOM	4481	C1	MAN	284D	62.583	54.175	74.656	1.00	67.56	BBBBB
ATOM	4257	CA	ASN	451	37.386	67.696	18.757	1.00	60.27	AAAAA	ATOM	4483	C2	MAN	284D	61.843	55.516	74.763	1.00	71.37	BBBBB
ATOM	4258	CB	ASN	451	38.695	66.945	18.781	1.00	58.04	AAAAA	ATOM	4484	O2	MAN	284D	62.728	56.582	74.422	1.00	74.58	BBBBB
ATOM	4259	CG	ASN	451	38.527	65.577	18.268	1.00	59.45	AAAAA	ATOM	4487	C3	MAN	284D	60.603	55.514	73.831	1.00	72.21	BBBBB
ATOM	4260	OD1	ASN	451	38.273	64.657	19.033	1.00	62.58	AAAAA	ATOM	4489	O3	MAN	284D	59.978	56.792	73.836	1.00	74.67	BBBBB
ATOM	4261	ND2	ASN	451	38.612	65.424	16.955	1.00	57.87	AAAAA	ATOM	4491	C4	MAN	284D	60.988	55.115	72.388	1.00	71.55	BBBBB
ATOM	4264	C	ASN	451	36.448	67.028	19.715	1.00	61.89	AAAAA	ATOM	4493	O4	MAN	284D	59.823	55.021	71.573	1.00	71.37	BBBBB
ATOM	4267	O	ASN	451	35.991	67.626	20.686	1.00	64.98	AAAAA	ATOM	4495	C5	MAN	284D	61.695	53.760	72.450	1.00	68.81	BBBBB
ATOM	4268	CA	ASN	452	35.275	64.944	20.807	1.00	68.31	AAAAA	ATOM	4497	O5	MAN	284D	62.865	53.867	73.288	1.00	68.38	BBBBB
ATOM	4269	CB	ASN	452	35.153	65.499	21.644	1.00	67.97	AAAAA	ATOM	4498	C6	MAN	284D	62.122	53.				

Face 1		Cleft 1		Face 2		Cleft 2		Face 3
(12D)	11N	10R	8D	(6G)	5P			
(35S)	33L	32L	30H	28Y	(27G)	26E	255I	259E
(61A)	59R	58F	56L	54Y	53E	242E	241F	256L
								263S
								262D
								305E
								305T
								310T
								312D
								313S
								335R
								(316S)
								315T
								336R
								(318Q)
								318Q
								319M
								(302C)
								300K
								282I
								284E
								(283R)
								276E
								(274M)
								272E
								279S
								240R
								(280G)
								270D
								138Y

Figure 2

(a)



(b)

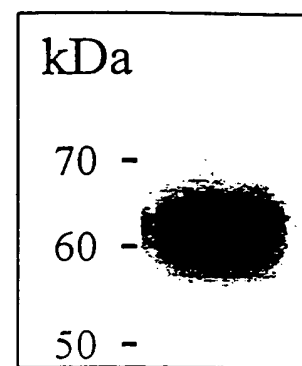
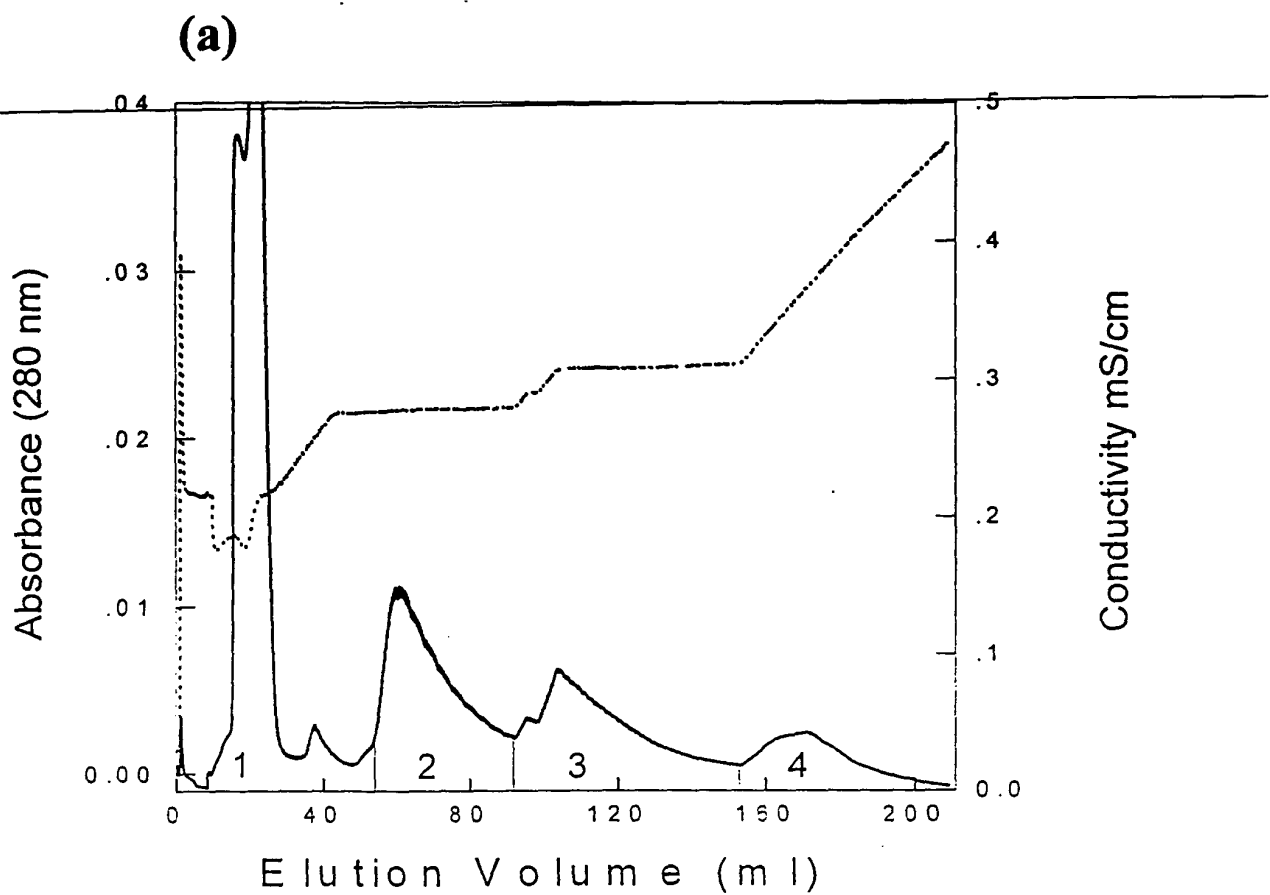
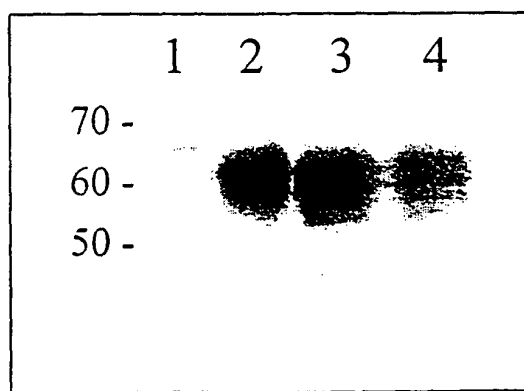


Figure 3



(b)



(c)

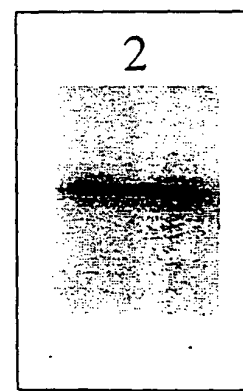


Figure 4

Figure 5

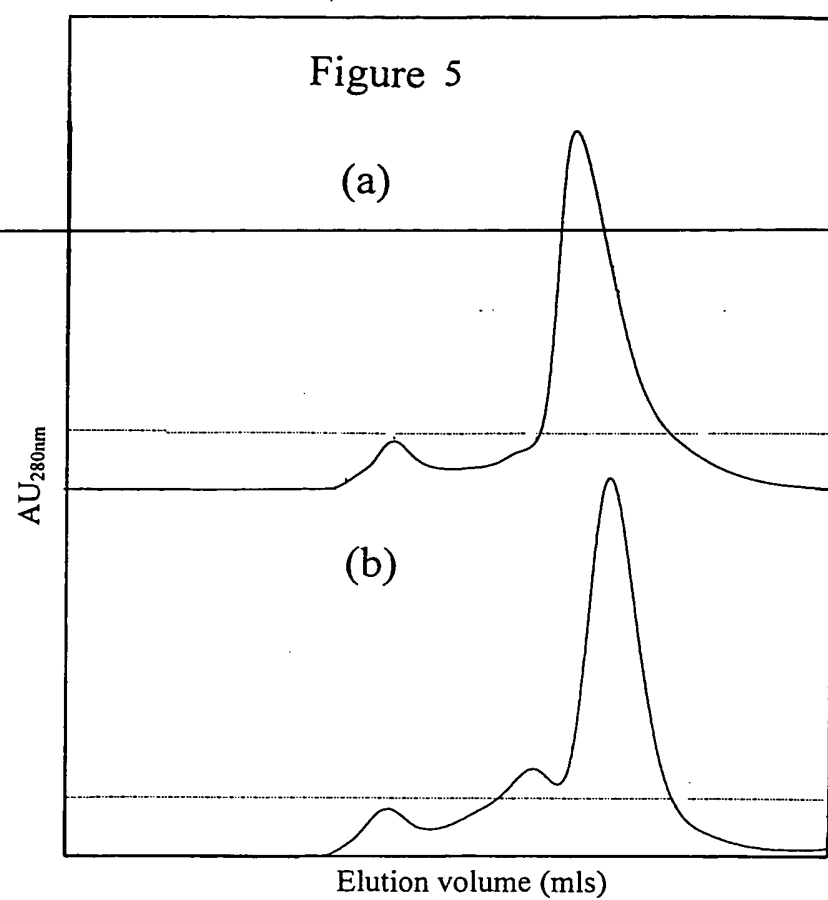
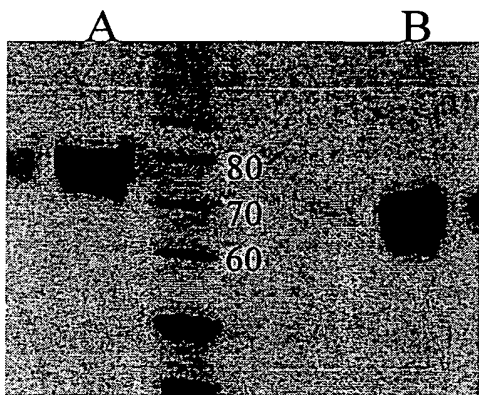
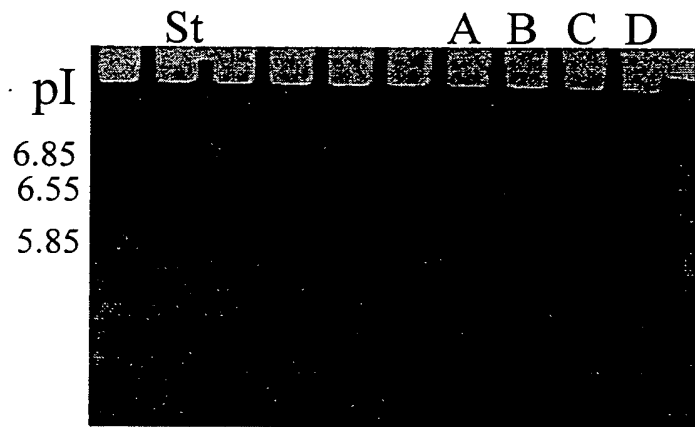


Figure 6

(a) SDS PAGE



(b) IEF pH3-7



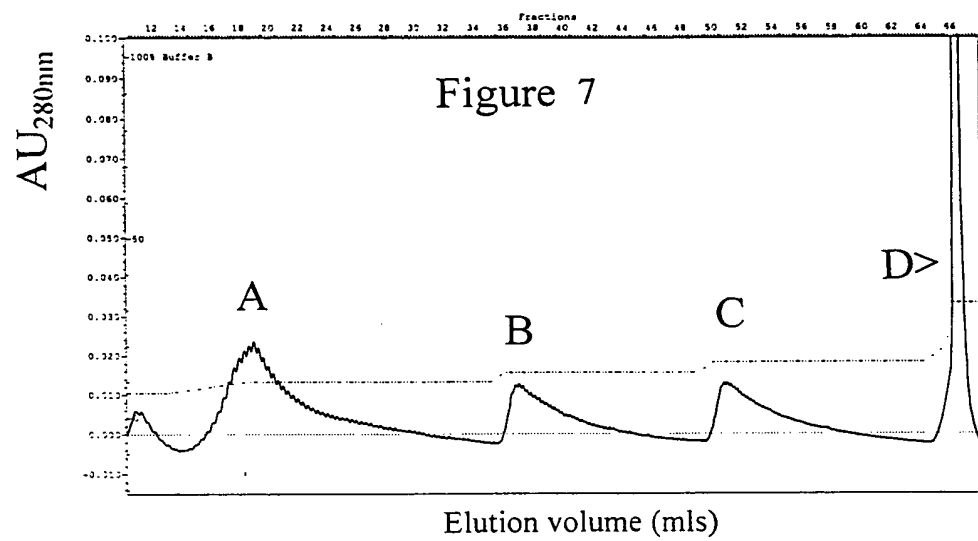




Figure 8

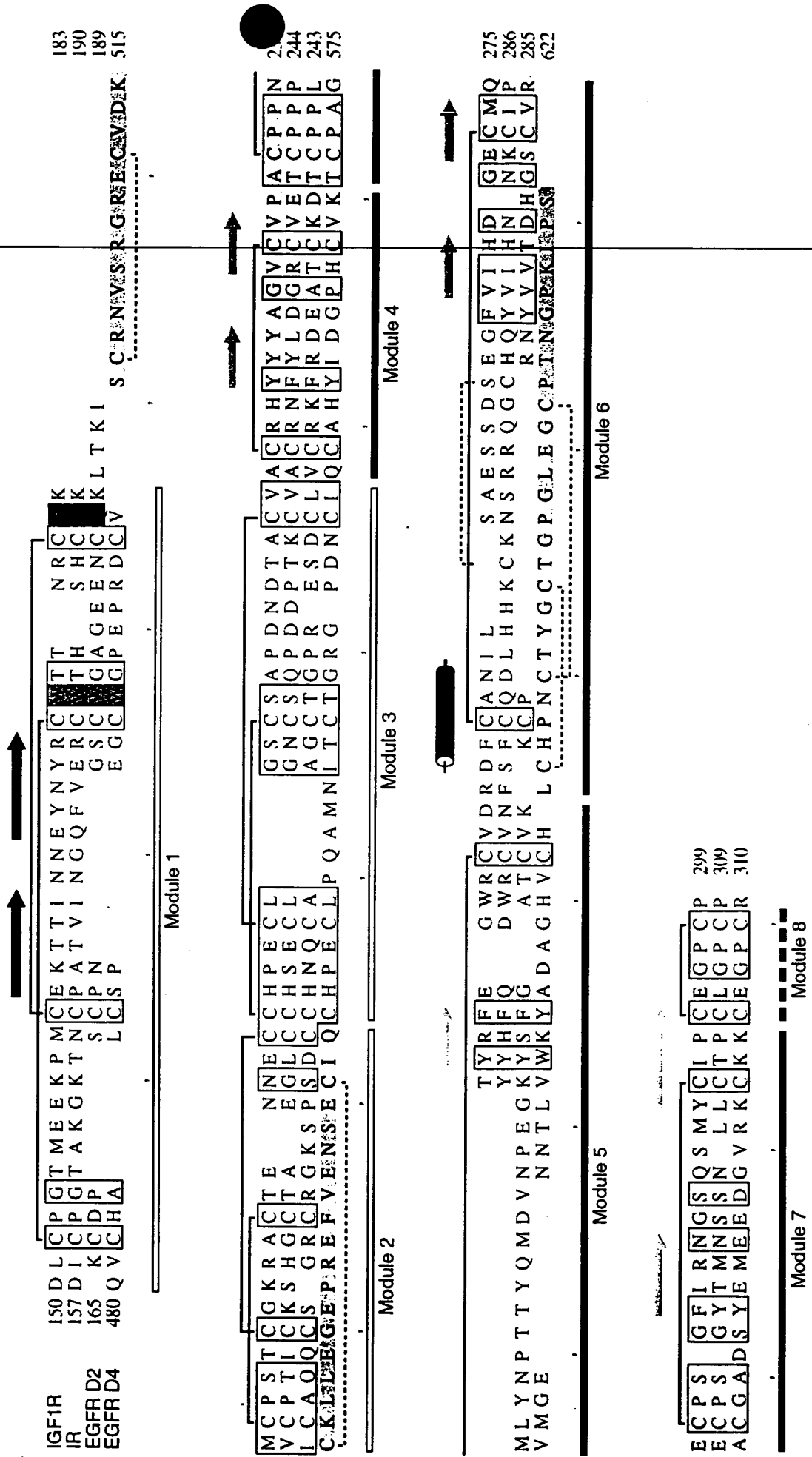


Figure 9b

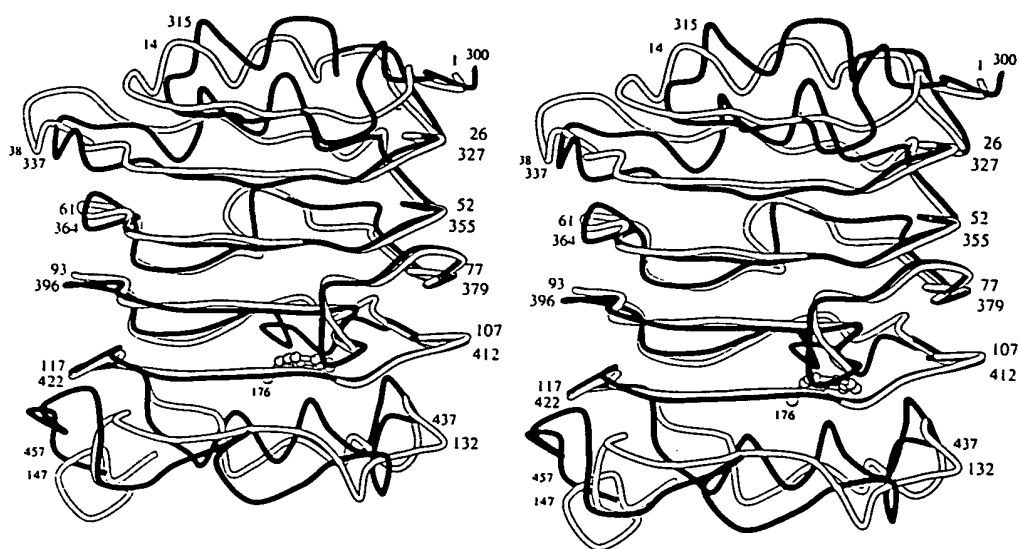


Figure 10

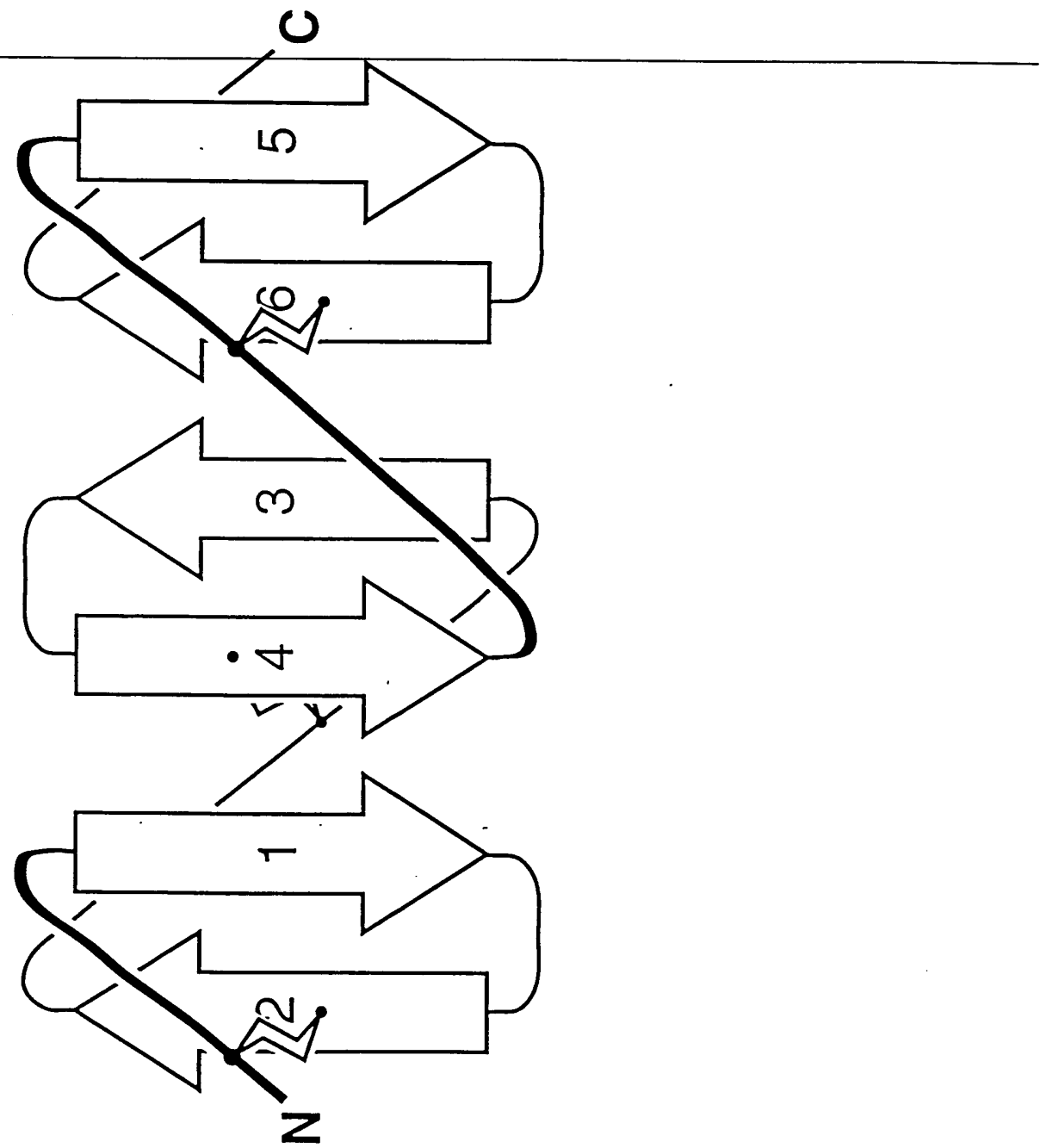


Figure 11

15/11

14/10

12/8

36/32

34/30

64/58

87/81

96/90

91/85

Figure 12

Figure 13: Sequence Alignment of hIGF-1R, hIR and hIRR ectodomains.

Derived by use of the PileUp program in the software package of the Genetics Computer Group, 575 Science Drive, Madison, Wisconsin, USA.

Symbol Comparison table: GenRunData:PileUpPep.Cmp CompCheck: 1254

GapWeight: 3.0
~~GapLengthWeight: 0.1~~

Name: Higflr	Len: 972	cheCk: 1781	Weight: 1.00
Name: Hir	Len: 972	cheCk: 2986	Weight: 1.00
Name: Hirr	Len: 972	cheCk: 9819	Weight: 1.00

*	*
HigflrEICGP GIDIRNDYQQ LKRL <u>EN</u> CTVI EGYLHILLIS K..AEDYRSY 43
Hir	HLYPGEVC.P GMDIRNNLTR LHE <u>LEN</u> CSVI EGHLQILLMF KTRPEDFRDL 49
HirrMNVC.P SLDIRSEVAE LROLENCSVV EGHLOILLMF TATGEDFRGL 45

Higflr	RFPKLTIVITE	YLLLF ^R VAGL	ESLGD ^L FPNL	<u>TVIRG</u> WKL ^F Y	NYALVIFEM ^T	93
Hir	SFPKLIMITD	YLLLF ^R VYGL	ESLKDLFPNL	<u>TVIRG</u> SRLFF	NYALVIFEM ^V	99
Hirr	SFPRLTQVTD	YLLLF ^R VYGL	ESLRDLPNL	AVIRGTRFL ^L	GYALVIFEMP	95

Higf1r	NLKDIGLYNL	R <u>N</u> ITRGAIRI	EKNADLCYLS	TVDWSLILDA	VSNNYIVGNK	143
Hir	HLKELGLYNL	M <u>N</u> ITRGCSVRI	EKNNELCYLA	TIDWSRILIDS	VEDNYIVLNK	149
Hirr	HLRDVALPAL	GAVLRGAVRV	EKNOELCHLS	TIDWGLLOPA	PGANHIVGNK	145

Higflr	PPK.ECGDLC PGTMEEKPM.	CEKTTINNEY NYRCWTTNRC	QKMCPSCTCGK	191
Hir	DDNEECDIC PGTAKGKTN.	CPATVINGQF VERCWTHSHC	QKVCPICKS	198
Hirr	LG.FECADVC PGVLGAAGEP	CAKTTEFSGHT DYRCWTSSHC	QBVCPCPHG	193

Higflr	RACTENNECC	HPECLGSCSA	PDNDTACVAC	RHYYYAGVCV	PACPPNTYRF	241
Hir	HGCTAEGLC	HSECLGNCSA	PDDPTKCVAC	RNFYLDGRVC	ETCPFPYYHF	248
Hir	MACTAPCECC	HTECTGCCSA	EDPDRGACVAC	RHLYKFGACT	WACTPCTYXO	243

Higfir	EGWRCVDRDF	CANILSAES. . . SDSEGFV	IHDGECMQEC	PSGFIRNGSQ	287	
Hir	QDWRCVNSF	CQDLHHKCKN	SRRQGCHQYV	IHNNKCIPEC	PSGYTMNSSN	298
Hirr	ESWRCVTAEP	CASLUSVPG	RASTEC	IHOGSCLAOC	PSGETBNSS	287

```

Higfir NNIASELENF MGLIEVVVTGY VKIRHSHALV SLSFLKNLRL ILGEEQLEGN 387
      Hir NNLAAELEAN LGLIEEISGY LKIRRSHALV SLSFFRKRLR IRGETLEIGN 397
      Hirr VNLFPOLQHS LGLVETITGF LKIKHSHALV SLGEEFKNLKL IRGDAVMDGN 385

```

Higflr	<u>Y</u> SFYVLDNQN	LQQLWDWDHR	<u>N</u> LTIKAGKMY	FAFNPKLCVS	EIYRMEVTG	437
Hir	<u>Y</u> SFYALDNQN	LRQLWDWSKH	<u>N</u> LTITQGKLF	FHYNPKLCLS	EIHKMEEVSG	447
Hirr	YTYLVLNDNON	LOOLGSWVAA	GLTIPVGKIX	FAFNPRLCLE	HIYRLEEVVG	435

							*	!End of	1-462 fragment	
Higfir	TKGRQSKGDI	NTRNNNGERAS	CESDV	LHFTS	TTTSKNRIII	TWHRYRPPDY				487
Hir	TKGRQERNDI	ALKTNGDQAS	CENEL	LKF SY	IRTSFDKILL	RWEPYWPPDF				497
Hirr	TRGRONKAEI	NPRTNGDRAA	COTRT	LRFVS	NVTEADRILL	RWERVEPLEA				485

Higfir	RDLISFTVYY KEAPFKNVTE YDGQDACGSN SWNMVDVDLP	PNKDV	532
Hir	RDLLGFMLFY KEAPYQNVTE FDGQDACGSN SWTVVDidPP LRSNDPKSQN		547
Hirr	RDLLSFIVYY KESPFQ NATE HVGPDACGTQ SWNLLDVELP L	SRTQ	530
* * * * *			
Higfir	EPGILLHGLK PWTQYAVYVK AVTLMVEND HIRGAKSEIL YIRT NASVPS		582
Hir	HPGWLMRGLK PWTQYAI F VK TL.VTFSDER RTYGAKSDII YVQTDATNPS		596
Hirr	EPGVTLASLK PWTQYAVFVR AITLTTEEDS PHQGAQSPIV YLRTLPAAPT		580
* * * * *			
Higfir	IPLDVLSASN <u>SSSQLIVKWN</u> PPSLPNGN <u>LS</u> YYIVRWRQRP QDG YLYRHN		632
Hir	VPLDPISVSN <u>SSSQIILKW</u> KPPSDP <u>NGNIT</u> HYLVFWERQA EDSELFELDY		646
Hirr	VPQDVISTSN <u>SSSHLLVRWK</u> PPTQRNGN <u>LT</u> YYLVLWQRLA EDGDLYLNDY		630
* * * * *			
Higfir	CSKD.KIPIR KYADGTIDIE EVTENPKTEV CGGEKGP <u>CCA</u> C . . . PKTEAE		678
Hir	CLKGLKLPSR TWS.PPFSE DSQKH <u>NOSE</u> . YEDSAGECCS C . . . PKTDSQ		691
Hirr	CHRGLRLPTS N.NDPRFDGE DGDPEAEME. SDCCP CQHPPPGQVL		673
-----><-----β			
Higfir	KQAEKEEAEY RKVFENFLHN SIFVPRPERK RRDVM OVANT TMSSRSR <u>NTT</u>		728
Hir	ILKELEESSF RKT FEDY LHN VVFVPRPSRK RRSLGDVG <u>NV</u> TVAVP . . . TV		738
Hirr	PPLEAQEASF QKKFENFLHN AITIPISPWK VTSINKSPQR D.SGRHRRAA		722
* * * * *			
Higfir	AA . DTYNIT DPEELETEYP FFESRVDNKE RTVISNLRPF TLYRIDIH <u>SC</u>		776
Hir	AAFP <u>NTSSTS</u> VPTSPEEHRP F . . EKVVNKE SLVISGLRH F TGYRIELQAC		786
Hirr	GPLRLGGN <u>SS</u> DFEIQEDKVP RE RAVLSGLRH F TEYRIDIHAC		764
* * * * *			
Higfir	NHEAEKLGCS ASN FV FARTM PAEGADDIPG PVTWEPRPEN SIFLKWP <u>PEPE</u>		826
Hir	NQDTPEERCS VAA YVSART M PEAKADDIVG PVTHEIFENN VVHLMW <u>QEPK</u>		836
Hirr	NHAAHTVGCS AATFV F ARTM PHREADGIPG KV WEASS KN SVLLRWLEPP		814
* * * * *			
Higfir	NPNGLILMYE IKYGS.QVED QREC VSRQ EY RKYGGAKLN R LNPGNY <u>TARI</u>		875
Hir	EPNGLIVLYE VS YRRY GDEE LHLCVSRKH F ALERGCR L R G LSPGNY <u>SVRI</u>		886
Hirr	DPNGLILKYE IKY RR LGEEA TVLCV SRL RY AKFGGVHL A LPPGNY <u>SARV</u>		864
* * * * *			
Higfir	QATSLSG <u>NGS</u> WTDPVFFYVQ AKTGYENFIH L		906
Hir	RATSLAG <u>NGS</u> WTEPTYFYVT DYLDVPSNIA K		917
Hirr	RATSLAG <u>NGS</u> WTDSVAFYIL GPEEEDAGGL H		895

Figure 14: Sequence Alignment of EGFR, ErbB2, ErbB3 and ErbB4 Ectodomains.

[For alignment on the IGF-1R fragment see Fig. 9]

Derived by use of the PileUp program in the software package of the Genetics Computer Group, 575 Science Drive, Madison, Wisconsin, USA.

Symbol comparison table: GenRunData.Pileuppep.Cmp CompCheck: 1254

GapWeight: 3.000
 GapLengthWeight: 0.100

Name: Erb3	Len: 649	Check: 4625	Weight: 1.00
Name: Erb4	Len: 649	Check: 790	Weight: 1.00
Name: Egfr	Len: 649	Check: 2381	Weight: 1.00
Name: Erb2	Len: 649	Check: 8174	Weight: 1.00

1 50
 Erb3 SEVGNSQAVC PGTLNGLSVT GDAENQYQTL YKLYERCEVV MGNLEIVL TG
 Erb4 ...SDSQSVC AGTENKLSSL SDLEQQYRAL RKYYENCEVV MGNLEITSIE
 Egfr ...LEEKKVC QGTSNKLQQL GTFEDHFLSL QRMFNNCEVV LGNLEITYVQ
 Erb2STQVC TGTDMKLRLP ASPETHLDML RHLYQGCQVV QGNLELTYLP

51 100
 Erb3 HNADLSFLQW IREVTGYVLV AMNEFSTLPL PNLRVVRGTQ VYDGKFAIFV
 Erb4 HNRDLSFLRS VREVTGYVLV ALNQFRYLPN ENLRIIRGKLYEDRYALAI
 Egfr RNYDLSFLKT IQEVAQGYVLI ALNTVERIPL ENLQIIRGNM YYENSYALAV
 Erb2 TNASLSFLQD IQEVAQGYVLI AHNQVRQVPL QRLRIVRGTQ LFEDNYALAV

101 150
 Erb3 MLNYN..... TNSSHA LRQLRLTQLT EILSGGGVYIE KNDKLCHMDT
 Erb4 FLNYR..... KDGNGFQ LQELGLKNLT EILNGGGVYVD QNKFLCYADT
 Egfr LSNYD..... ANKT.G LKELPMRNLQ EILHGAVRFS NNPALCNVES
 Erb2 LDNGDPLNNT TPVTGASPQG LRELQLRSLT EILKGGVLIQ RNPQLCYQDT

151 200
 Erb3 IDWRDIVRDR ...DAEIVVK DNGRSCPPCH EVC.KGRCWG PGSEDCQTLT
 Erb4 IHWQDIVRNP WPSNLTLVST NGSSGCGRCH KSC.TGRCWG PTENHCQTLT
 Egfr IQWRDIVSSD FLSNMSMDFQ NHLGSCQKCD PSCPNGSCWG AGEENCQKLT
 Erb2 ILWKDIFHKN NQLALTLIDT NRSRACHPCS PMCKGSRCWG ESSEDCQSLT

201 250
 Erb3 KTICAPQCNG HCFGPNPNQC CHDECAGGCS GPQDTDCFAC RHFNDSGACV
 Erb4 RTVCAEQCQDG RCYGPYVSDC CHRECAGGCS GPKDTDCFAC MNFNDSGACV
 Egfr KIICAQQCQSG RCRGKSPSDC CHNQCAAGCT GPRESDCLVC RKFRDEATCK
 Erb2 RTVCAGG.C.A RCKGPLPTDC CHEQCAAGCT GPKHSDCLAC LHFNHSGICE

251 300
 Erb3 PRCQPQLVYN KLTFQLEPNP HTKYQYGGVC VASCPhNFVV .DQTSCVRAC
 Erb4 TQCPQTGVYN PTTFQLEHNF NAKTYGAFC VKKCPHNFVV .DSSSCVRAC
 Egfr DTCPPMLYN PTTYQMDVNP EGKYSFGATC VKKCPRNYVV TDHGSCVRAC
 Erb2 LHCPLALVTYN TDTFESMPNP EGRTFGASC VTACPYNVLS TDVGSCTLVC

301 350
 Erb3 PPDKMEV.DK NGLKMCEPCG GLCPKACEGT GSGSRF..QT VDSSNIDGFW
 Erb4 PSSKMEV.EE NGIKMCKPCT DICPKACDGI GTGSLMSAQV VDSSNIDKFI
 Egfr GADSYEM.EE DGVRKCKKCE GPCRKVCNGI GIGEFKDSLs INATNIKHF
 Erb2 PLHNQEVTAE DGTQRCEKCS KPCARVCYGL GMEHLREVRA VTSANIQEFA

351 400
 Erb3 NCTKILGNLD FLITGLNGDP WHKIPALDPE KLNVFRTVRE ITGYLNIQSW
 Erb4 NCTKINGNLI FLVTGIHGDY YNAIEAIDPE KLNVFRTVRE ITGFLNIQSW
 Egfr NCTSISGDLH ILPVAFRGDS FTHTPPPLDPQ ELDILKTVKE ITGFLLIQAW
 Erb2 GCKKIFGSLA FLPESFDGDP ASNTAPLQPE QLQVFETLEE ITGYLYISAW

401 450
 Erb3 PPHMHNFNSVF SNLTTIGGRS LYNRGFSLLI MKNLNVTSLG FRSLKEISAG
 Erb4 PPNMTDFSVF SNLVTIGGRV LYS.GLSLLI LKQQGITSQ FQSLKEISAG

Egfr	PENRTDLHAF ENLEIIRGRT KQHGQFSLAV VS.LNITSLG LRSLKEISDG		
Erb2	PDSL PDL SVF QNLQVIRGRI LHNGAYSL.T LQGLGISWLG LRSLRELGSG		
451 End L2 domain> 500			
Erb3	RIYISANRQL CYHHSLNWTK VL RGPTTEERL DIKHNRPRRD CVA	EGKVCDP	
Erb4	NIYITDNSNL CYYHTINWTT LF.STINQRI VIRDNRKAEN CTA	EGMVCNH	
Egfr	DVIISGNKNL CYANTINWKK LF.GTSGQKT KIISNRGENS CKA	TGQVCHA	
Erb2	LALIHHTHNL CFVHTVPWDQ LFRNP.HQAL LHTANRPEDE CVG	EGLACHQ	
501 550			
Erb3	LCSSGGCWGP GPGQCLSCRN YSRGGVCVTH CNFLNGEPRE FAHEAECFSC		
Erb4	LCSSDGCWGP GPDQCLSCRN FSRGRICIES CNLYDGEFRE FENG SICVEC		
Egfr	LCSPEGCWGP EPRDCVSCRN VSRGRECVDK CKLLEGEPRE FVENSECIQC		
Erb2	LCARGHWCWGP GPTQCVNCSQ FLRGQECVVE CRVLQGLPRE YVNARHCLPC		
551 600			
Erb3	HPECQPME.G TATCNGSGSD TCAQCAHFRD GPHCVSSCPH GVLGA.KGP.		
Erb4	DPQCEKMEDG LLTCHGPGPD NCTKCSHFKD GPNCVEKCPD GLQGA.NSF.		
Egfr	HPECLPQAMN I.TCTGRGPD NCIQCAHYID GPHCVKTCPA GVMGENNTL.		
Erb2	HPECQPQN.G SVTCFGPEAD QCVACAHYKD PPFCVARCPS GVKPDLSYMP		
601 649			
Erb3	IYKYPDVQNE CRPCHENCTQ GCKGPELQDC L.....GQT.		
Erb4	IFKYADPDRE CHPCHPNCTQ GCNGPTSHDC IYYPWTGHST LPQHARTPL		
Egfr	VWKYADAGHV CHLCHPNCTY GCTGPGLEG C PTNGPKIPS.		
Erb2	IWKFPDEEGA CQPCPINCTH SCVLDLDDKGC PAEQRASPLT S.....		

Figure 15. Classification of Cys-rich modules

C2-4 denote modules with the 1-3/2-4 double disulphide bond connections.
 C1-2 for the single disulphide bonded modules and
 C1-2t for stabilised beta turn.

First Cys-rich region
C2-4 modules

		1	2	3	4		
Higfir	152	CPGTMEEKPM-CEKTTINNEVINYRCWTTMRC	QKM			184	(1st)
Hir	159	CPGTAKGKTL-CPATVINGQEVERCWTTHSHC	QKV			191	(1st)
Hirr	154	CPG/LGAAGEPCAKTTESGHDTDYRCWTSSHC	QRV			187	(1st)
Egfr	166	CDPSCPNG-SCWGAG-EENC	QKLTKII			190	(1st)
hErb2	174	CSPHCKGS-RCWGES-SEDC	QSLTRTV			198	(1st)
hErb3	167	CHEVCKG--RCWGPG-SEDC	QTLTKTI			190	(1st)
hErb4	167	CHKSCCTG--RCWGPT-ENHC	QTLTRTV			190	(1st)
Higfir	185	CPSTOGK-RACTEN---NEC				200	(2nd)
Hir	192	CP TICKS-HGCTAE---GLC				207	(2nd)
Hirr	188	CP--CPHGMACTAR---GEC				202	(2nd)
Egfr	191	CAQQCNSG--RCRGKS-PSDC				207	(2nd)
hErb2	199	CAGGCA---RCKGPL-PTDC				214	(2nd)
hErb3	191	CAPOCNG--HCFGPN-PNQC				207	(2nd)
hErb4	191	CAEQCDG--RCYGPY-VSDC				207	(2nd)
Higfir	201	CH2ECLG--SCSAPNDTAC	VA			220	(3rd)
Hir	208	CHSECLG--NCSQPDDPTKC	VA			227	(3rd)
Hirr	203	CHTECLG--GCSQPEDPRAC	VA			222	(3rd)
Egfr	208	CHHQCAA--GCTGPR-ESEC	LV			226	(3rd)
hErb2	215	CHEQCAA--GCTGPK-HSDC	LA			233	(3rd)
hErb3	208	CHDECAG--GCSGPQ-PTDC	FA			226	(3rd)
hErb4	208	CHRECAG--GCSGPK-PTDC	FA			226	(3rd)

C1-2 modules

Higfir	231	CRHYY---YAGVC	VPA		233	(4th)
Hir	238	CRMFY---LDGRC	VET		240	(4th)
Hirr	233	CRHLY---FQGAC	LWA		235	(4th)
Egfr	237	CRHFR---DEATC	KDT		239	(4th)
hErb1	234	CIHEN---HSGIC	ELH		248	(4th)
hErb3	237	CRHFN---DSGAC	VPR		239	(4th)
hErb4	237	CRHFN---DSGAC	VTQ		239	(4th)
Higfir	234	CFENTYRFEQWRC	VDRDF		251	(5th)
Hir	241	CFEFETYHEQDWRC	VHESF		259	(5th)
Hirr	236	CFEFETYQYESWRC	VTAER		253	(5th)
Egfr	240	CFPLMLYNEFTTYQIDWVPEKGKISFGATC	VKK		270	(5th)
hErb2	247	CFALVTYHTDTFESIIPNFEGRYTFEGASC	VTA		277	(5th)
hErb3	240	CPQPLVYINKLTQLEPNPHTKYQYGGVC	VAS		270	(5th)
hErb4	240	CPQPLVYINPTTFQLEHHENMAKYTYGAFC	VKK		270	(5th)
Higfir	252	CAWILSAESSDSEG.....FVIHD.GEC	MQE		276	(6th)
Hir	259	CC. LHHKCKNSRRQGCHQYVIHN.NKC	IPE		287	(6th)
Hirr	254	CA. LHSVPGRAST.....FGHQ.GSC	LAQ		276	(6th)
Egfr	271	CFRNYVVTDHGSC	VRA		286	(6th)
hErb1	278	CFRNYLSTDVGSC	TLV		293	(6th)
hErb3	271	CFHNEVV.DQTSC	VRA		285	(6th)
hErb4	271	CFHNEVV.DSSSC	VRA		285	(6th)
Higfir	277	CFSS. FIRNGSQ-SNYC	IP		293	(7th)
Hir	288	CFSS. VTHNSSH--LLC	TP		303	(7th)
Hirr	278	CFSG. FTRNISS--SIFC	HK		293	(7th)
Egfr	297	CAADSTENE-EDGVRKC	KK		304	(7th)
hErb1	294	CPHNQEVTAEDGTQRC	EK		312	(7th)
hErb3	296	CPFDKNEVDKH-GLRHC	EP		303	(7th)
hErb4	296	CPSSHNEVEENI-GIRHC	KP		303	(7th)

C1-2t module

hIgflr	294	CEGPC	298	(8th)
Hir	304	CLGPC	308	(8th)
Hirr	294	CEGLC	298	(8th)
hEgfr	305	CEGPC	309	(8th)
hErb2	313	CSKPC	317	(8th)
hErb3	304	CGGLC	308	(8th)
hErb4	304	CTDIC	308	(8th)

Second Cys-rich region.**C2-4 modules**

hEgfr	482	CHALCSP-----EGCWGPEPRDCVS	501	(1st)
hErb2	490	CHQLCAR-----GHCWGPQPTQCVN	509	(1st)
hErb3	481	CDPLCSS-----GGCWGPQPGQCLS	500	(1st)
hErb4	481	CNHLCSS-----DGCWGPQPDQCLS	500	(1st)
Egfr	534	CHPECLPQAM-NITCTGRGPDNC IQ	557	(4th)
hErb2	542	CHPECQPQNG-SVTCFGPEADQC VA	565	(4th)
hErb3	533	CHPECQPMEG-TATCNGSGSDTC AQ	556	(4th)
hErb4	533	CDPQCEKMEDGLLTCHGPQPDNC TK	557	(4th)
hEgfr	596	CHPNCTY-----GCTGPGLEGC PTNGPKIPS/	621	(7th)
hErb2	605	CPINCTH-----SCVLDLDDKGC PAEQRAQRASPLTS/	632	(7th)
hErb3	594	CHENCTQ-----GCKGPELQDC LGQT/	614	(7th)
hErb4	595	CHPNCTQ-----GCNGPTSHDC IYYPWTGHSTLPQHARTPL	630	(7th)

C1-2 modules

hEgfr	502	CRNVS---RGREC VDK	514	(2nd)
hErb2	510	CSQFL---RGQEC VEE	522	(2nd)
hErb3	501	CRNYS---RGGVC VTH	513	(2nd)
hErb4	501	CRRFS---RGRIC IES	513	(2nd)
hEgfr	515	CKLLEGEPEFVENSEC IQ	533	(3rd)
hErb2	523	CRVLQGLPREYVNARHC LP	541	(3rd)
hErb3	514	CNFLNCEPEFAHEAEC FS	532	(3rd)
hErb4	514	CNLYDGEFREFENGSI C VE	532	(3rd)
hEgfr	558	CAHYI---DGPHC VKT	570	(5th)
hErb2	566	CAHYK---DPPFC V-A	578	(5th)
hErb3	557	CAHFR---DGPHC V-S	569	(5th)
hErb4	558	CSHFK---DGPNC VEK	570	(5th)
hEgfr	571	CPAGVMGENNTL-VWKYADAGHVC HL	595	(6th)
hErb2	579	CPSGVKPDLSYMPIWKFPDEEGAC QP	604	(6th)
hErb3	570	CPHGVLGAKG--PIYKYPDVQNEC RP	593	(6th)
hErb4	571	CPDGLQGANS--FIFKYADPDREC HP	594	(6th)

See Pattern is:

IR family:	C2-4, C2-4, C2-4, C1-2, C1-2, C1-2, C1-2, C1-2t
EGFR family: 1st	C2-4, C2-4, C2-4, C1-2, C1-2, C1-2, C1-2, C1-2t
2nd	C2-4, C1-2, C1-2, C2-4, C1-2, C1-2, C2-4

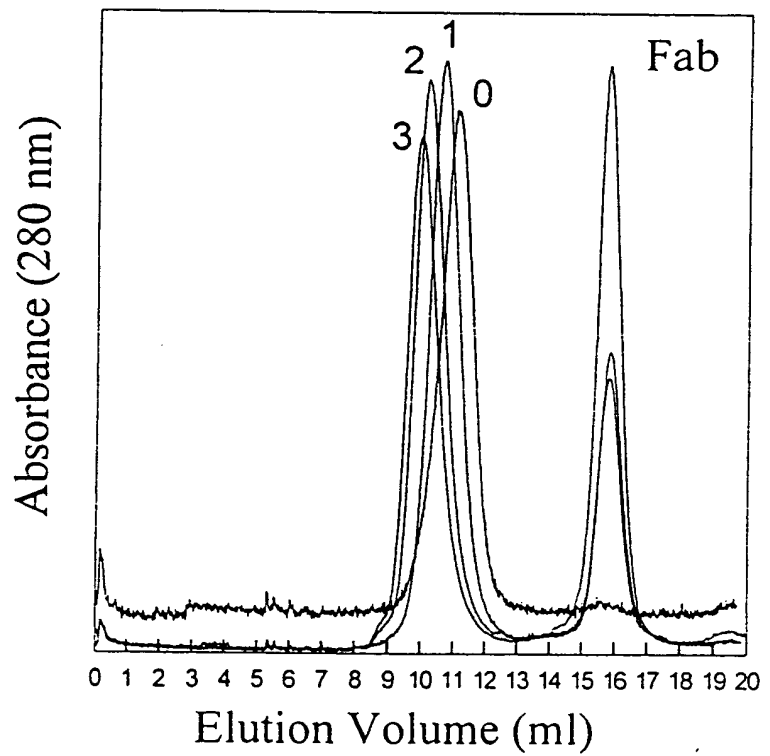
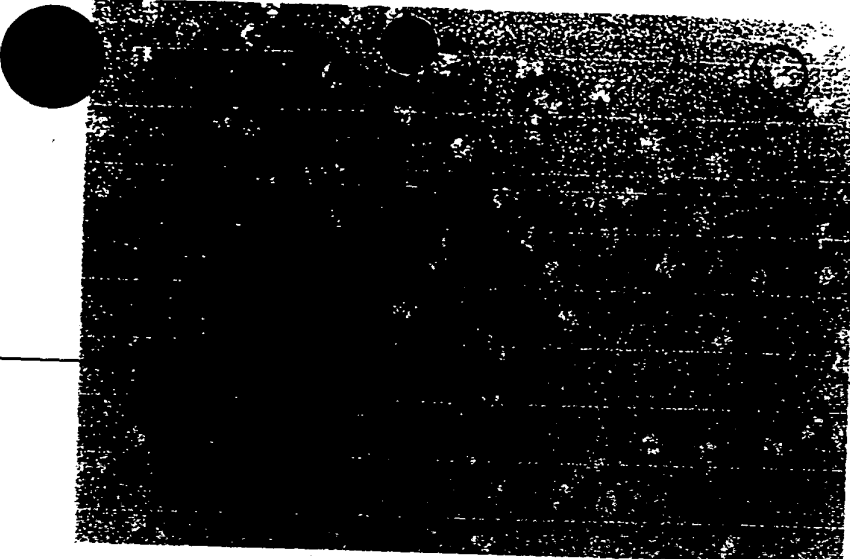
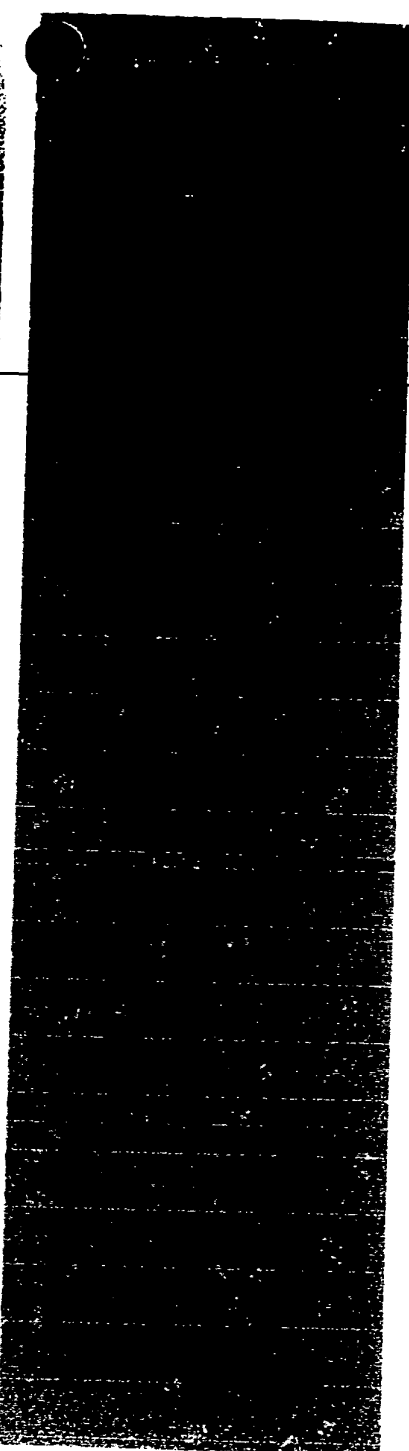


Figure 16

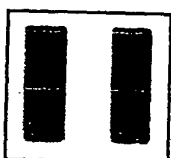


(b)



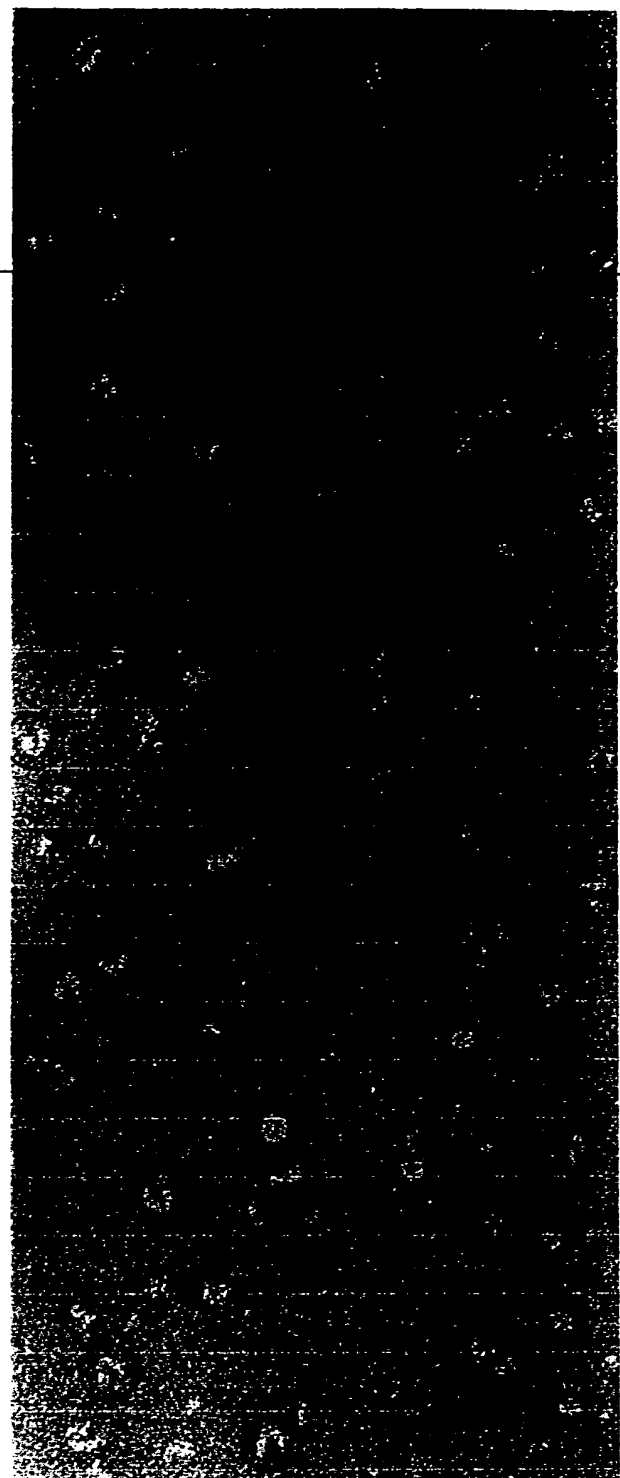
(c)

Figure 17





(a)



(b)



Figure 18

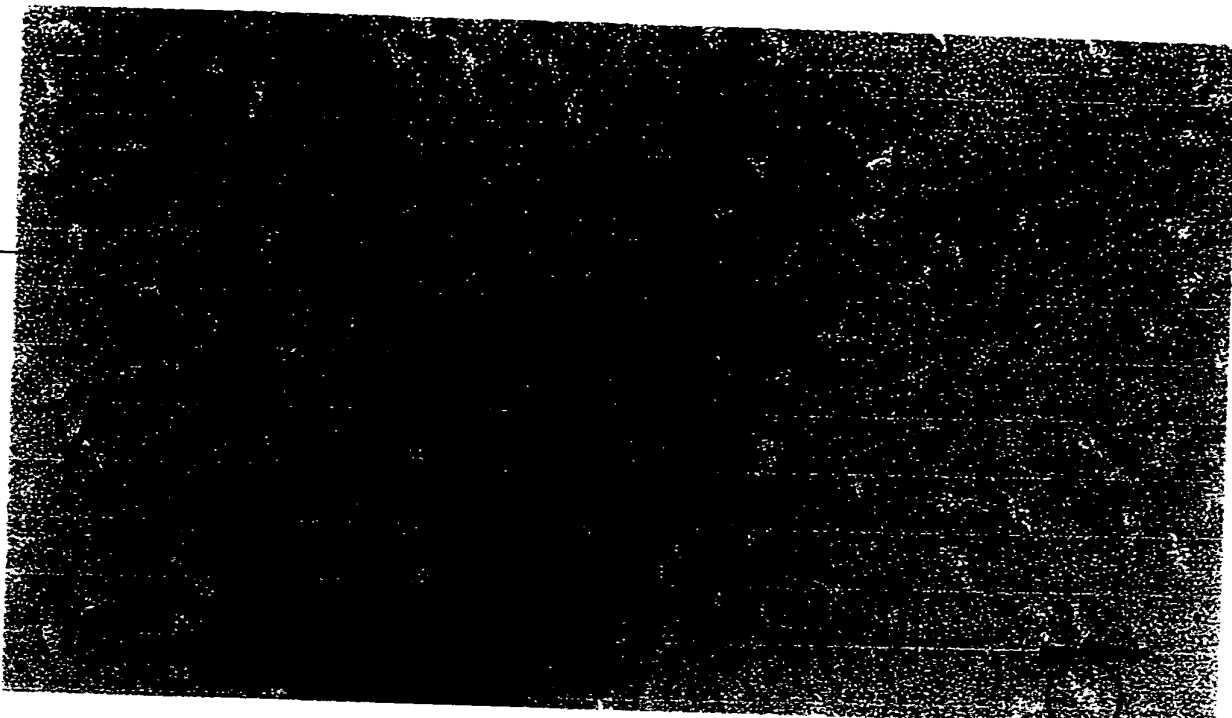


Figure 19

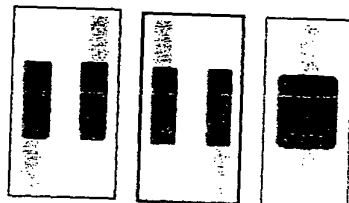


Figure 20

(a)



(b)

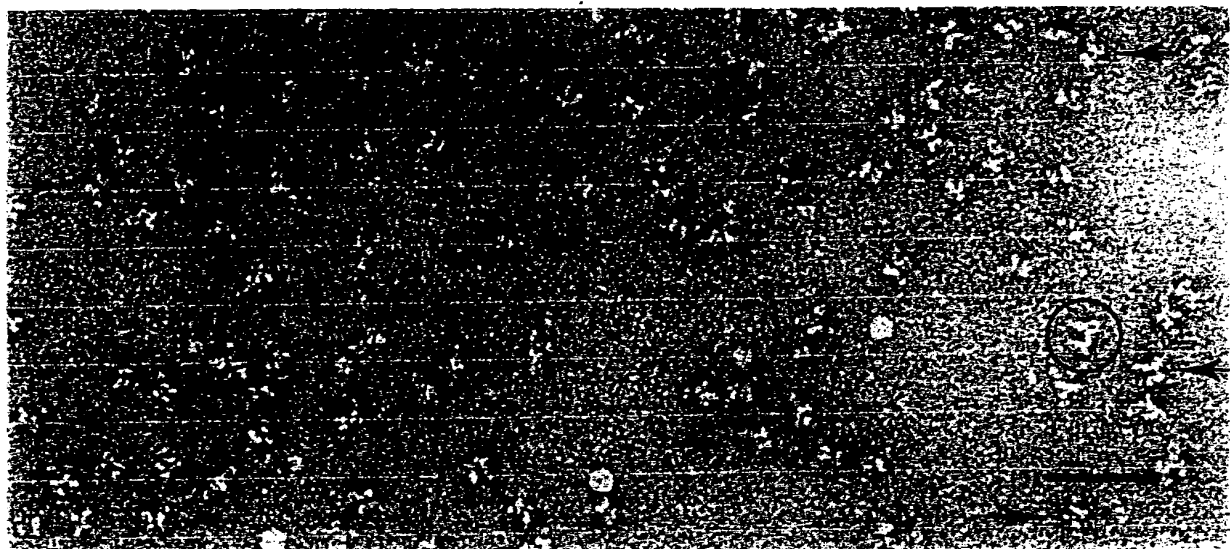


Figure 21



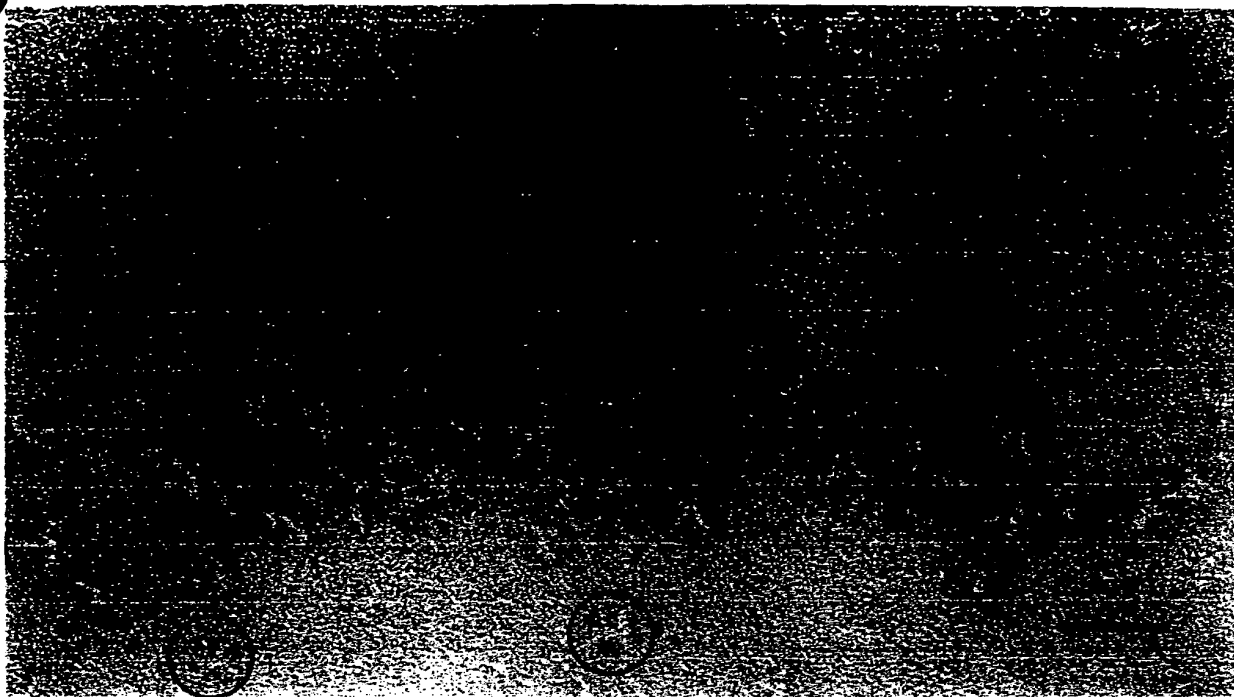


Figure 22

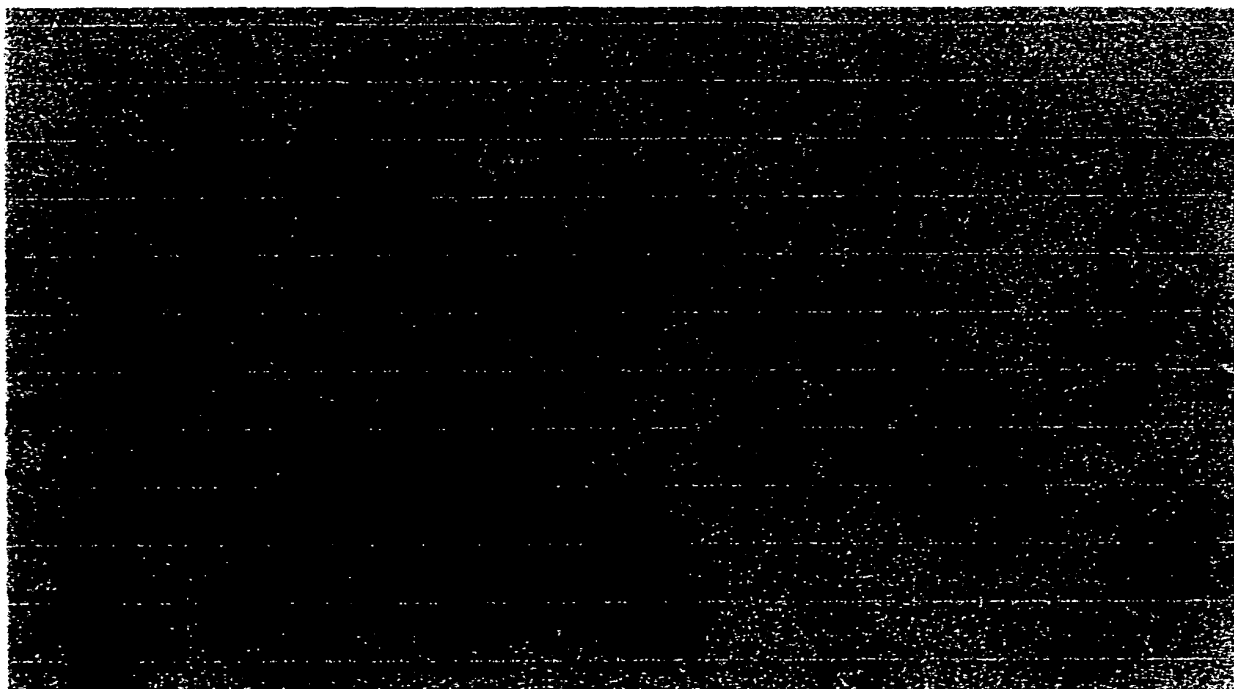


Figure 23

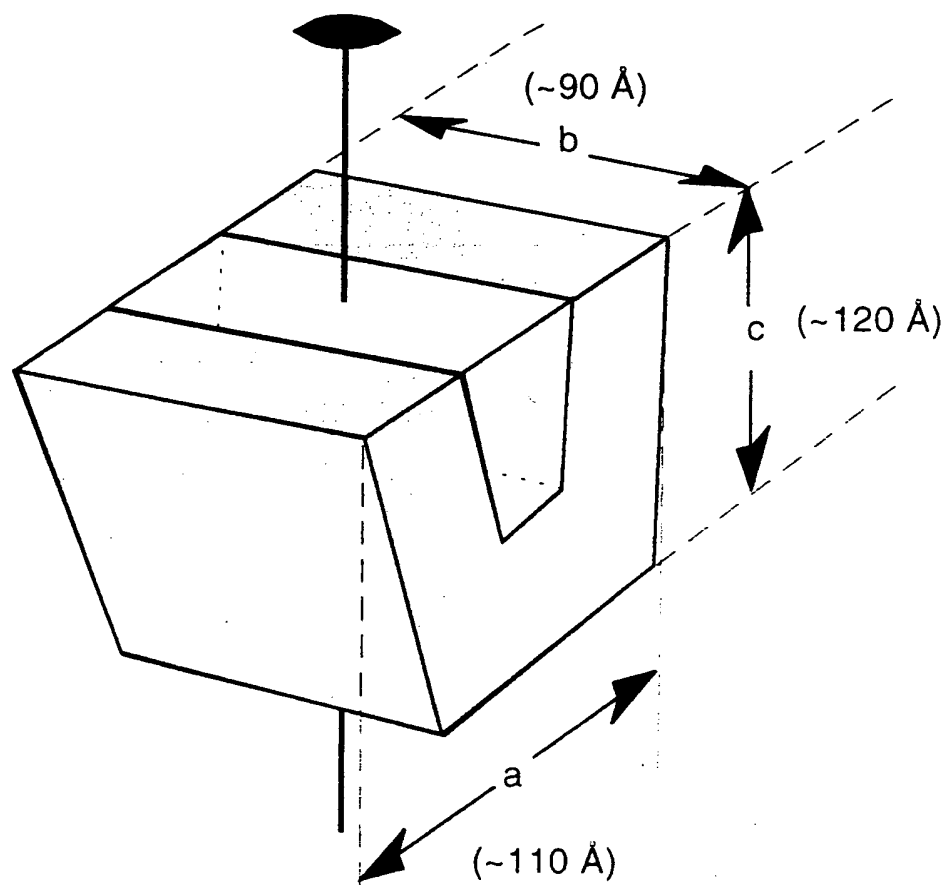


Figure 24

